Numerical Modeling of Friction in Lubricated Cold Rolling

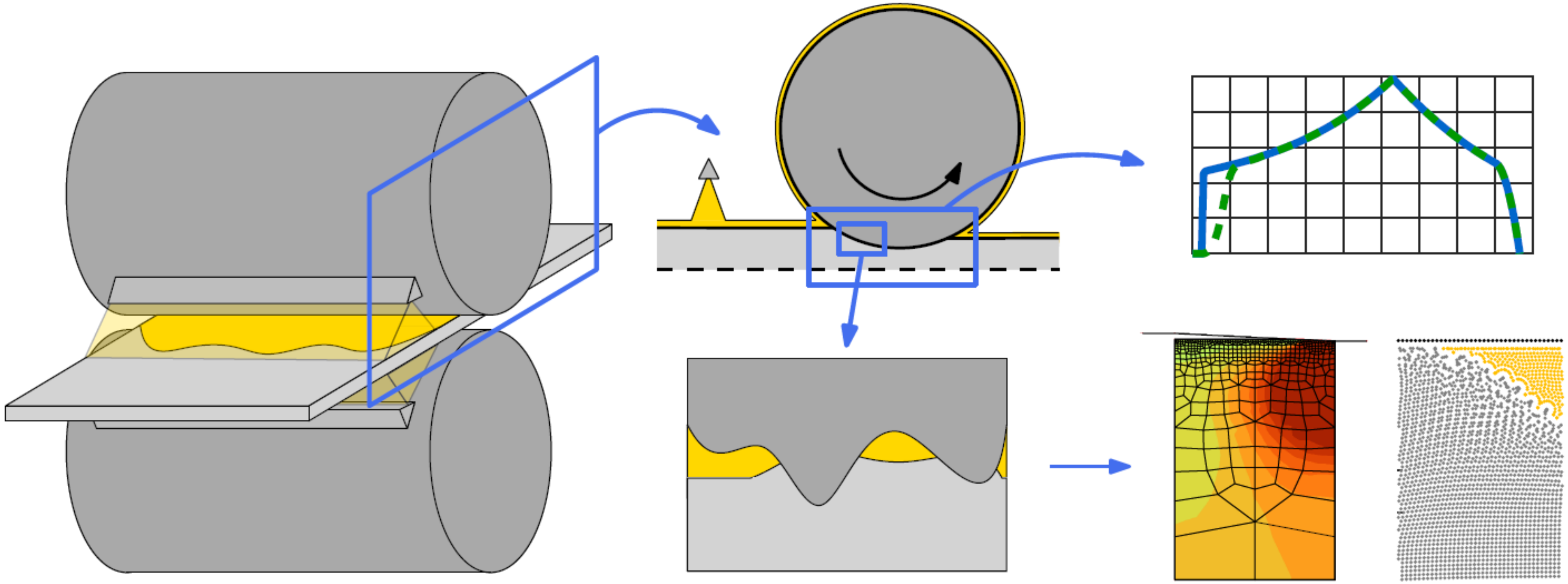

Dominik BOEMER

MN2L Research Group, University of Liège, Belgium

PhD Thesis Defense Liège May 5th, 2020

Outline

1. **Introduction**
2. Experimental data
3. Metalub model
4. Metalub results
5. FE asperity flattening in Metalub
6. SPH asperity flattening
7. Conclusion and outlook

1.1 Rolling in the steel production

Steel slab
Thickness: ~250 mm

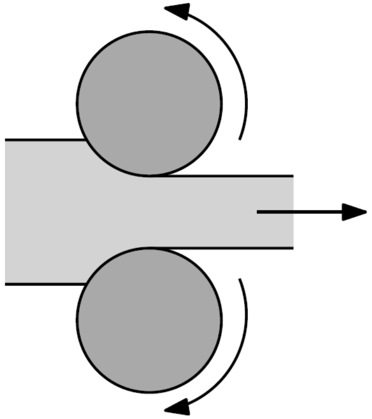

Rolling

Car body
~0.8 mm

Tin can
~0.2 mm

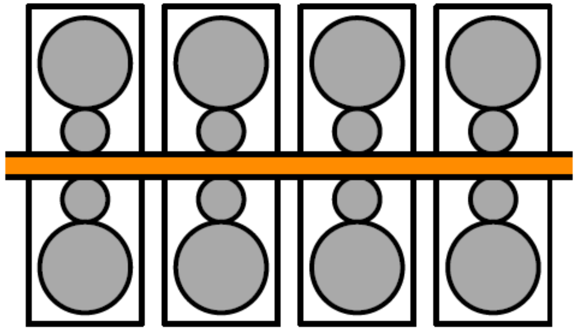

Hot rolling at ~1000°C

Intermediate thickness:
1.5 - 5 mm

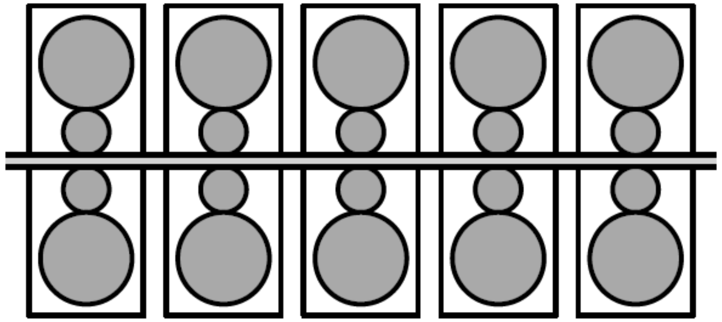

Cold rolling at ~100°C

1.2 Cold rolling

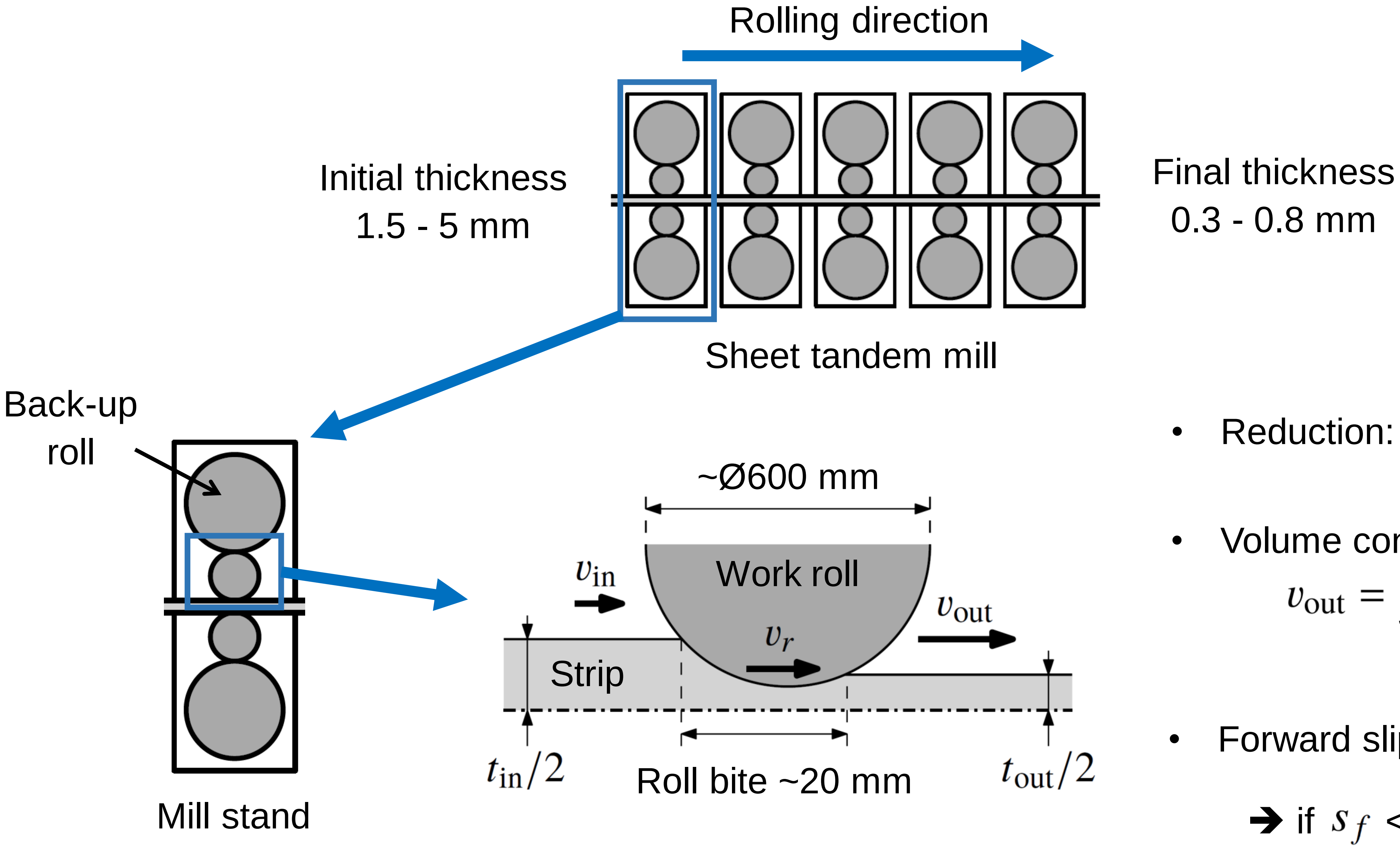

- Reduction: $r = \dfrac{t_{\mathrm{in}} - t_{\mathrm{out}}}{t_{\mathrm{in}}}$
- Volume conservation:

$$v_{\mathrm{out}} = \underbrace{(t_{\mathrm{in}}/t_{\mathrm{out}})}_{> 1} v_{\mathrm{in}}$$

- Forward slip: $s_f = \dfrac{v_{\mathrm{out}} - v_r}{v_r}$

➔ if $s_f < 0$, skidding

1.3 Conventional lubrication

- Conventionally, recirculating lubrication systems with an oil-in-water emulsion
  - Passive: constant oil concentration, …
  - Mixed lubrication

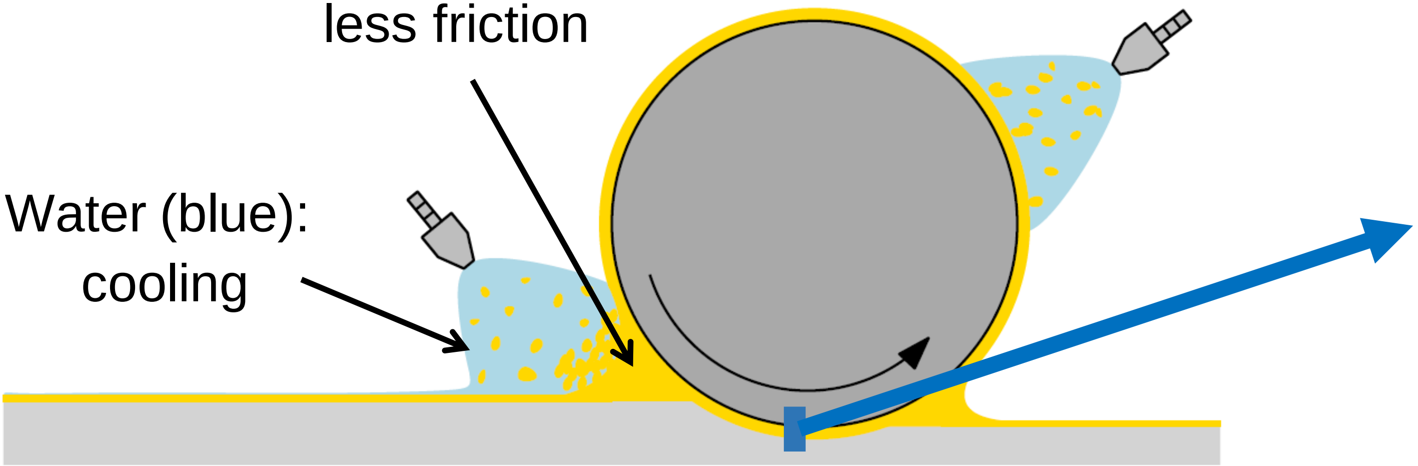

Oil (yellow): less friction

Water (blue): cooling

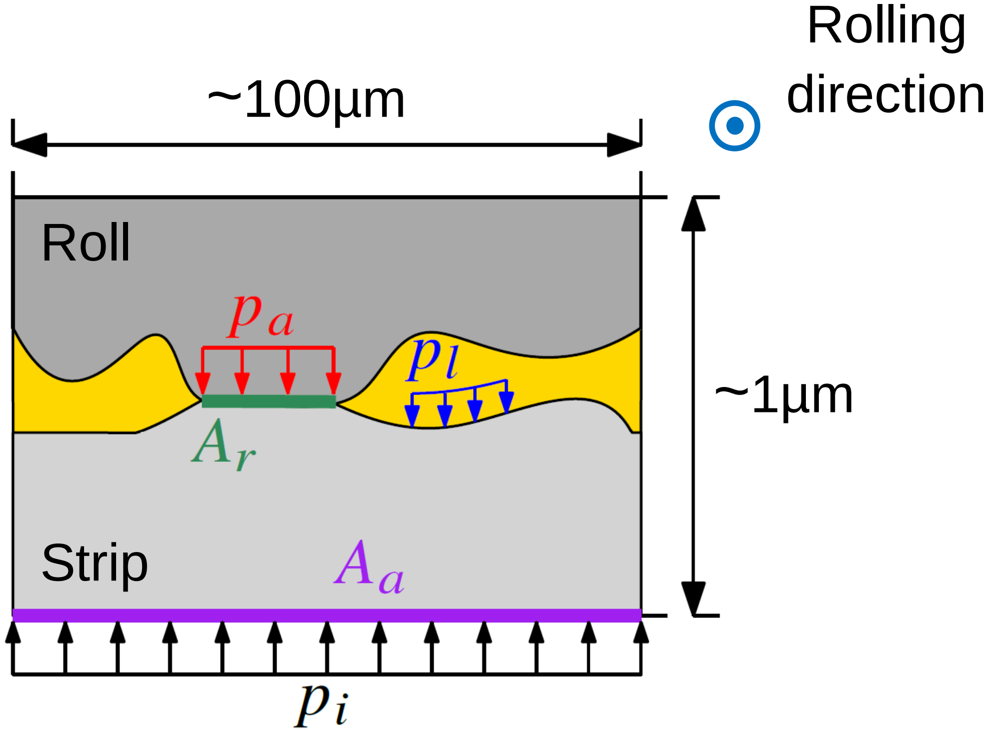

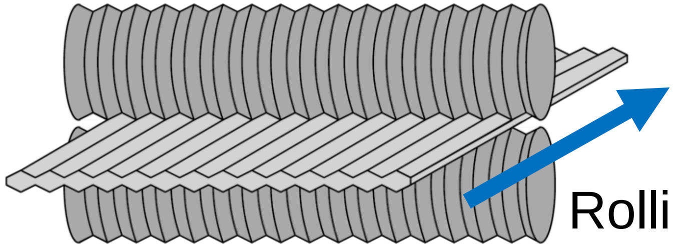

Roughness grooves along rolling direction due to roll grinding (magnified)

Rolling direction

- Relative contact area: $A = A_r / A_a$
- Interface pressure: $p_i = A p_a + (1 - A) p_l$
- Interface shear stress: $\tau_i = A \tau_a + (1 - A) \tau_l$

$\tau_a \gg \tau_l$

1.3 Friction and rolling force

- Friction and yield stress σ_Y increase the rolling force:

$$\tau_i \nearrow \quad \rightarrow \quad \sigma_x \searrow \quad \xrightarrow[\sigma_Y = \text{constant}]{\text{Von Mises}} \quad p_i \nearrow \quad \rightarrow \quad F_r = \int p_i \, \mathrm{d}x \nearrow$$

Interface shear stress due to friction

Stress in rolling direction (< 0, compression)

Interface pressure (> 0, compression)

Rolling force

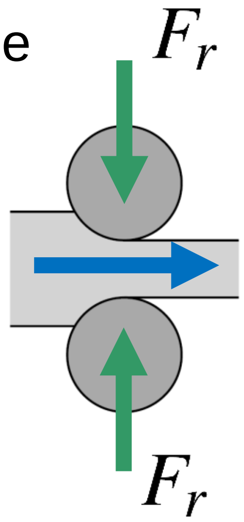

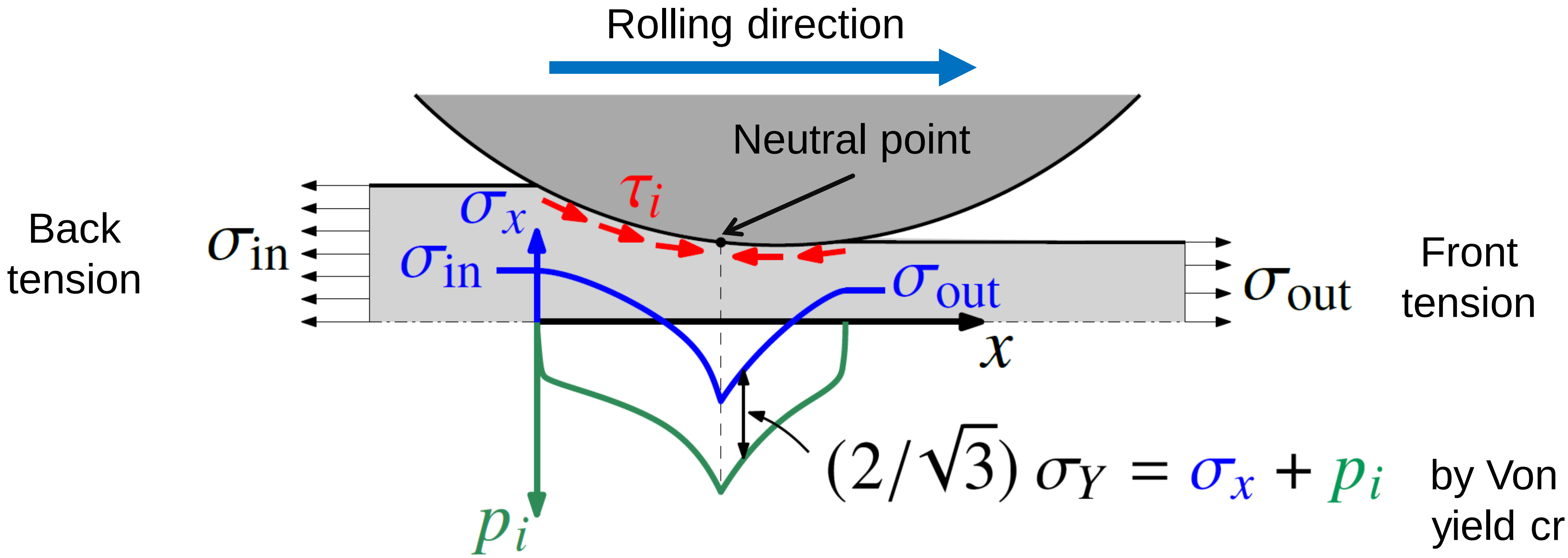

$$(2/\sqrt{3})\,\sigma_Y = \sigma_x + p_i$$ by Von Mises yield criterion

1.4 Industrial problem

- Demand for harder and thinner sheet products by car manufacturers

  ➔ lighter cars, lower fuel consumption, less CO2

- This implies a greater rolling force.

- Technological constraint: rolling force limited by the mill stand

- If friction was minimized for a given mill stand, while preventing skidding:
  - Harder and thinner products could be rolled;
  - Energy consumption of rolling could be decreased;
  - Roll wear could be reduced;
  - …

1.4 Industrial problem

- Necessity of friction control [Laugier et al., 2014]
  - Computed decrease of rolling force, if effective coefficient of friction is decreased from 0.05 to 0.04
  - For a reduction of 25% and fixed front and back tensions
  - Strong dependence for hard and thin products

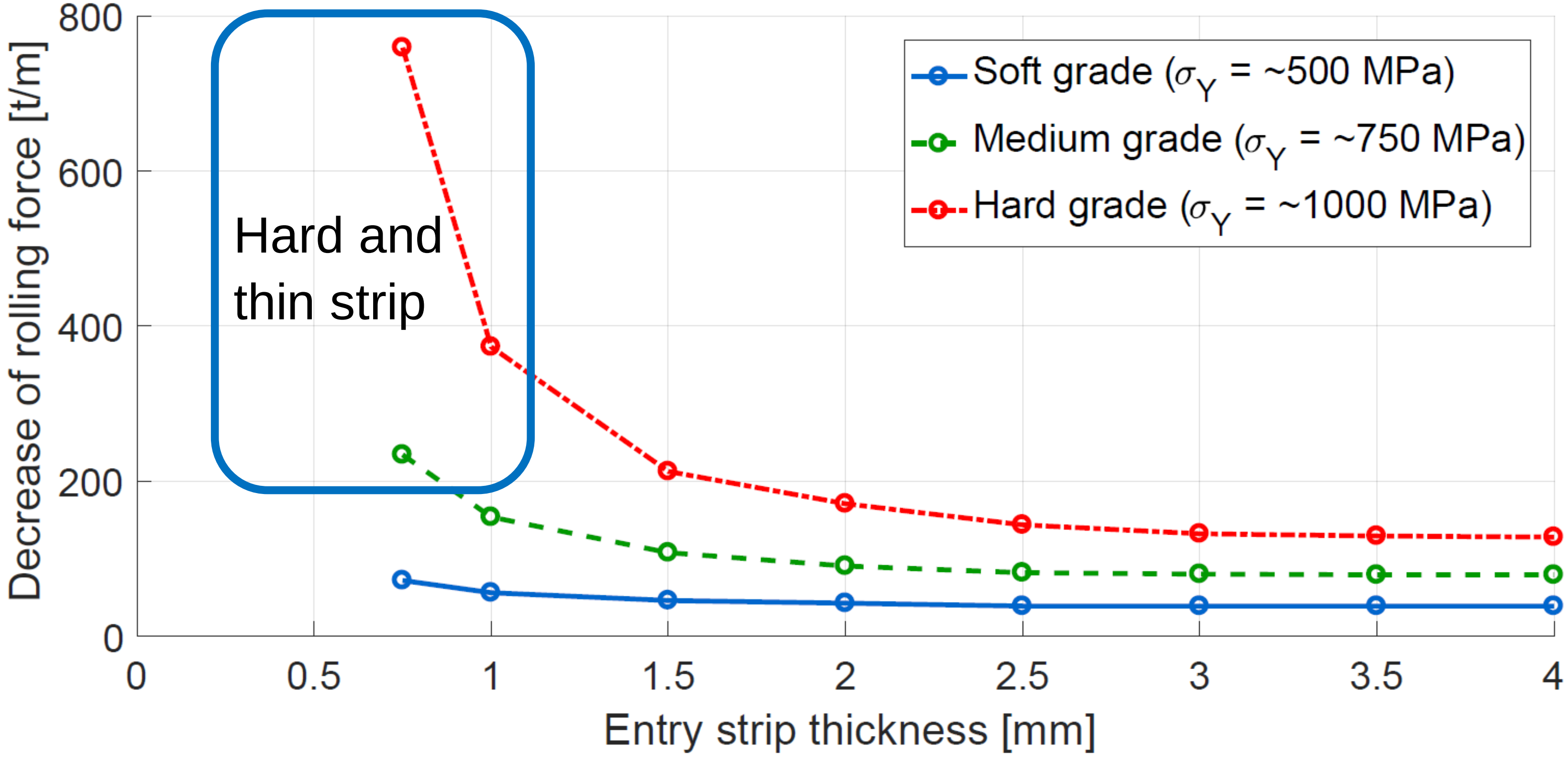

➔ Friction control required

1.5 Solution: flexible lubrication

- Flexible lubrication (FL) concept
  - Active: continuous control of friction
  - By adjusting lubrication conditions depending on rolling conditions

- Application of concept: control of oil concentration by additional FL system

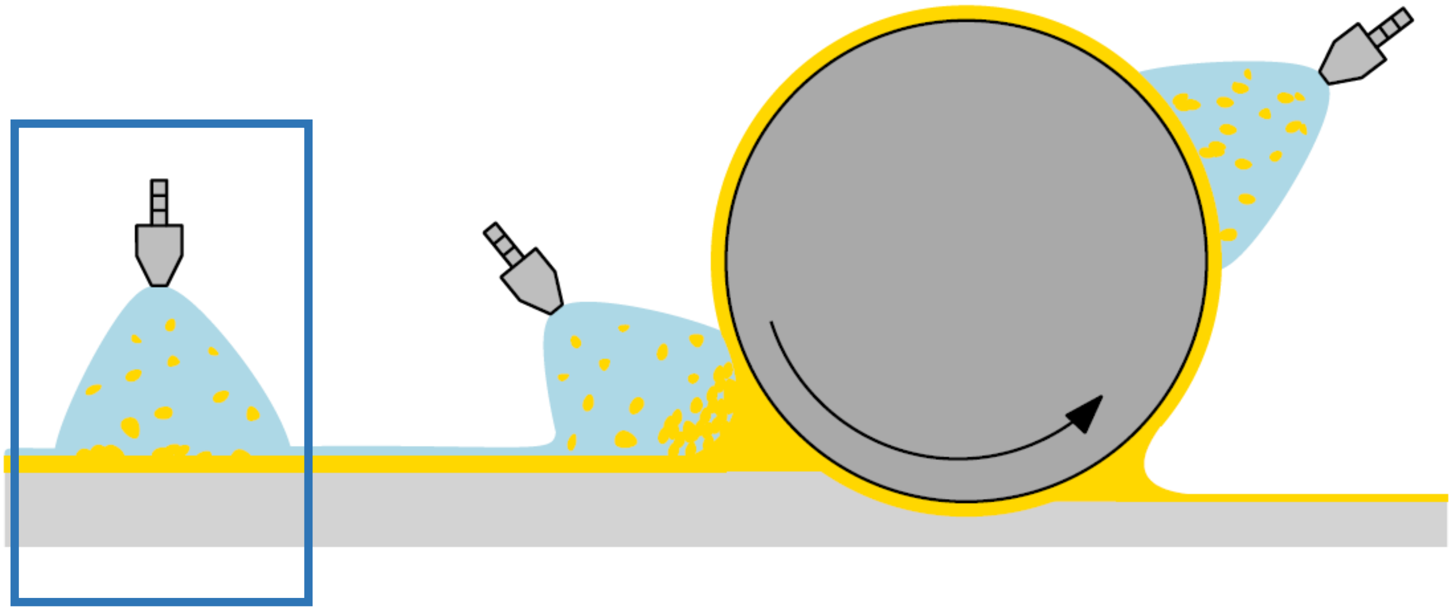

Additional flexible
lubrication system

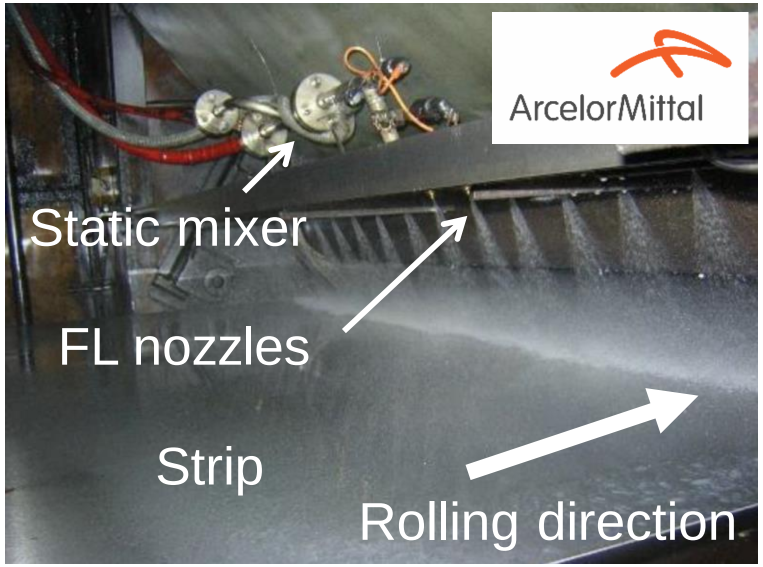

[Laugier et al., 2011]

1.5 Solution: flexible lubrication

- Predictive tool
    - To determine optimal lubrication conditions (e.g. oil concentration, viscosity, …)
    - Depending on rolling conditions (e.g. rolling speed, product characteristics, …)

- Extensive research in the past

- BUT no complete tool exists because:
    - Some physical mechanisms cannot be modeled satisfactorily, yet;
    - Individual models of mechanisms could not be combined in one full model, yet.

1.6 Objectives

- General objective:

Accurately model friction in lubricated cold rolling to minimize friction while preventing skidding by flexible lubrication

- In this thesis:

1. Determine physical mechanisms to model by most extensive experimental data.
2. Re-derive, document and extend the Metalub rolling model.
3. Evaluate predictive capabilities and shortcomings of Metalub by this data.
4. Introduce MPH lubrication by Finite Element (FE) asperity flattening in Metalub.
5. Explore Smoothed Particle Hydrodynamics (SPH) to model MPH lubrication.

Outline

1. Introduction
2. **Experimental data**
3. Metalub model
4. Metalub results
5. FE asperity flattening in Metalub
6. SPH asperity flattening
7. Conclusion and outlook

2.1 Experimental setup

- Objective: determine physical mechanisms and validation data
- Semi-industrial pilot mill by courtesy of ArcelorMittal (March 2014)
- Most comprehensive data available:
  - Roughness measurements
  - Thermo-piezoviscous material laws of the lubricants
  - Hardening laws of strips by plane strain compression tests
  - Large design space:
    - Rolling speeds
    - Rolled products
    - Lubrication conditions
    - Reductions

$\Big\} \longrightarrow$

- Rolling force
- Forward slip

➔ Post-processed: library with 112 rolling scenarios

[Legrand et al., 2015]

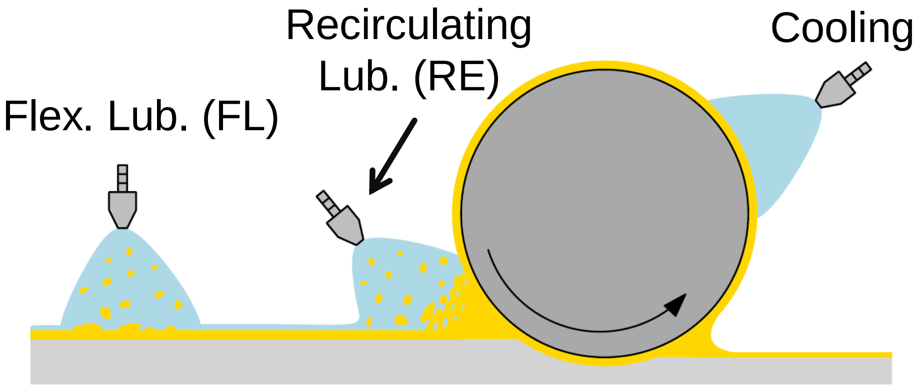

2.2 Analysis of experimental data – Influence of rolling speed

- Hydrodynamic effect (Test 5B, pure oil)

$$v_r \nearrow \quad \rightarrow \quad h_t \nearrow \quad \rightarrow \quad A \searrow \quad \rightarrow \quad \overline{\mu} \searrow \quad \rightarrow \quad F_r \searrow, \quad s_f \searrow$$

Rolling speed Oil film thickness Relative contact area Friction Rolling force Forward slip

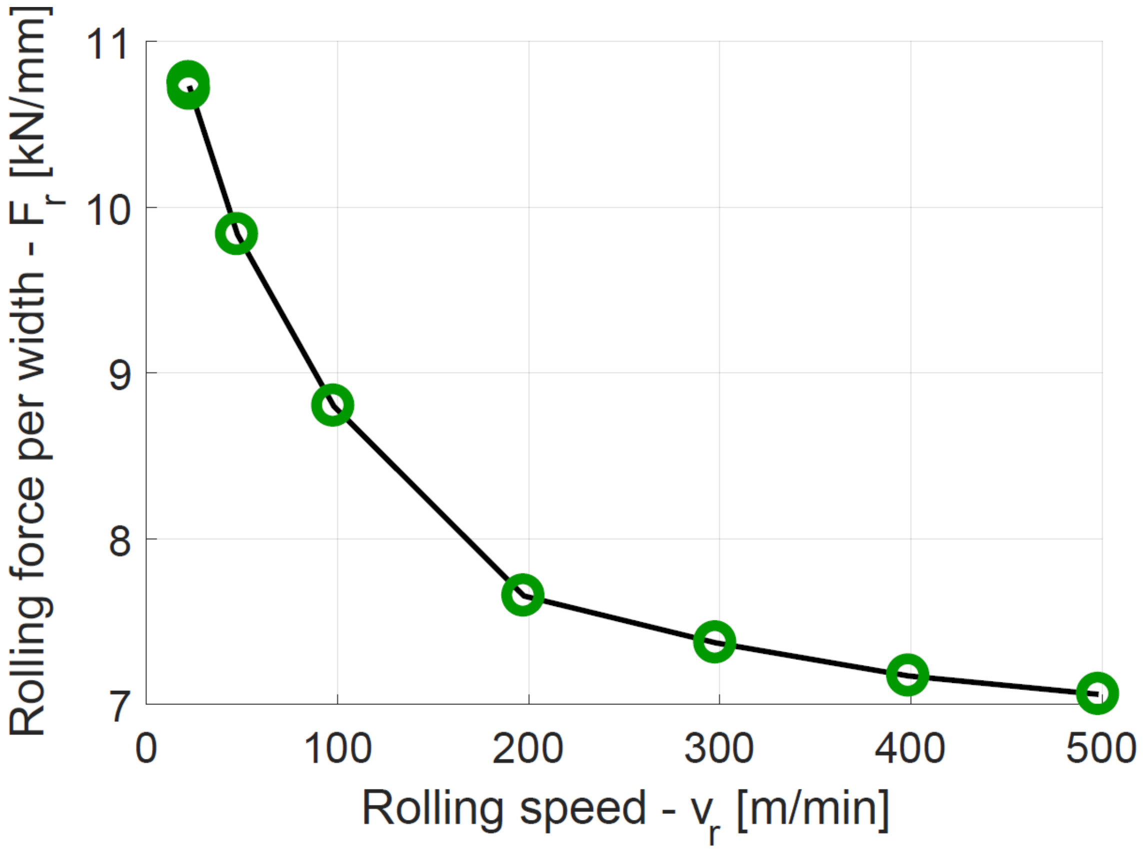

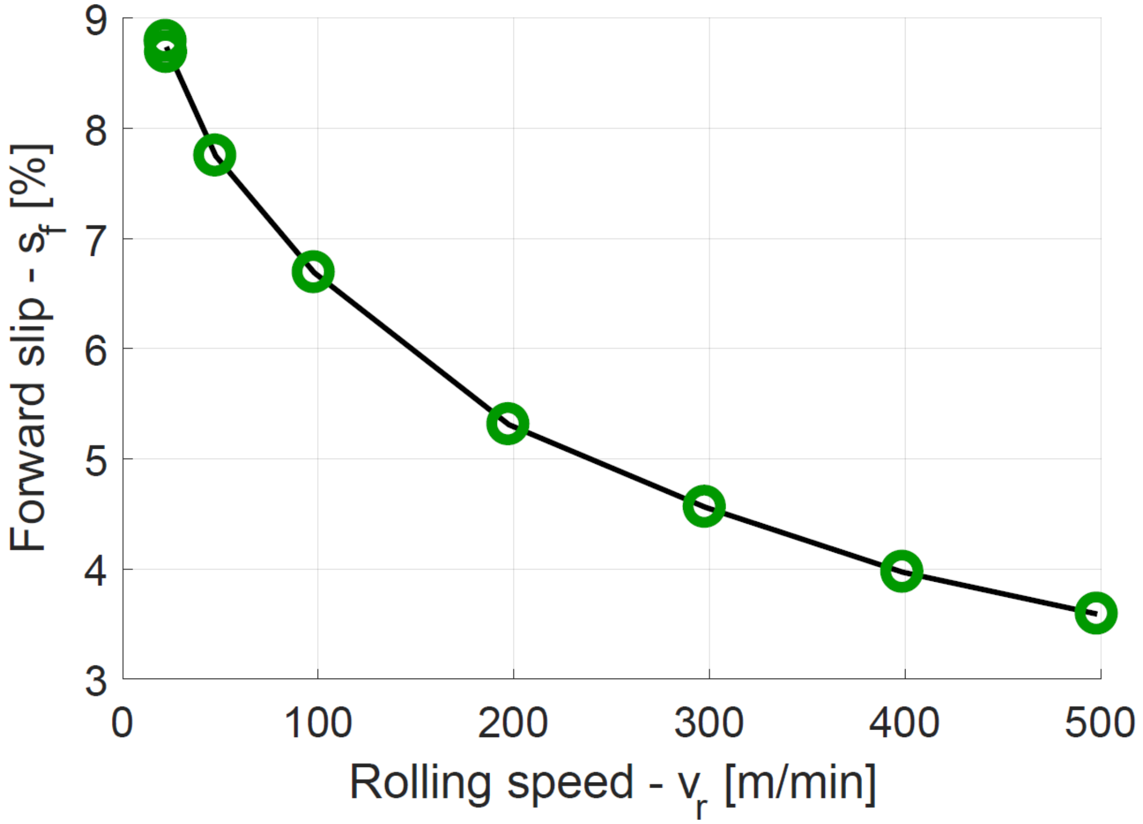

2.2 Analysis of experimental data – Influence of rolling speed

- Viscoplasticity (Test 6, pure oil, different rolled product)

$$v_r \nearrow \quad \rightarrow \quad \overline{D}_p \nearrow \quad \rightarrow \quad \sigma_Y \nearrow \quad \rightarrow \quad F_r \nearrow$$

Rolling speed | Effective plastic strain rate | Yield stress | Rolling force

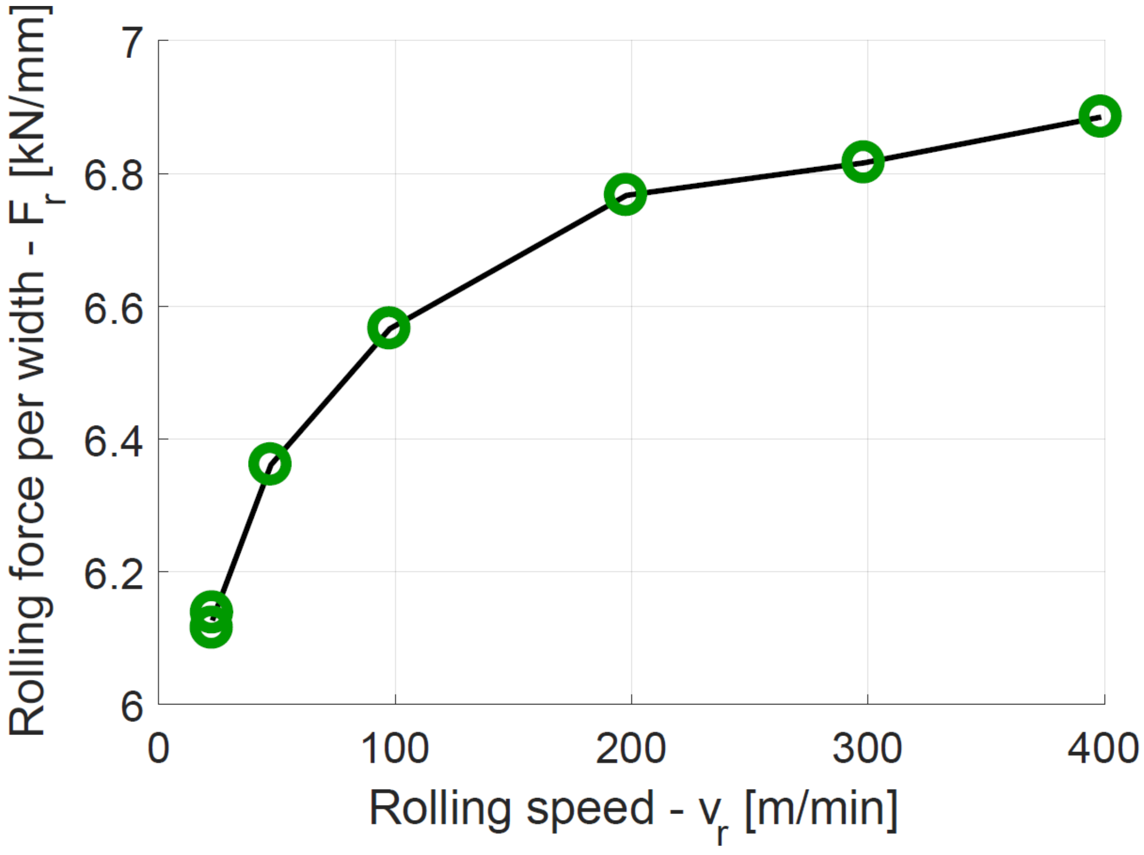

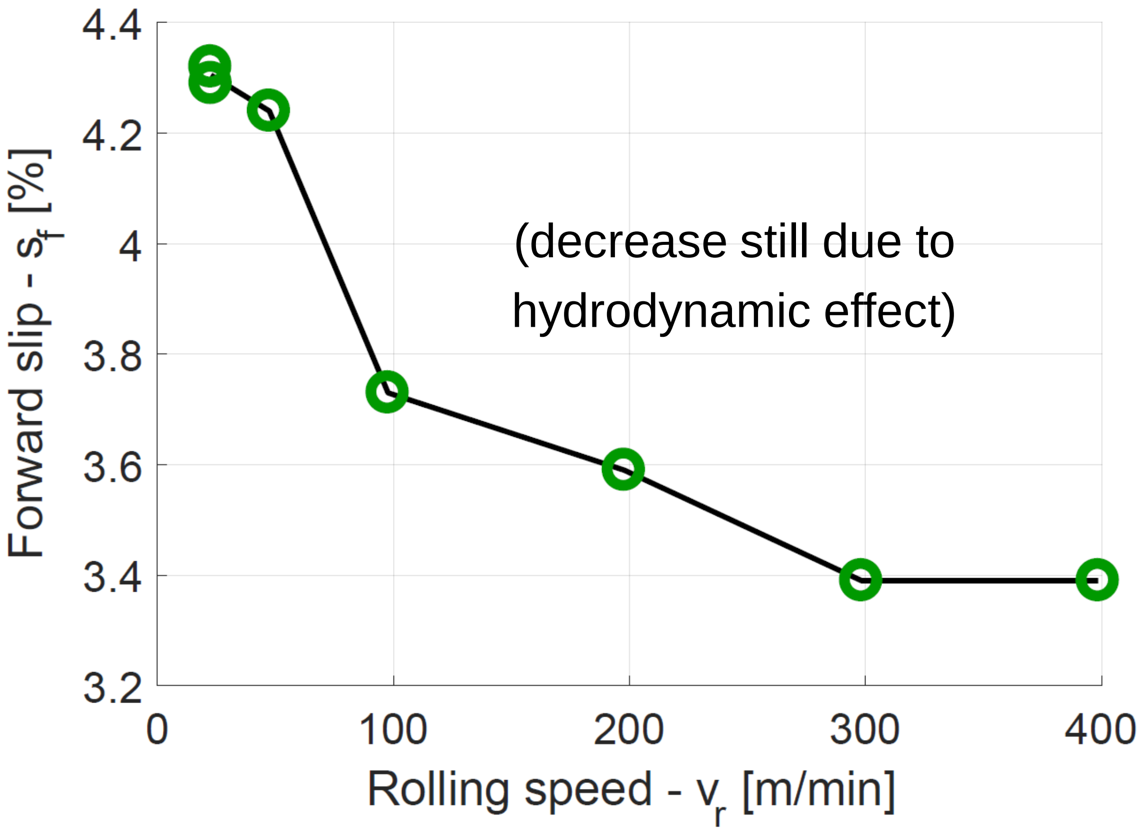

(decrease still due to hydrodynamic effect)

2.2 Analysis of experimental data – Influence of lubricant quantity

- **Starvation** (Tests 5B and 4A)

$$h_L \searrow \xrightarrow{\text{Condition}} h_t \searrow \rightarrow A \nearrow \rightarrow \overline{\mu} \nearrow \rightarrow F_r \nearrow, \; s_f \nearrow$$

$h_L \searrow$	$h_t \searrow$	$A \nearrow$	$\overline{\mu} \nearrow$	$F_r \nearrow$	$s_f \nearrow$
Oil film thickness provided by lub. syst.	Oil film thickness in roll bite	Relative contact area	Friction	Rolling force	Forward slip

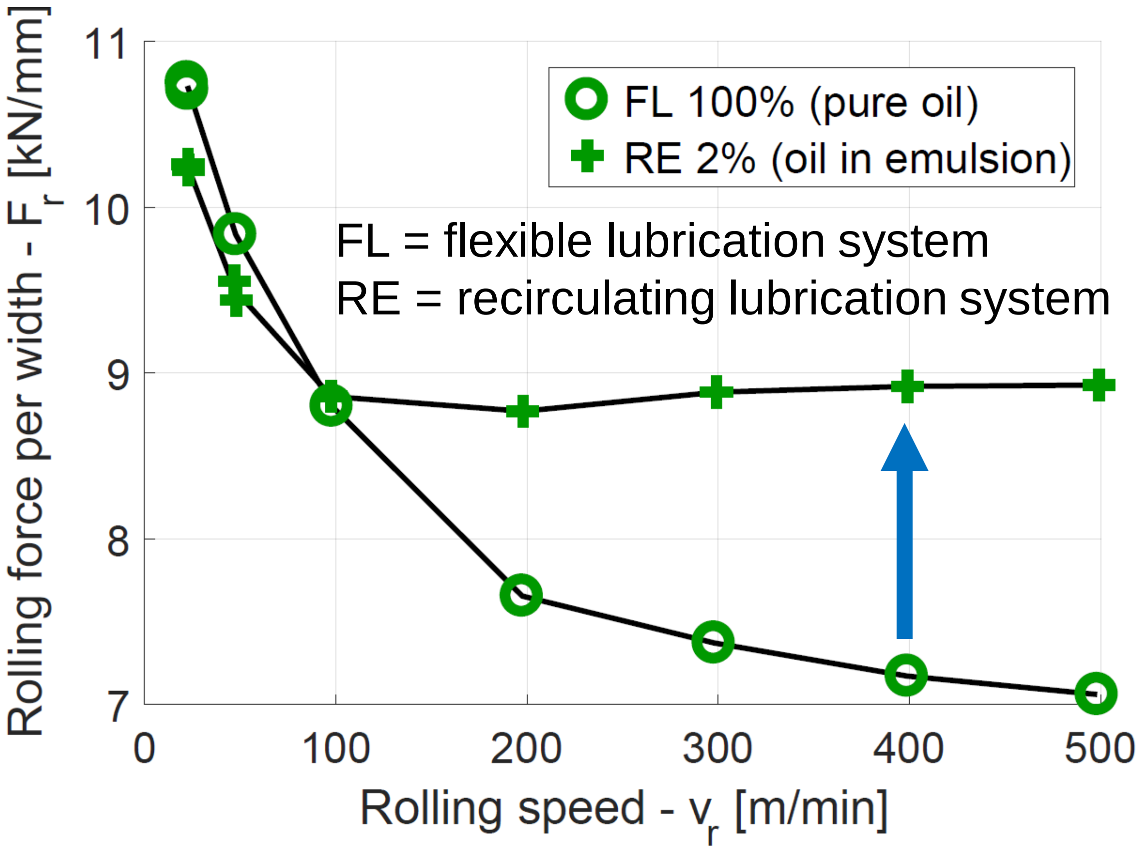

FL = flexible lubrication system
RE = recirculating lubrication system

Condition:

- If less oil is provided to roll bite than it can absorb:

- Otherwise, film thickness in roll bite unchanged:

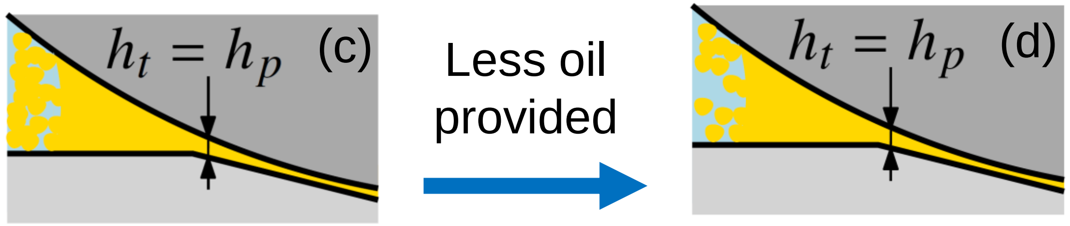

h_p: maximum film thickness in full-flooded lubrication

2.2 Analysis of experimental data – Influence of lubricant quantity

- Starvation (Tests 5B, 4A and 5A)

➔ Friction control by flexible lubrication

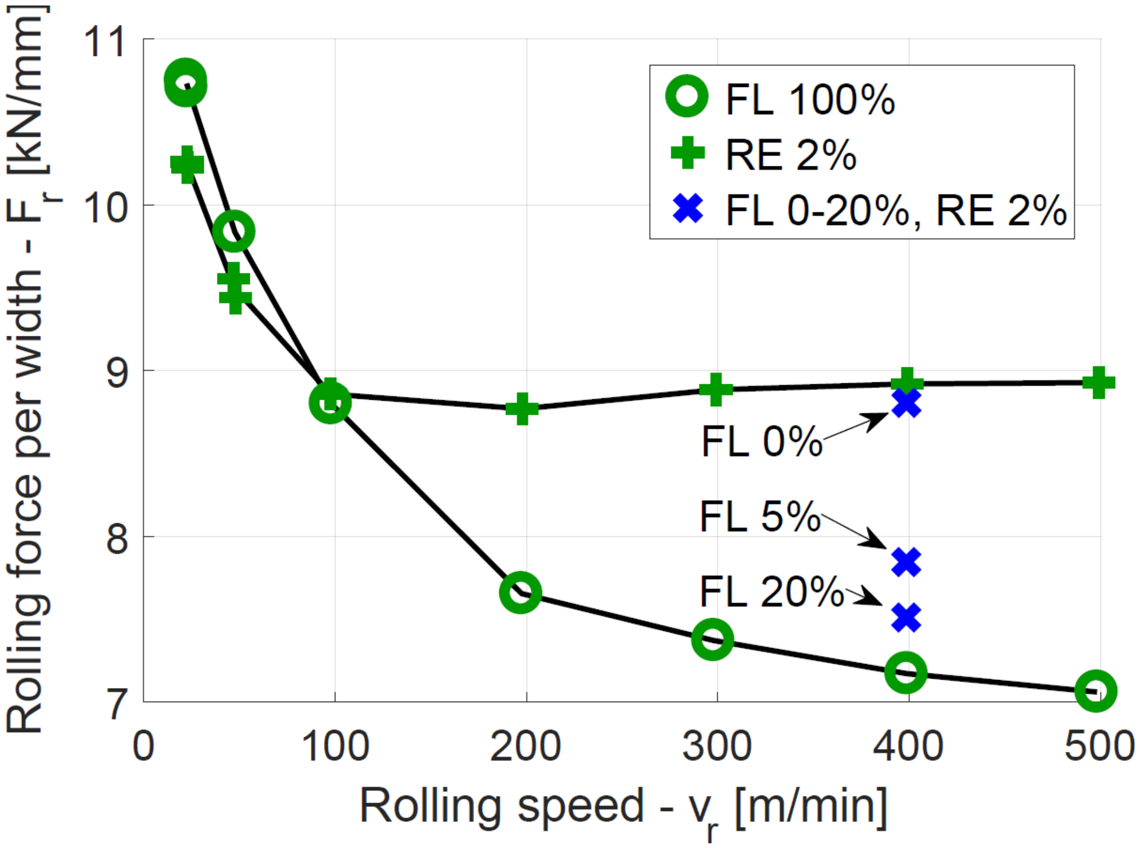

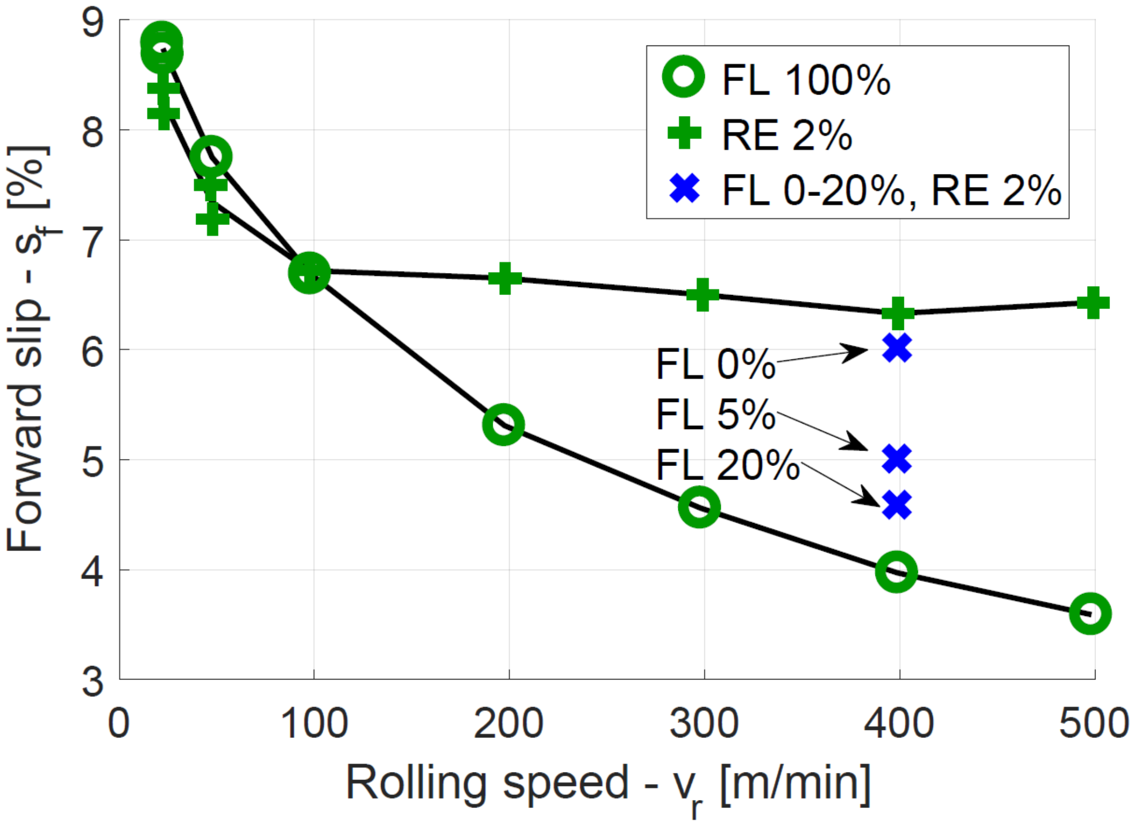

FL = flexible lubrication system; RE = recirculating lubrication system

2.2 Analysis of experimental data – Influence of reduction

- Geometrical effect (Test 8)

$$r \nearrow \quad \rightarrow \quad l_{\mathrm{rb}} \nearrow \quad \rightarrow \quad F_r \nearrow, \quad s_f \nearrow$$

Reduction — Length of roll bite — Rolling force — Forward slip

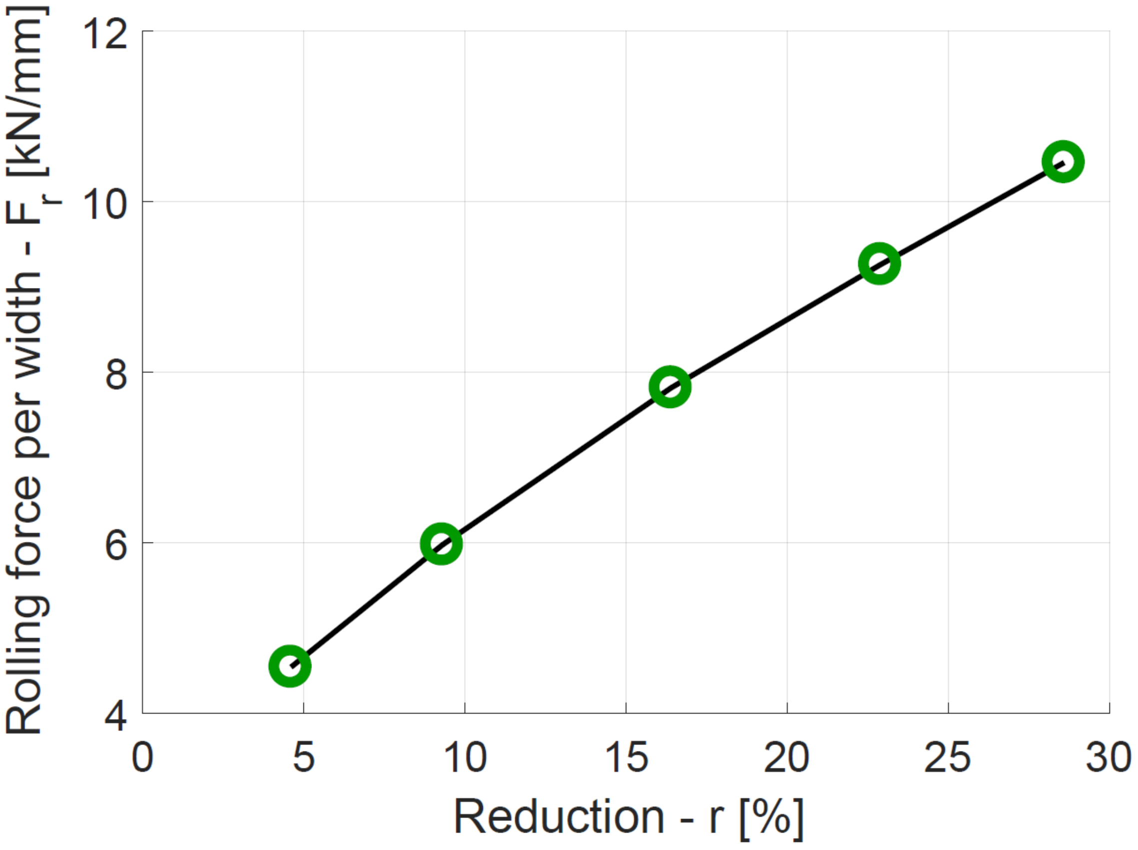

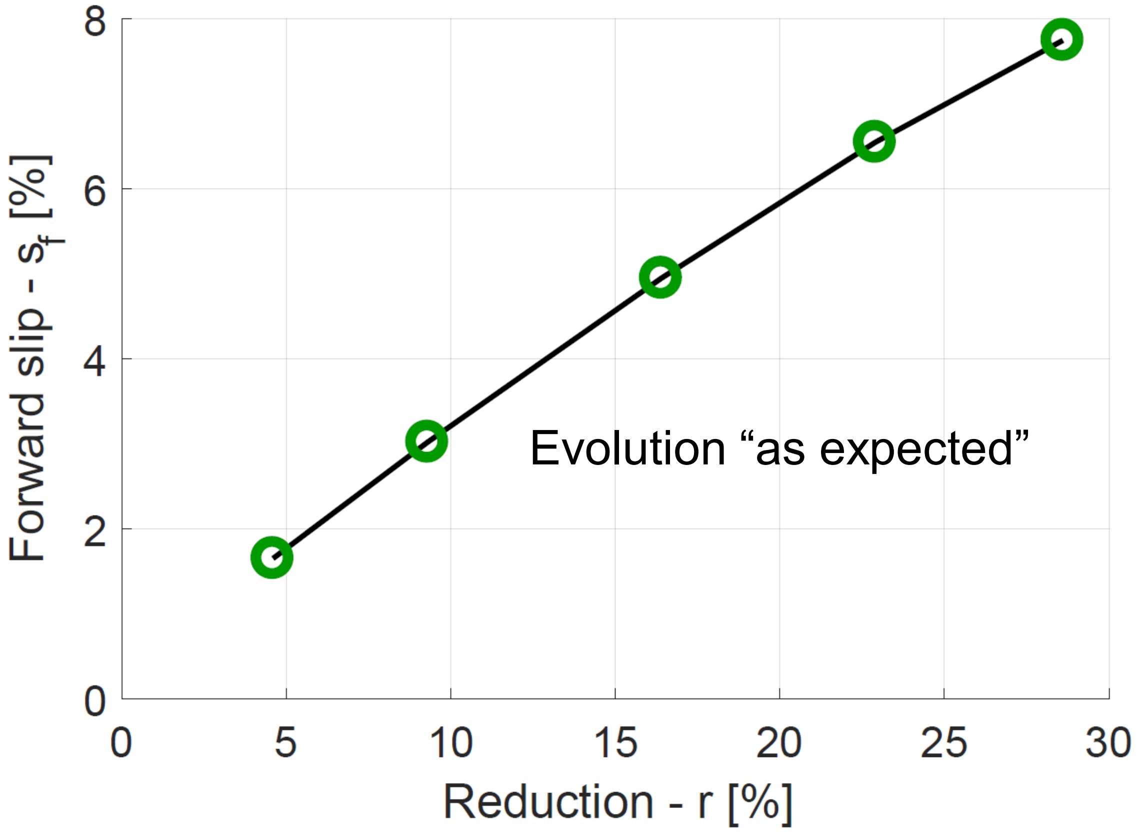

2.2 Analysis of experimental data – Influence of reduction

- Micro-plasto-hydrodynamic/static (MPH) lubrication (Test 7, different rolled product)

$$r \nearrow \quad \rightarrow \quad p_l \nearrow \quad \rightarrow \quad A \searrow \quad \rightarrow \quad \overline{\mu} \searrow \quad \rightarrow \quad F_r \searrow , \quad s_f \searrow$$

$r \nearrow$	$p_l \nearrow$	$A \searrow$	$\overline{\mu} \searrow$	$F_r \searrow$	$s_f \searrow$
Reduction	Lubricant pressure	Relative contact area	Friction	Rolling force	Forward slip

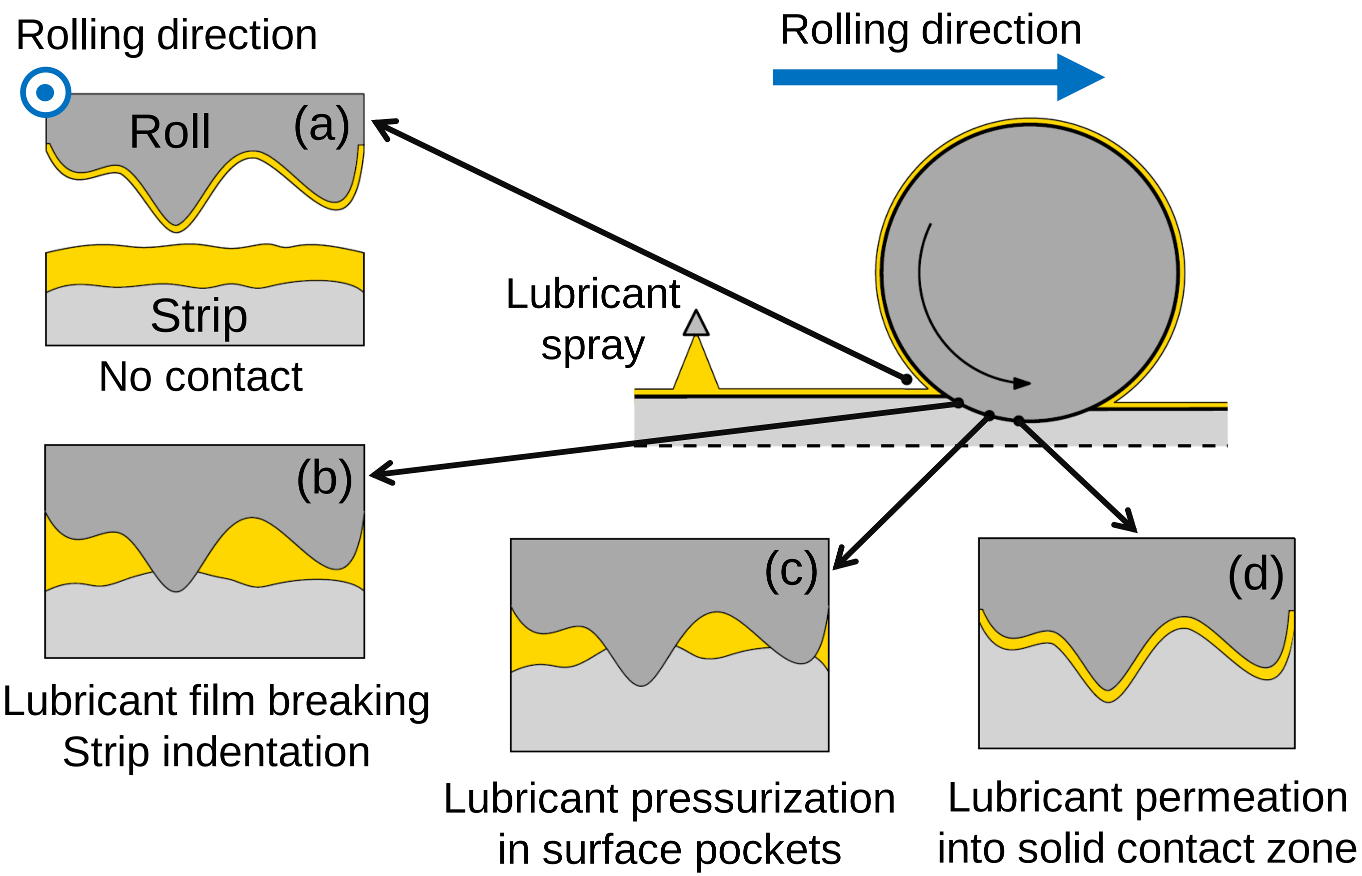

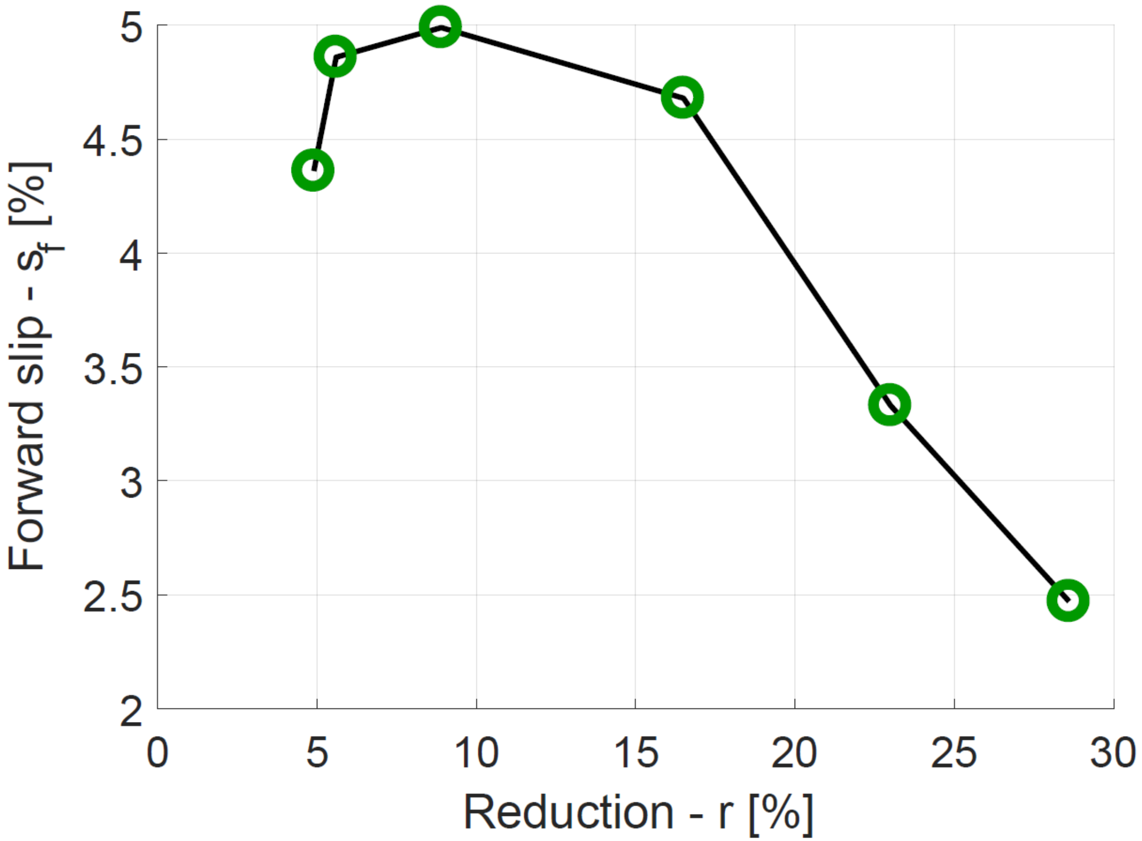

2.3 Intermediate conclusion

- Interacting mechanisms to include in model, mainly:
    - Hydrodynamic effect
    - Starvation
    - Viscous friction
    - Work hardening
    - Viscoplasticity
    - Geometrical effect
    - Asperity flattening
    - MPH lubrication

- Post-processed validation data

Outline

3.1 Objective

- Highly-specialized modeling codes

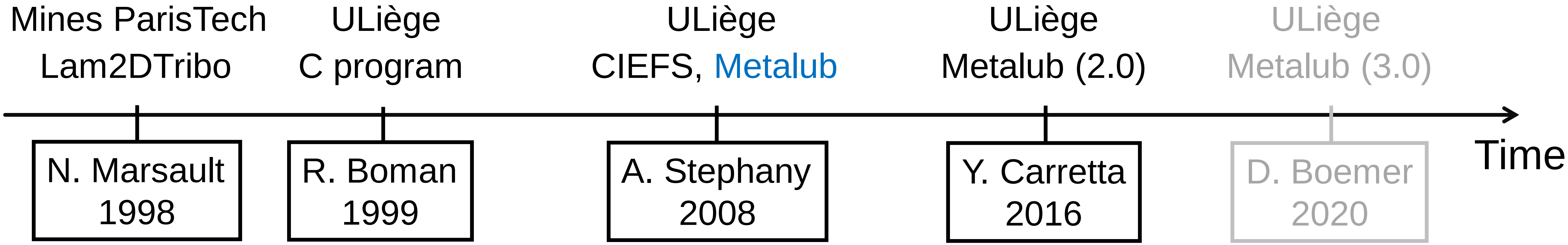

- Shortcomings:
  - Different versions
  - No consistent documentation
  - Some physical mechanisms not yet modeled

- Objective: re-derive, document and extend (in blue in the following slides) the Metalub model

3.2 System of equations

- Mechanics of the strip
  - Slab method: 1D, neglected internal shear stresses

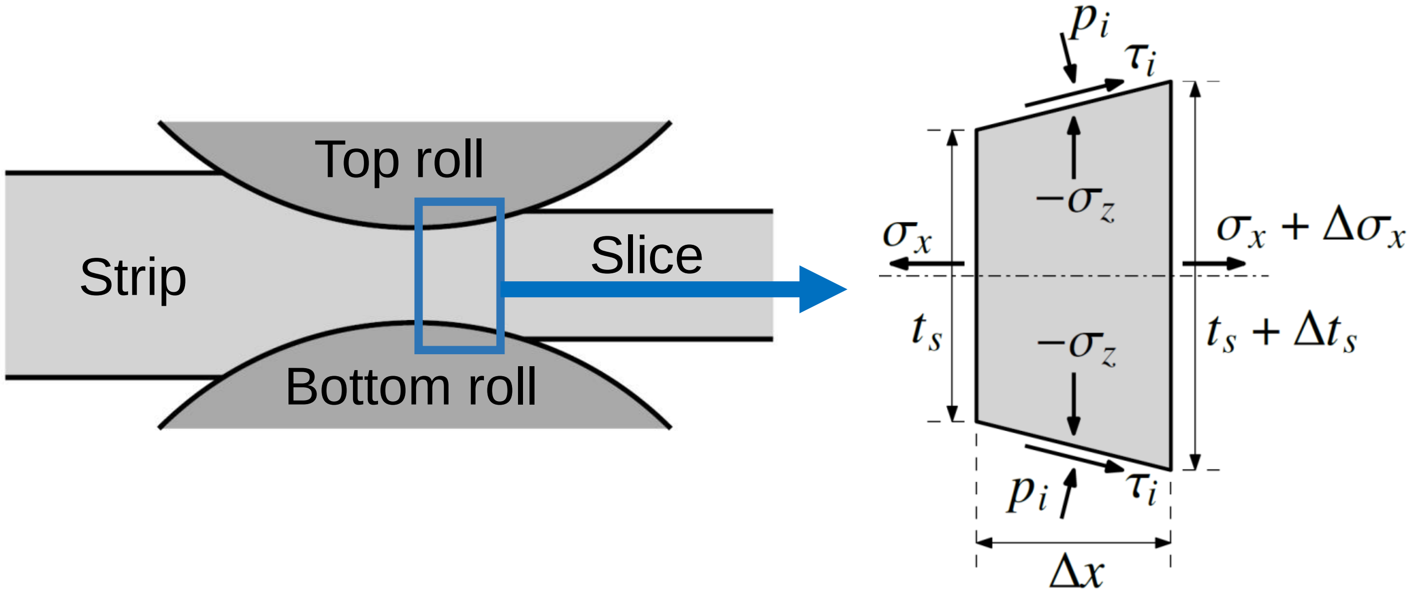

$$\frac{\partial(\sigma_x\, t_s)}{\partial x} = -p_i \frac{\partial t_s}{\partial x} - 2\tau_i$$

$$\sigma_z = -p_i + \frac{1}{2}\tau_i \frac{\partial t_s}{\partial x}$$

  - Material laws
    - Elastoplasticity
    - Viscoplasticity (new)
    - Thermoplasticity (new)

Effective plastic strain rate

Strip temperature

$$\sigma_Y(\overline{\epsilon}^p, \overline{D}^p, T_s) = \left[A + B\left(\overline{\epsilon}^p\right)^n\right]\left(1 + \eta_s \ln \frac{\overline{D}^p}{\overline{D}_0^p}\right)\left[1 - \left(\frac{T_s - T_0}{T_m - T_0}\right)^m\right]$$

Yield stress

Effective plastic strain

[Johnson and Cook, 1983]

3.2 System of equations

- Roll flattening models
  - Rigid: circular or non-circular
  - Adapted radius: Hitchcock (1935), Bland and Ford (1952)
  - Elastic deformation: Jortner et al. (1960); Meindl (2001, new)

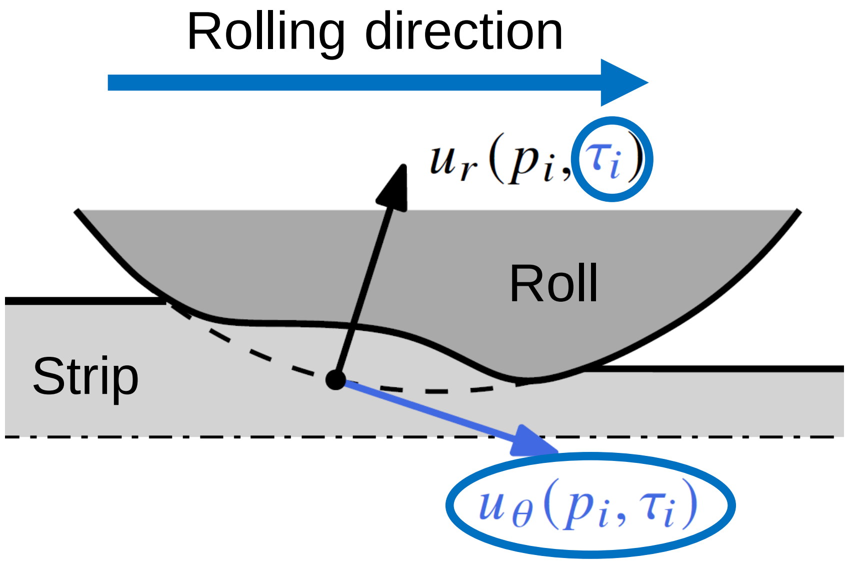

- Geometric contact description

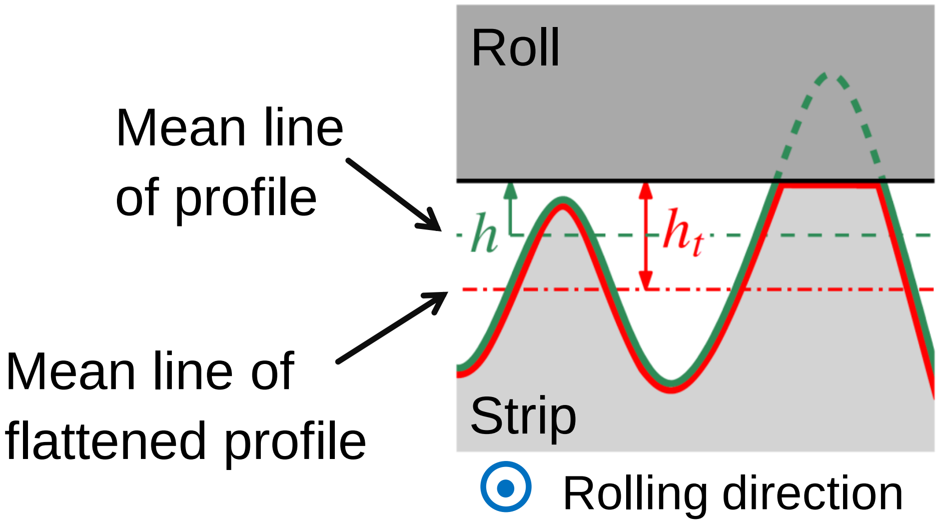

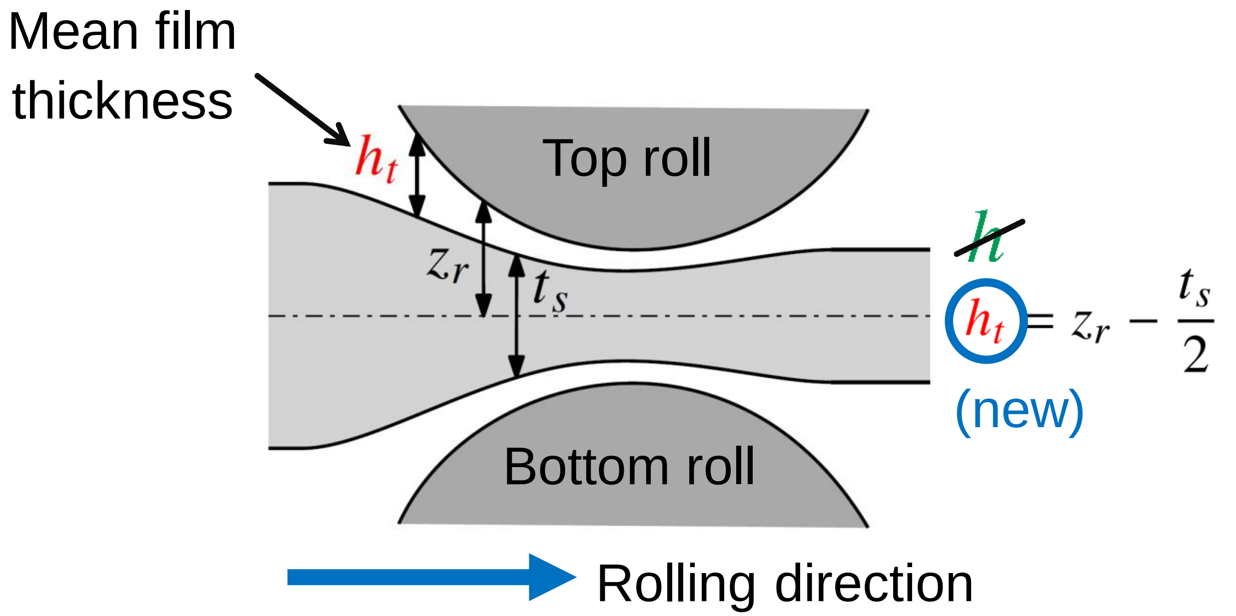

3.2 System of equations

- Asperity flattening models
  - Relation between:
    - Relative contact area A
    - Pressure on top of asperities p_a
    - Lubricant pressure p_l
    - Plastic strain rate of the strip along rolling direction D_x^p
  - Analytical models in Metalub:
    - Wilson and Sheu (1988, by upper bound results)
    - Marsault and Sutcliffe (1998, by slip line results)
    - Sutcliffe (1999) based on Korzekwa et al. (1992, by FE results, new)

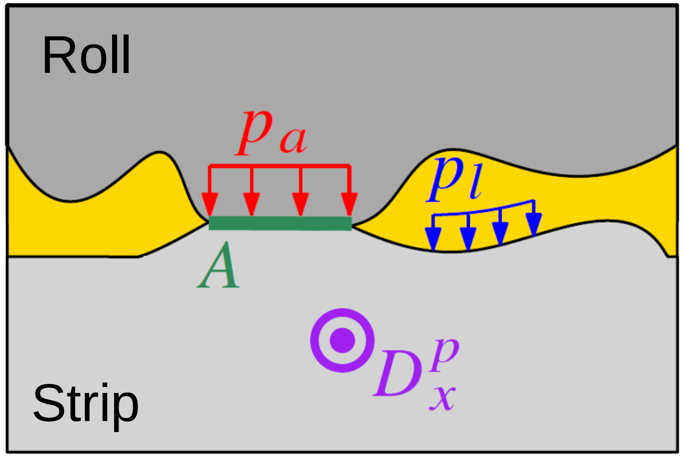

⊙ Rolling direction

3.2 System of equations

- Lubricant flow
  - Average Reynolds equation with flow factors (corrected) to include roughness

$$\frac{\partial p_l}{\partial x} = \frac{12\eta}{\phi_x h_t^3}\left(\frac{v_s + v_r}{2}h_t + \frac{v_s - v_r}{2}R_q\phi_s - Q\right)$$

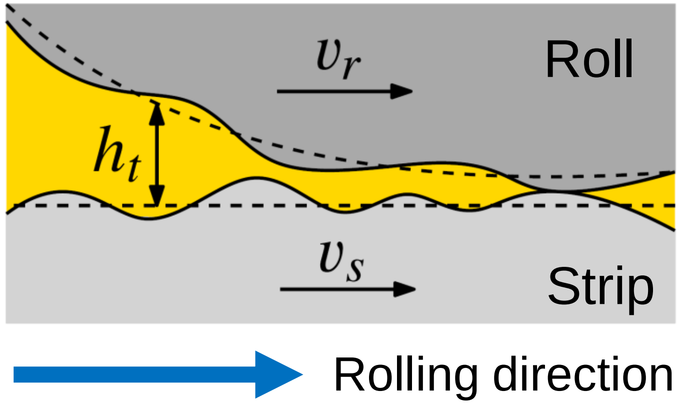

  - Lubricant shear stress (shear stress factors, new)

$$\tau_l = \frac{\eta(v_r - v_s)}{h_v} \quad \text{with} \quad h_v = \frac{h_t}{1 - A}$$

$$\tau_l = \begin{cases} \frac{\eta(v_r - v_s)}{h}(\phi_f - \phi_{fs}) - \phi_{fp}\frac{h}{2}\frac{\partial p_l}{\partial x} & \text{, if } h > 0 \\ \frac{\eta(v_r - v_s)}{h_v} - \frac{h_v}{2}\frac{\partial p_l}{\partial x} & \text{, otherwise.} \end{cases}$$

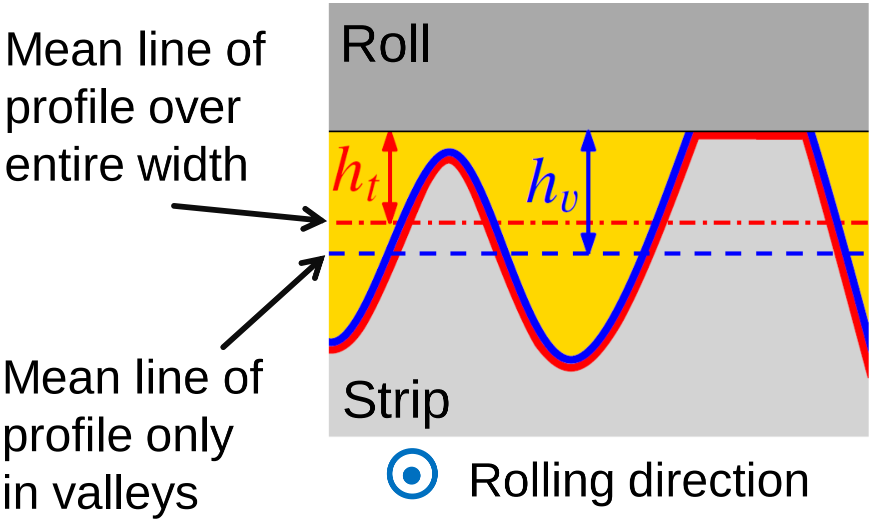
Mean line of profile over entire width

Mean line of profile only in valleys

3.2 System of equations

- Thermal model (new)
  - In the past, coupling with ThermRoll code (Mines ParisTech, Bouache et al., 2009) but abandoned with Stephany's Metalub version
  - Strip temperature T_s : adiabatic heating due to plastic deformation and friction

$$\frac{\partial T_s}{\partial x} = \frac{1}{\rho_s c_s v_s}\left[\overbrace{\beta_s\left(D_x^p \sigma_x + D_z^p \sigma_z\right)} + \overbrace{\frac{\tau_i (v_r - v_s)}{t_s}}\right]$$

Taylor-Quinney coefficient ≈ 0.9

  - Lubricant temperature T_l :
    - Isothermal: $T_l = T_l^0$
    - Strip temperature: $T_l = T_s$ or $T_l = \begin{cases} T_l^0 & \text{, if } T_s < T_l^0 \\ T_s & \text{, otherwise} \end{cases}$
    - Heating due to friction: $\frac{\partial T_l}{\partial x} = \frac{\beta_l}{\rho_l c_l v_s} \frac{\tau_i (v_r - v_s)}{h_t}$ β_l : percentage of friction energy

3.3 Full Metalub model

- Division of roll bite into zones depending on:
    - Contact status
    - Deformation mode (elastic or elastoplastic)
    - High-speed hypothesis: $p_l = p_i$

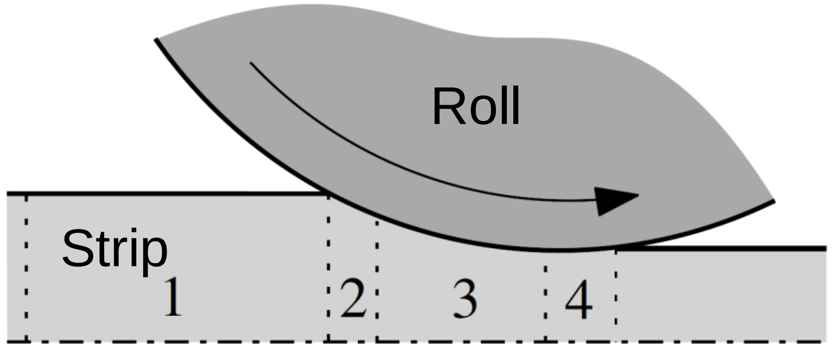

- System of equation for each zone

- Zones:

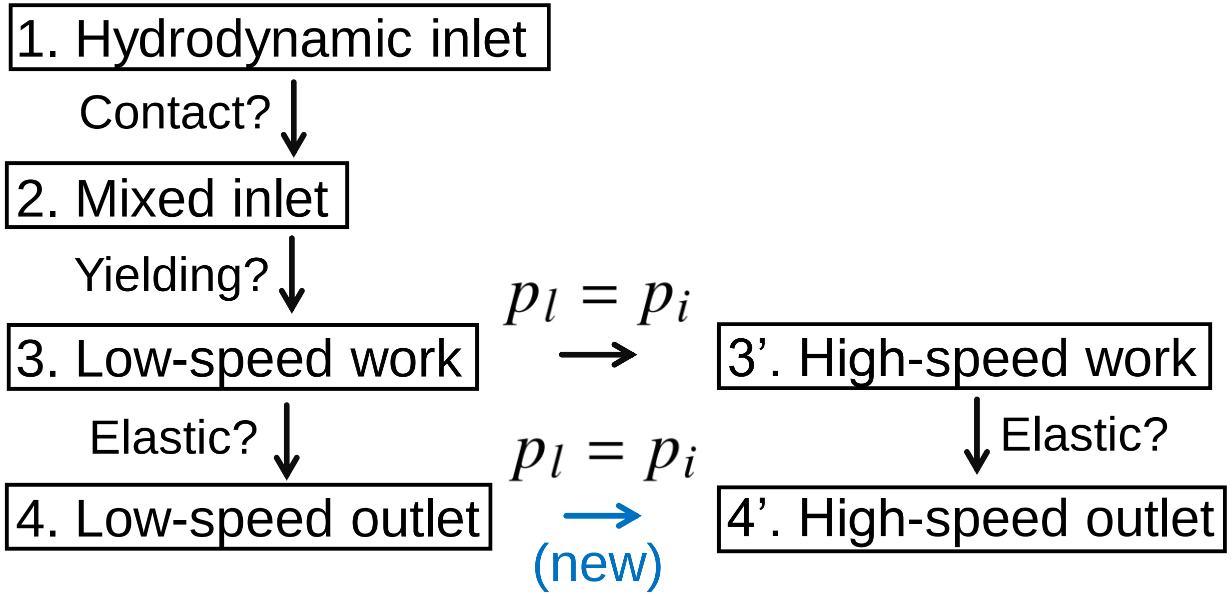

1. Hydrodynamic inlet

Contact? ↓

2. Mixed inlet

Yielding? ↓

3. Low-speed work $\xrightarrow{p_l = p_i}$ 3'. High-speed work

Elastic? ↓ ↓ Elastic?

4. Low-speed outlet $\xrightarrow{p_l = p_i}$ (new) 4'. High-speed outlet

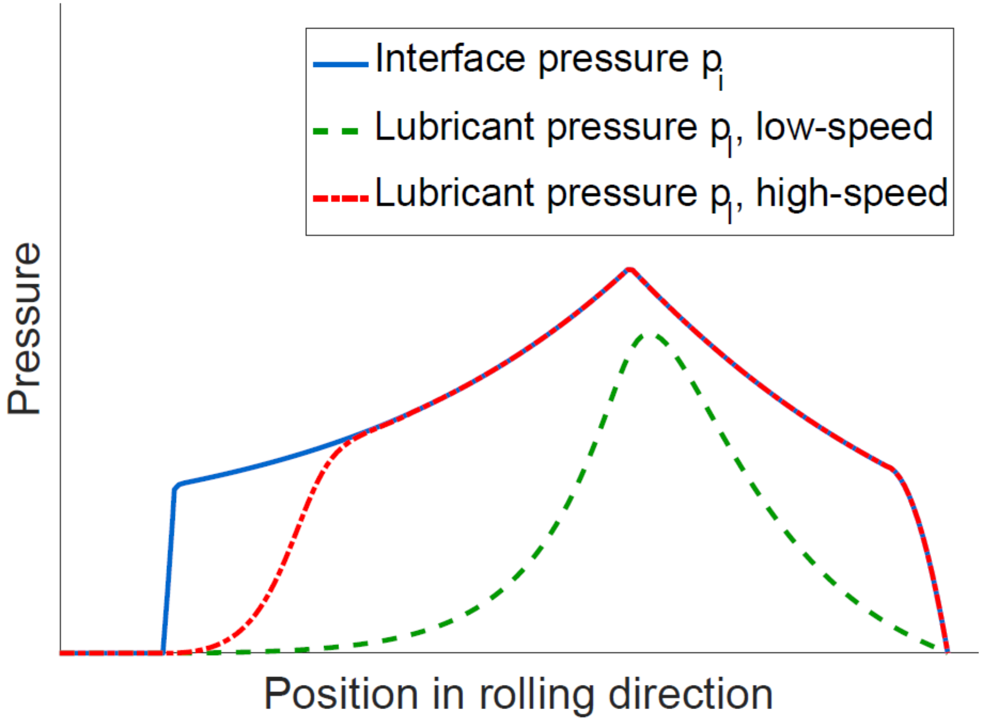

3.3 Full Metalub model

- Illustration: short version of system of equations in low-speed work zone (documentation, unification)

$$
\begin{aligned}
z_r &= z_r(x) \\
h_t &= z_r - \frac{t_s}{2} \\
h_t &\overset{\text{cpl}}{=} h_t(x) \\
h &= h(h_t) \\
A &\overset{\cancel{\text{cpl}}}{=} A(h) \\
A &\overset{\text{cpl}}{=} A(x) \\
\sigma_Y &= \sigma_Y(\overline{\epsilon}^p, \overline{D}^p, T_s) \\
\tau_Y &= \frac{\sigma_Y}{\sqrt{3}} \\
H_a &\overset{\cancel{\text{cpl}}}{=} \frac{p_a - p_l}{\tau_Y} \text{ or } \frac{p_a}{\tau_Y} \\
E_p &\overset{\cancel{\text{cpl}}}{=} E_p(A, H_a) \\
p_i &= A p_a + (1 - A) p_l \text{ or } A p_a \\
\tau_a &= \tau_a(v_s, v_r, p_a, \tau_Y) \\
T_l &= T_l(T_l^*, T_s, T_l) \text{ or } / \\
\eta &= \eta(p_l, T_l) \text{ or } / \\
\tau_l &= \tau_l\left(h, h_t, A, \eta, v_s, v_r, \frac{\partial p_l}{\partial x}\right) \text{ or } 0
\end{aligned}
$$

Without coupling?

With coupling?

$$
\begin{aligned}
\tau_i &= A\tau_a + (1 - A)\tau_l \text{ or } A\tau_a \\
\phi_x &= \phi_x(h_t) \text{ or } / \\
\phi_s &= \phi_s(h_t) \text{ or } / \\
\frac{\partial p_l}{\partial x} &= \frac{12\eta}{\phi_x h_t^3}\left(\frac{v_s + v_r}{2} h_t + \frac{v_s - v_r}{2} R_q \phi_s - Q\right) \text{ or } 0 \\
\frac{\partial(\sigma_x t_s)}{\partial x} &= -p_i \frac{\partial t_s}{\partial x} - 2\tau_i \\
\sigma_z &= -p_i \\
\epsilon_x^e &= \frac{1}{E_s}\left[\sigma_x - \nu_s(\sigma_y + \sigma_z)\right] \\
\sigma_y &= \nu_s(\sigma_x + \sigma_z) \\
\epsilon_z^e &= \frac{1}{E_s}\left[\sigma_z - \nu_s(\sigma_x + \sigma_y)\right] \\
h_{i,s} &= h_{i,s}(\overline{\epsilon}^p, \overline{D}^p, T_s) \\
\beta_1 &= \frac{1}{\frac{2}{3}\sigma_Y^2\left(1 + \frac{h_{i,s}}{3G_s}\right)}
\end{aligned}
$$

With lubricant?

Without lubricant?

$$
\begin{aligned}
\dot{s}_x &= \frac{2G_s}{3}\left[\left(2 - 3\beta_1 s_x^2\right) D_x - (1 + 3\beta_1 s_x s_z) D_z\right] \\
\dot{s}_z &= \frac{2G_s}{3}\left[-(1 + 3\beta_1 s_x s_z) D_x + \left(2 - 3\beta_1 s_z^2\right) D_z\right] \\
\dot{s}_x &= v_s \frac{\partial s_x}{\partial x} \\
\dot{s}_z &= v_s \frac{\partial s_z}{\partial x} \\
0 &= s_x + s_y + s_z \\
D_x &= \frac{\partial v_s}{\partial x} \\
D_z &= \frac{v_s}{t_s}\frac{\partial t_s}{\partial x} \\
\dot{p} &= -K_s(D_x + D_z) \\
\dot{p} &= v_s \frac{\partial p}{\partial x} \\
D_x^e &= v_s \frac{\partial \epsilon_x^e}{\partial x}
\end{aligned}
$$

$$
\begin{aligned}
D_z^e &= v_s \frac{\partial \epsilon_z^e}{\partial x} \\
0 &= D_x^p + D_y^p + D_z^p \\
D_y^p &= 0 \\
D_z &= D_z^e + D_z^p \\
\frac{\partial h}{\partial x} &= \frac{-D_x^p \bar{l}}{v_s E_p} \\
\overline{D}^p &= v_s \frac{\partial \overline{\epsilon}^p}{\partial x} \\
\overline{D}^p &= \sqrt{\frac{2}{3}\left[(D_x - D_x^e)^2 + (D_z - D_z^e)^2\right]} \\
s_x &= \sigma_x + p \\
s_z &= \sigma_z + p \\
s_y &= \sigma_y + p \\
\frac{\partial T_s}{\partial x} &= \frac{1}{\rho_s c_s v_s}\left[\beta_s\left(D_x^p \sigma_x + D_z^p \sigma_z\right) + \frac{\tau_i(v_r - v_s)}{t_s}\right] \\
\frac{\partial T_l}{\partial x} &= \frac{\beta_l}{\rho_l c_l v_s}\frac{\tau_i(v_r - v_s)}{h_t}
\end{aligned}
$$

3.3 Full Metalub model

- General Metalub algorithm
    - Based on 4 nested adjustment loops
    - Convergence not straightforward
    - Improvements of robustness
        - Removal of unnecessary criteria
        - Initial conditions closer to solution

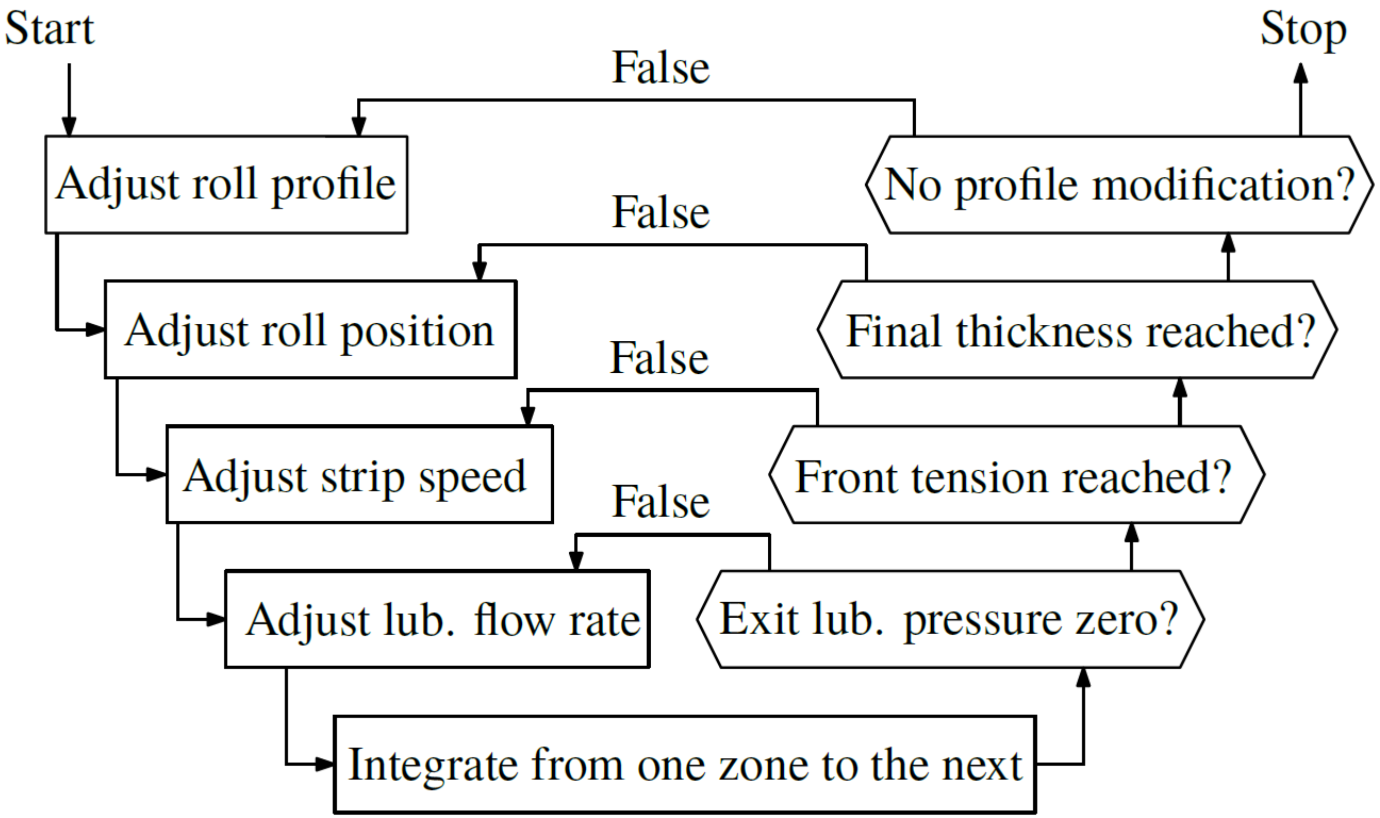

3.4 Metalub implementation

- Implemented in C++ with Python interface and Graphical User Interface in PyQt

  ➔ Completely refactored (21k lines in 169 core C++ files with ~200 regression tests)

  ➔ Improved robustness and coding style in a spirit of continuity

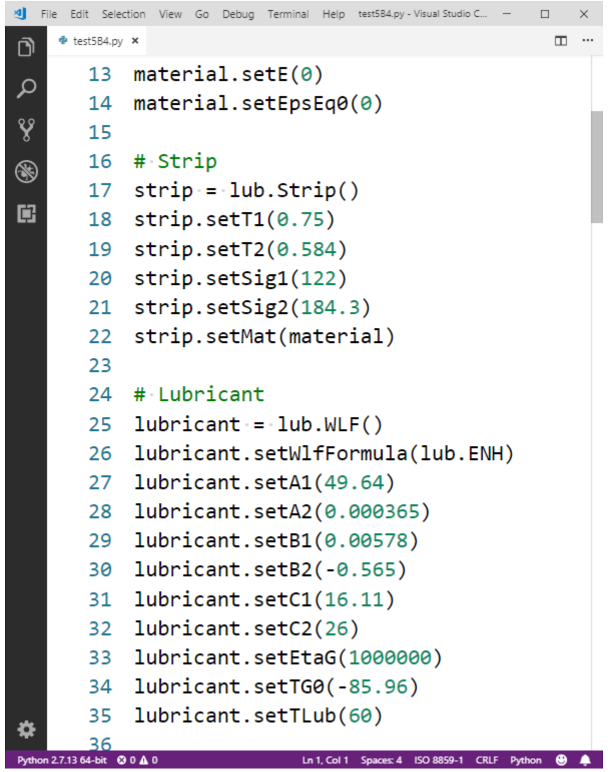

```python
material.setE(0)
material.setEpsEq0(0)

# Strip
strip = lub.Strip()
strip.setT1(0.75)
strip.setT2(0.584)
strip.setSig1(122)
strip.setSig2(184.3)
strip.setMat(material)

# Lubricant
lubricant = lub.WLF()
lubricant.setWlfFormula(lub.ENH)
lubricant.setA1(49.64)
lubricant.setA2(0.000365)
lubricant.setB1(0.00578)
lubricant.setB2(-0.565)
lubricant.setC1(16.11)
lubricant.setC2(26)
lubricant.setEtaG(1000000)
lubricant.setTG0(-85.96)
lubricant.setTLub(60)
```

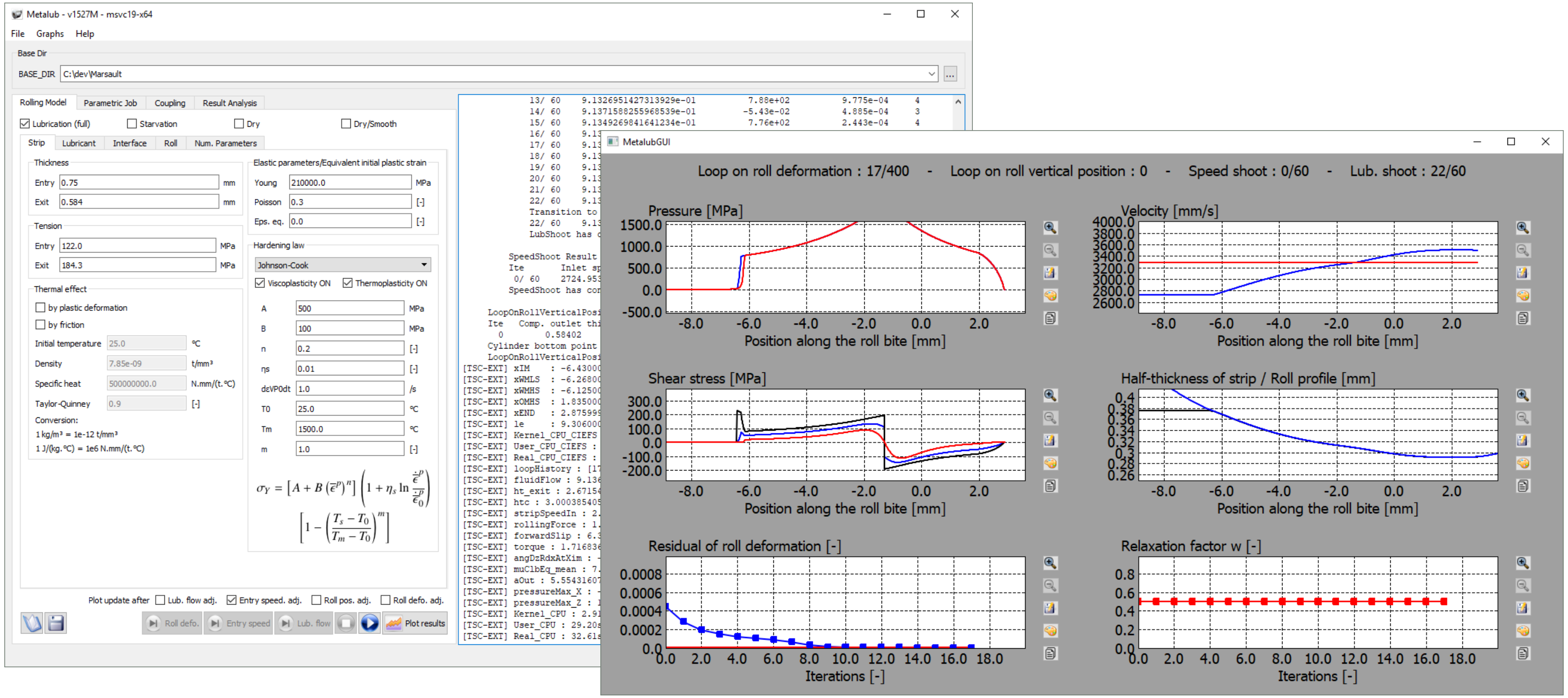

BASE_DIR: C:\dev\Marsault

☑ Lubrication (full) ☐ Starvation ☐ Dry ☐ Dry/Smooth

Thickness
Entry: 0.75 mm
Exit: 0.584 mm

Tension
Entry: 122.0 MPa
Exit: 184.3 MPa

Thermal effect
☐ by plastic deformation
☐ by friction
Initial temperature: 25.0 °C
Density: 7.85e-09 t/mm³
Specific heat: 500000000.0 N.mm/(t.°C)
Taylor-Quinney: 0.9 [-]
Conversion:
1 kg/m³ = 1e-12 t/mm³
1 J/(kg.°C) = 1e6 N.mm/(t.°C)

Elastic parameters/Equivalent initial plastic strain
Young: 210000.0 MPa
Poisson: 0.3 [-]
Eps. eq.: 0.0 [-]

Hardening law: Johnson-Cook
☑ Viscoplasticity ON ☑ Thermoplasticity ON
A: 500 MPa
B: 100 MPa
n: 0.2 [-]
ηs: 0.01 [-]
dεVP0dt: 1.0 /s
T0: 25.0 °C
Tm: 1500.0 °C
m: 1.0 [-]

$$\sigma_Y = \left[A + B\left(\bar{\epsilon}^p\right)^n\right]\left(1 + \eta_s \ln \frac{\dot{\bar{\epsilon}}^p}{\dot{\bar{\epsilon}}_0^p}\right) \left[1 - \left(\frac{T_s - T_0}{T_m - T_0}\right)^m\right]$$

Plot update after ☐ Lub. flow adj. ☑ Entry speed. adj. ☐ Roll pos. adj. ☐ Roll defo. adj.

```
        13/ 60    9.1326951427313929e-01          7.88e+02          9.775e-04     4
        14/ 60    9.1371588255968539e-01         -5.43e-02          4.885e-04     3
        15/ 60    9.1349269841641234e-01          7.76e+02          2.443e-04     4
        16/ 60    9.13
        17/ 60    9.13
        18/ 60    9.13
        19/ 60    9.13
        20/ 60    9.13
        21/ 60    9.13
        22/ 60    9.13
        Transition to
        22/ 60    9.13
        LubShoot has c

    SpeedShoot Result
    Ite       Inlet sp
     0/ 60    2724.953
    SpeedShoot has con

  LoopOnRollVerticalPosi
  Ite   Comp. outlet thi
    0        0.58402
  Cylinder bottom point
  LoopOnRollVerticalPosi
[TSC-EXT] xIM    : -6.43000
[TSC-EXT] xWMLS  : -6.26800
[TSC-EXT] xWMHS  : -6.12500
[TSC-EXT] xOMHS  : 1.835000
[TSC-EXT] xEND   : 2.875999
[TSC-EXT] le     : 9.306000
[TSC-EXT] Kernel_CPU_CIEFS
[TSC-EXT] User_CPU_CIEFS :
[TSC-EXT] Real_CPU_CIEFS :
[TSC-EXT] loopHistory : [17
[TSC-EXT] fluidFlow : 9.136
[TSC-EXT] ht_exit : 2.67154
[TSC-EXT] htc : 3.000385405
[TSC-EXT] stripSpeedIn : 2.
[TSC-EXT] rollingForce : 1.
[TSC-EXT] forwardSlip : 6.3
[TSC-EXT] torque : 1.716836
[TSC-EXT] angDzRdxAtXim : -
[TSC-EXT] muClbEq_mean : 7.
[TSC-EXT] aOut : 5.55431607
[TSC-EXT] pressureMax_X : -
[TSC-EXT] pressureMax_Z : 1
[TSC-EXT] Kernel_CPU : 2.91
[TSC-EXT] User_CPU : 29.20s
[TSC-EXT] Real_CPU : 32.61s
```

Loop on roll deformation : 17/400 - Loop on roll vertical position : 0 - Speed shoot : 0/60 - Lub. shoot : 22/60

Outline

4.1 Numerical parameter calibration

- Objective: evaluate predictive capabilities and shortcomings of the Metalub model

- First systematic calibration of numerical parameters
  - In the past: numerous parameters, calibration by trial and error
  - Now: less parameters, systematic choice

➔ numerical error estimation, reduced computation time, prevention of non-convergence

$$\boxed{\begin{cases} x_{12} \\ \Delta x_1 \\ \Delta x_2 \end{cases} \Rightarrow \mathrm{tol}_Q} \Rightarrow \mathrm{tol}_{\sigma_\mathrm{out}} \Rightarrow \begin{cases} \mathrm{tol}_{t_\mathrm{out}} \\ x_{12} \\ x_{23} \\ \Delta\theta_1 \\ \Delta\theta_2 \\ \Delta\theta_3 \\ w^{(0)} \end{cases} \Rightarrow \begin{cases} \mathrm{tol}_R \\ \Delta x_{\mathrm{extr},1} \\ \Delta x_{\mathrm{extr},2} \end{cases} \Rightarrow \begin{cases} \mathrm{tol}_{\overline{F}_r} \\ \mathrm{tol}_{s_f} \end{cases}$$

Integration steps

Front tension tolerance

Numerical parameters of the adjustment loop, layer by layer

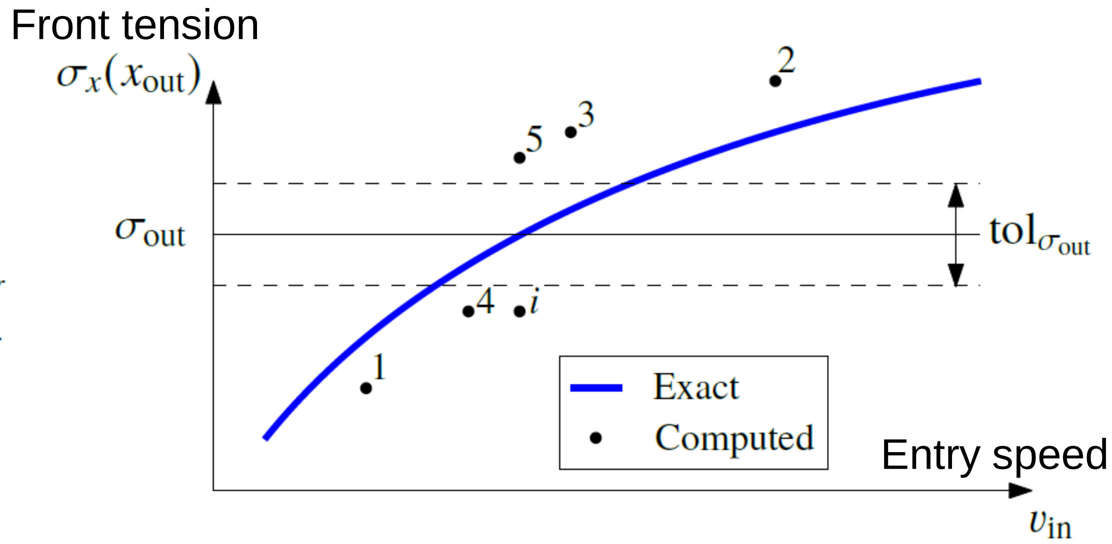

Non-convergence, if tolerances of inner loops not strict enough

4.2 Physical parameter calibration

- Hydrodynamic effect (Test 5B, pure oil)
  - Overall improvement of old predictions, especially the forward slip
  - Hypotheses (of new predictions):
    - Adjustment: boundary coefficient of friction, thermoplasticity coefficient (instead of yield stress)
    - Constant lubricant temperature at roll bite entry
    - Neglected lubricant shear stress in roll bite

} Shortcoming: missing prediction of lubricant temperature

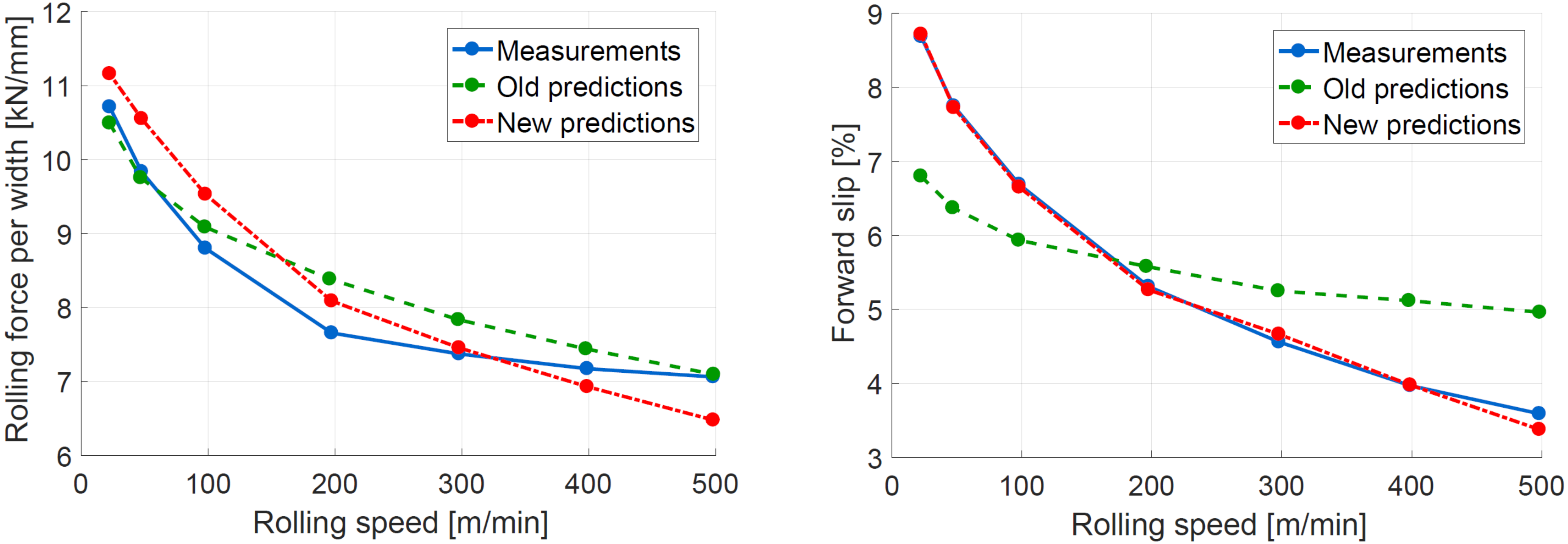

4.2 Physical parameter calibration

- Starvation (Test 4A, 2% oil emulsion)
    - Overall improvement of old predictions
    - Hypotheses (of new predictions):
        - The same as previously
        - Manually adjusted lubricant film thickness $h_{t,\mathrm{in}}$ at entry of roll bite

➔ Shortcoming: missing prediction of this entry film thickness

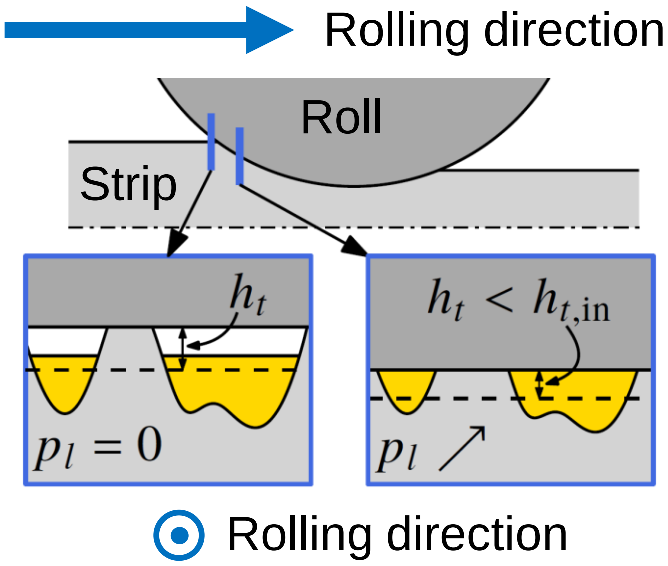

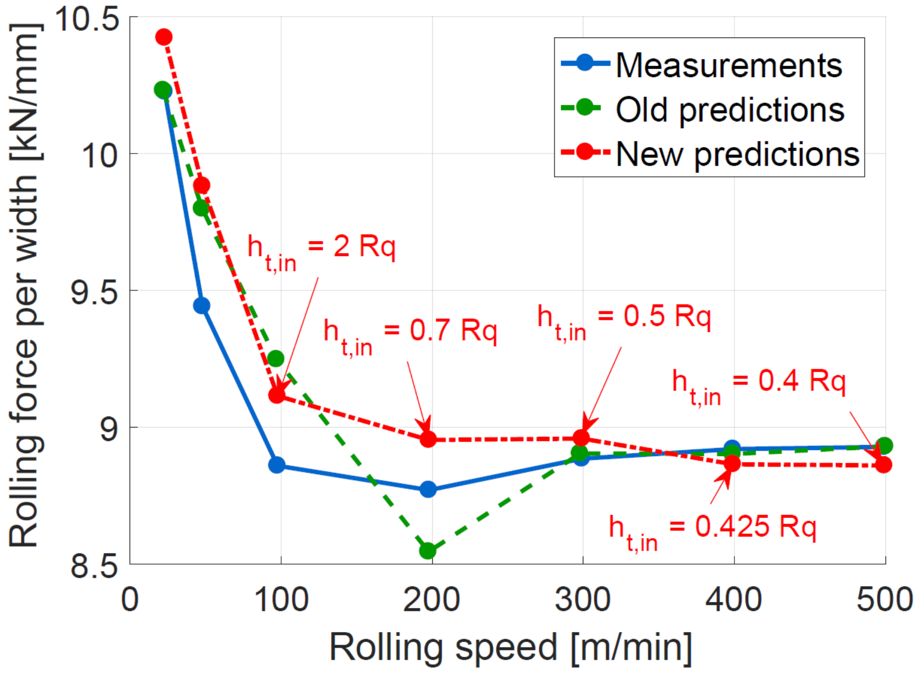

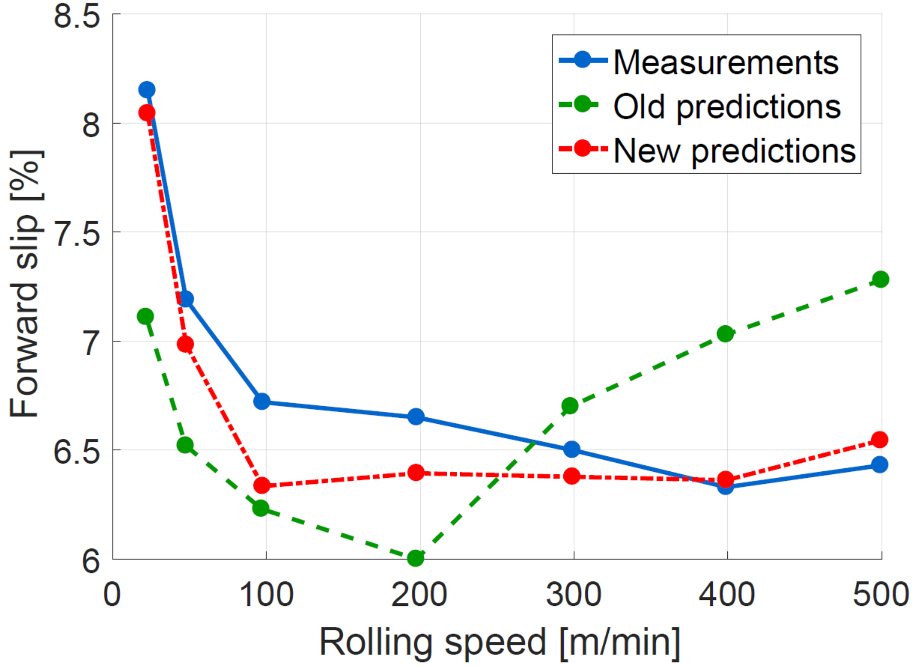

Rq = Composite root-mean-square roughness of roll and strip

4.2 Physical parameter calibration

- Viscoplasticity (Test 6, pure oil, different rolled product)
  - Significant improvement of old predictions obtained by wrong starvation hypothesis
  - Hypotheses (of new predictions):
    - The same as previously (but no starvation)
    - Adjusted viscoplasticity coefficient (the same for all rolling speeds)

      ➔ Shortcoming: viscoplasticity coefficient not identified by experimental testing

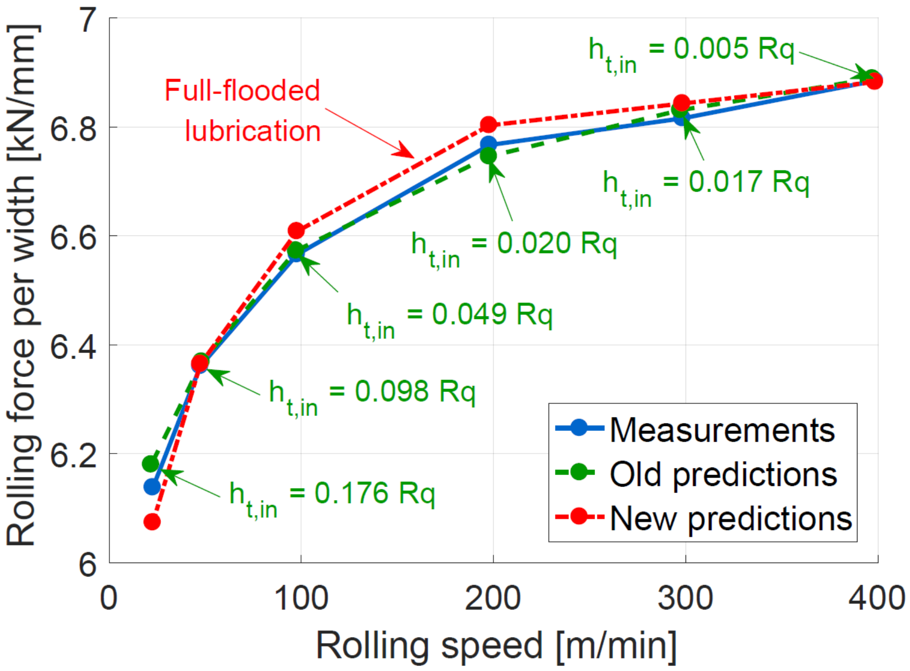

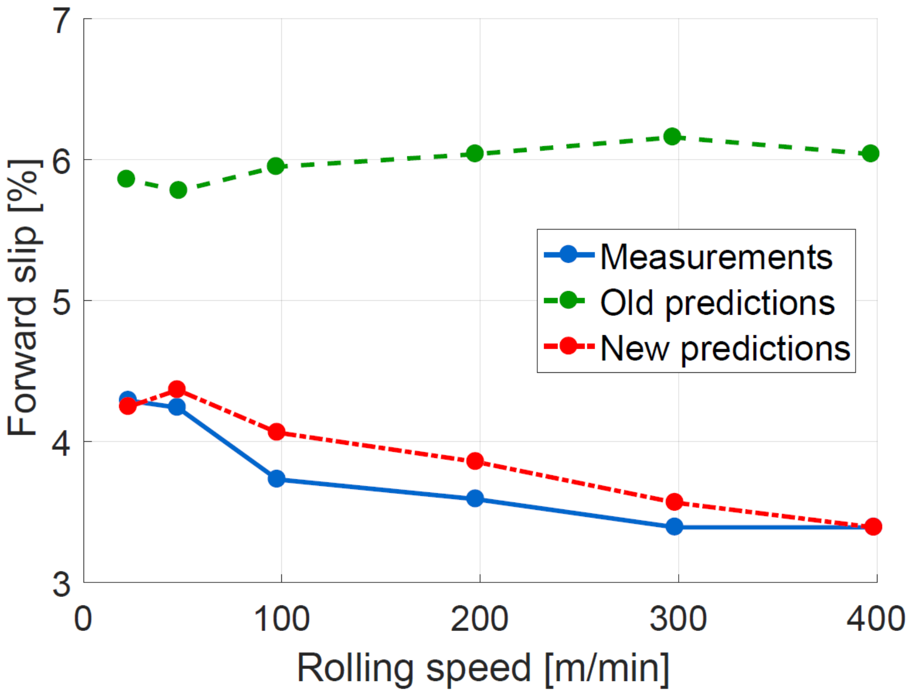

4.2 Physical parameter calibration

- Influence of thickness reduction (Test 8)
  - Overall good prediction (no old prediction available)
  - Improvement by decreasing the boundary coefficient of friction μ_C with reduction
    - ➔ Suggests micro-plasto-hydrodynamic/static lubrication

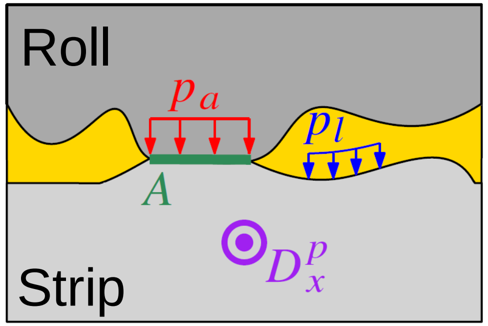

⦿ Rolling direction

$$\tau_a = \mu_C p_a$$

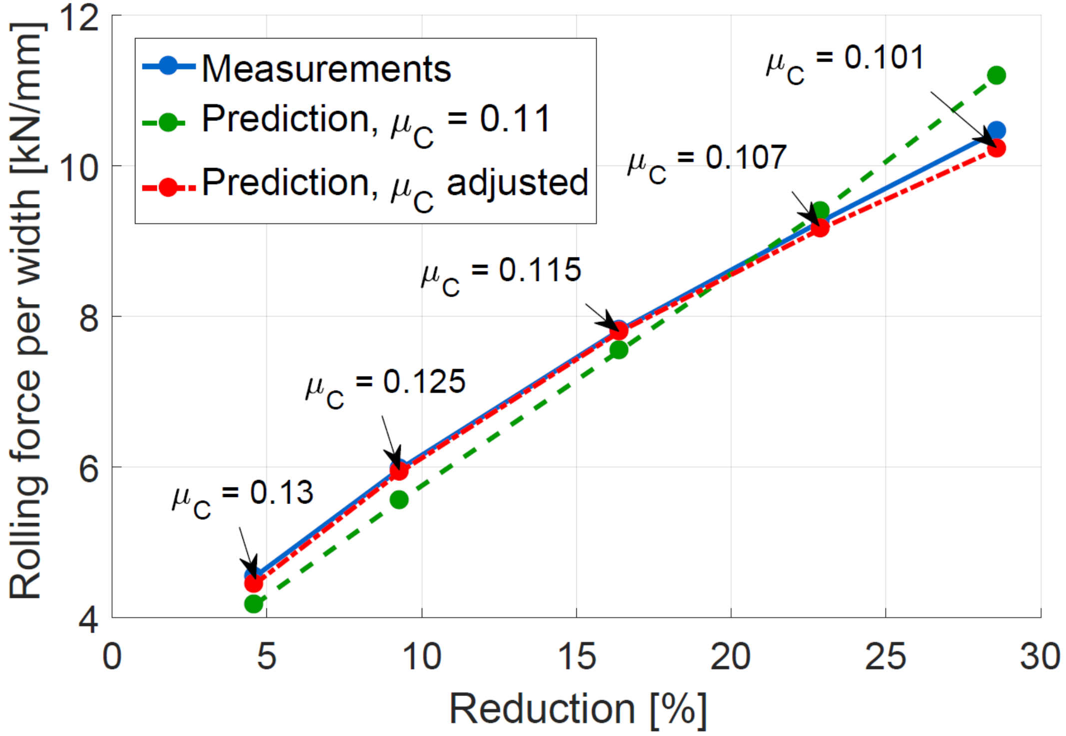

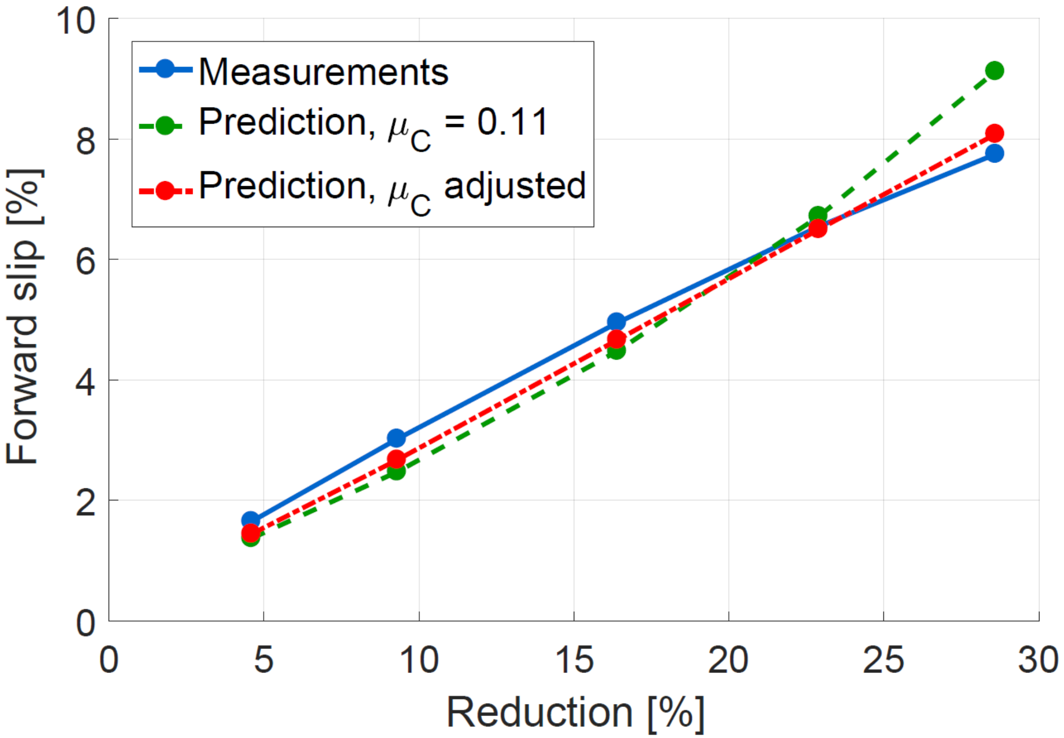

4.2 Physical parameter calibration

- Micro-plasto-hydrodynamic/static (MPH) lubrication (Test 7)
  - More significant influence of this mechanism
    - ➔ Shortcoming: missing prediction of MPH lubrication
    - ➔ Clear need for modeling MPH lubrication

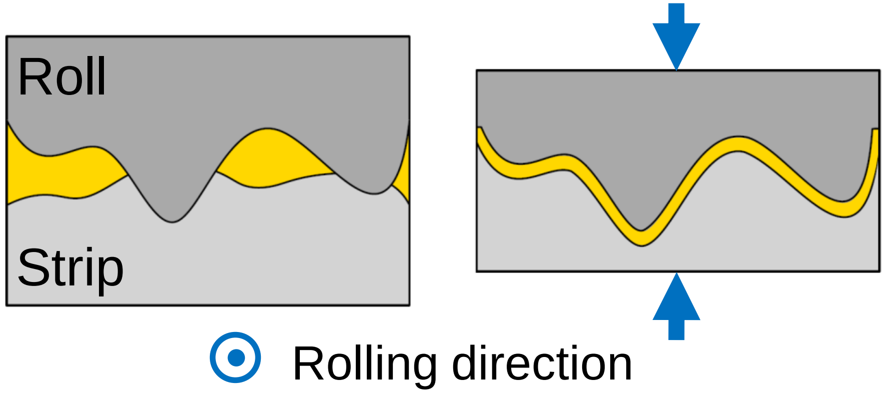

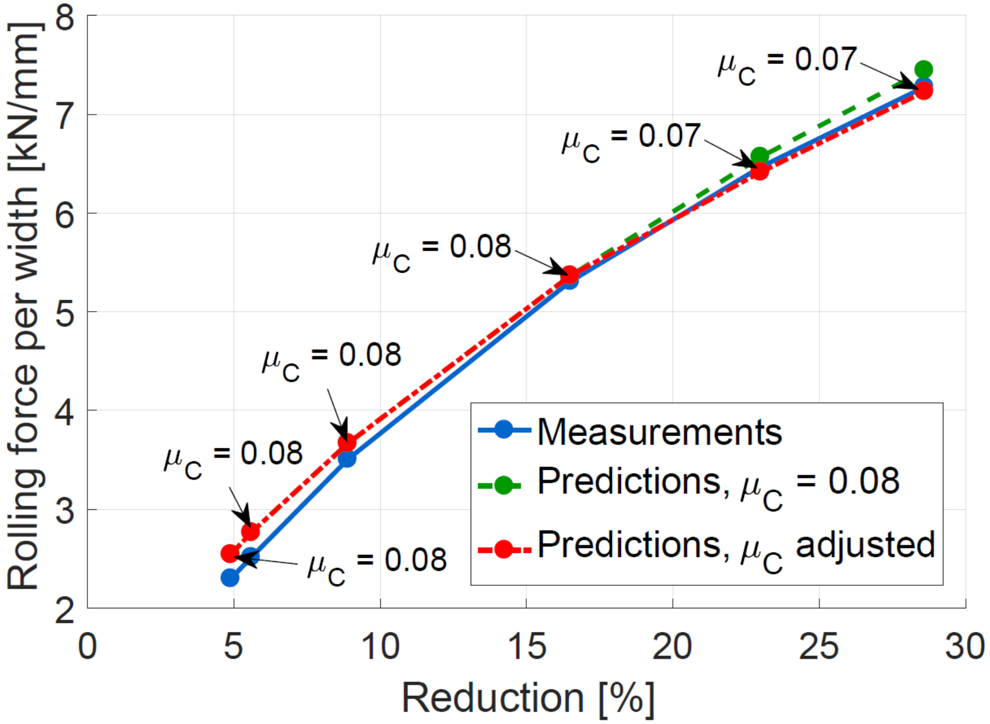

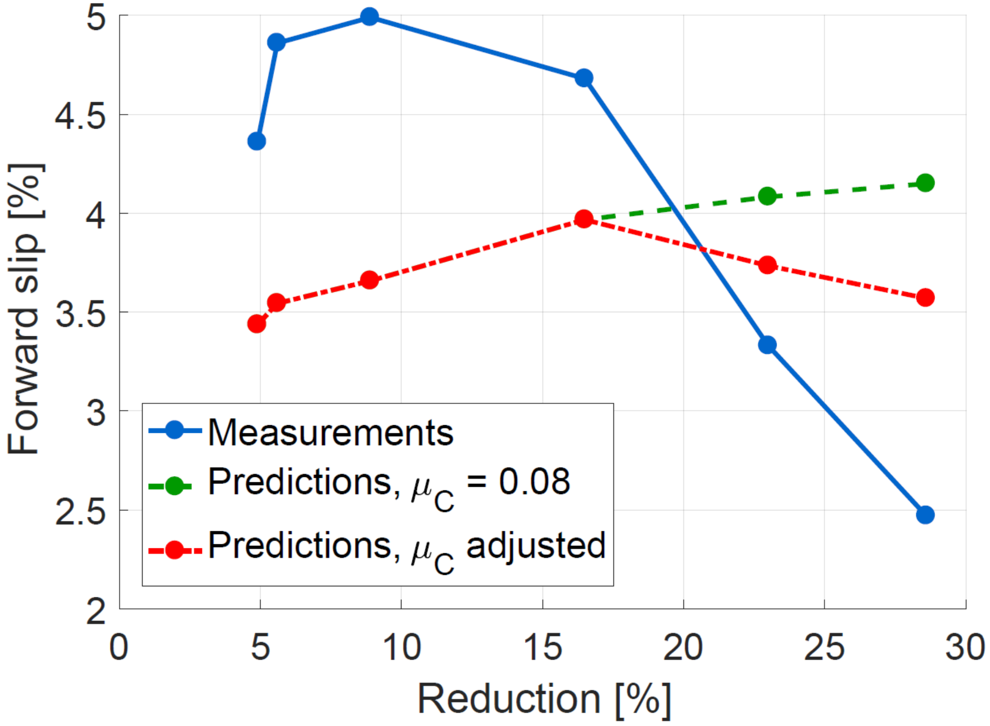

Outline

5.1 Asperity flattening

- Conventionally, the relative contact area A is computed by analytical equations, like Wilson and Sheu:

$$E_p = \frac{1}{0.515 + 0.345A - 0.860A^2}\left(\frac{2}{H_a} - \frac{1}{2.571 - A - A\ln(1-A)}\right)$$

$$\text{with} \begin{cases} E_p = \text{ non-dimensional form of } D_x^p \\ H_a = \text{ non-dimensional form of } (p_a - p_l) \end{cases}$$

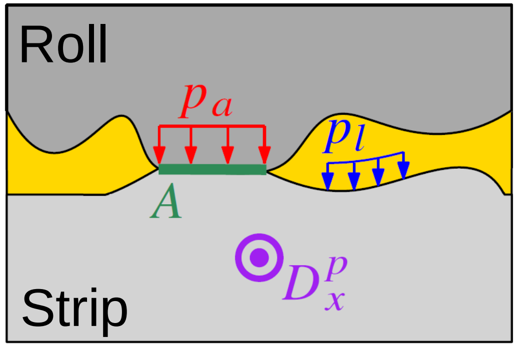

Rolling direction

- Limitations:
  - Simplified geometry: flat indenters
  - Simplified material law: rigid perfectly plastic
  - Approximate method: upper-bound method
  - No MPH lubrication

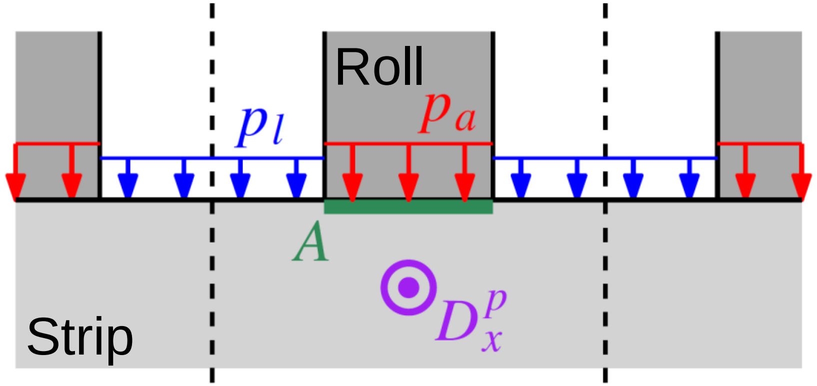

Rolling direction

- Objective: introduce an enhanced FE asperity flattening model with MPH lubrication in Metalub

5.2 Carretta’s coupling procedure

- Carretta (2017): first finite element (FE) model capable of simulating MPH lubrication in strip drawing
  - Strip drawing with lubricant pocket
  - Simulated in in-house FE solver Metafor
  - Lubricant flow by Arbitrary Lagrangian Eulerian (ALE)
    - Uncoupled flow from FE mesh to prevent mesh distortions
    - Artificial lubricant pipes required for lubricant permeation

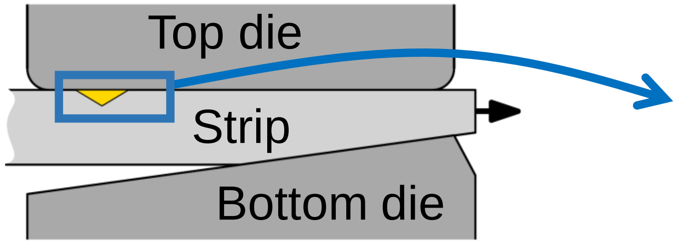

Strip drawing

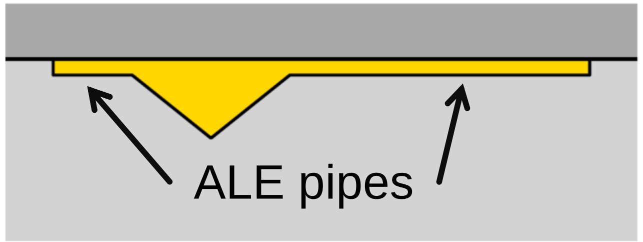

Lubricant pocket with artificial pipes in FE model

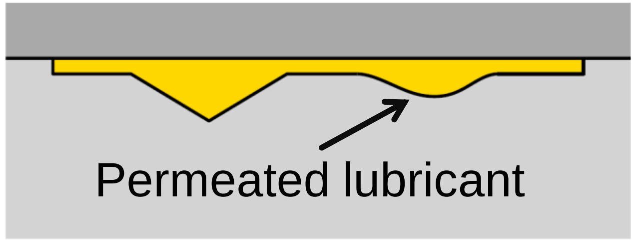

Permeation of lubricant from pocket into solid contact zone

5.2 Carretta’s coupling procedure

- MPH lubrication in cold rolling
  - Coupling procedure between Metalub and Metafor
  - FE asperity flattening model similar to previous lubricant pocket in strip drawing
    - Lubricant pipes introduced by shifted contact tool to allow permeation
    - Pressure increase in valleys “opens” pipes and decreases contact ➔ MPH lubrication

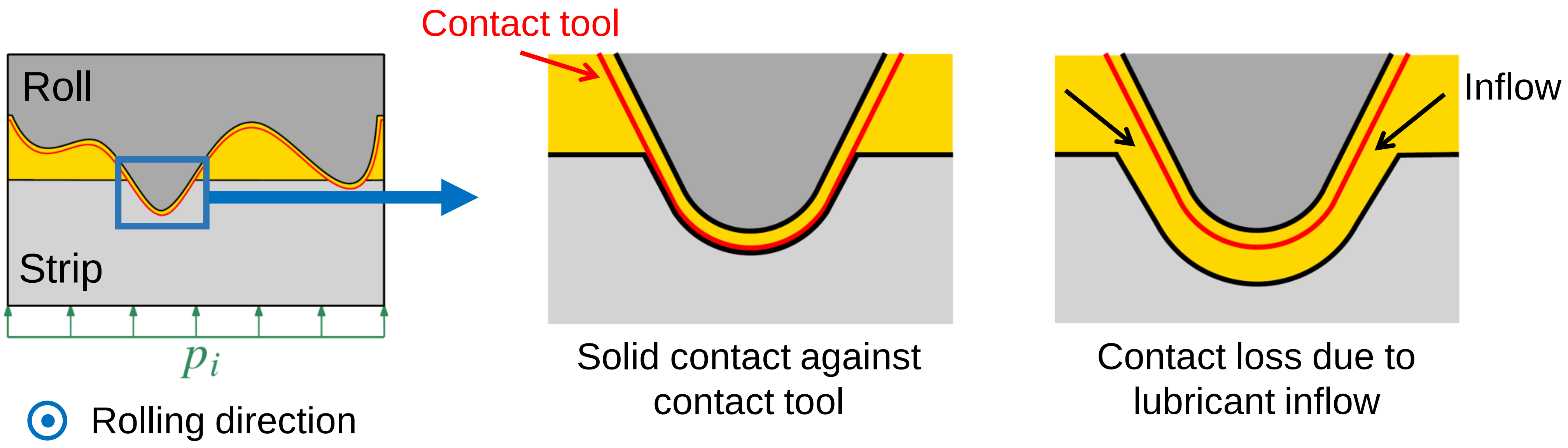

Solid contact against contact tool

Contact loss due to lubricant inflow

  - Converged only, if lubricant pressure not updated based on FE results

    ➔ No real convergence, since influence of FE model on lubricant pressure not considered

5.3 New coupling procedure

- Simplified model for gradual improvement towards MPH lubrication
- New FE asperity flattening model
  - Roll modeled by fixed rigid contact tool
  - Strip modeled by FE method
  - Interface pressure p_i pushes strip against roll
  - Strip cannot deform laterally
  - Generalized plane strain state
    - Strip elongation $l_{x,s}$ due to rolling
  - Lubricant pressure p_l of Metalub applied where no contact exists between roll and strip

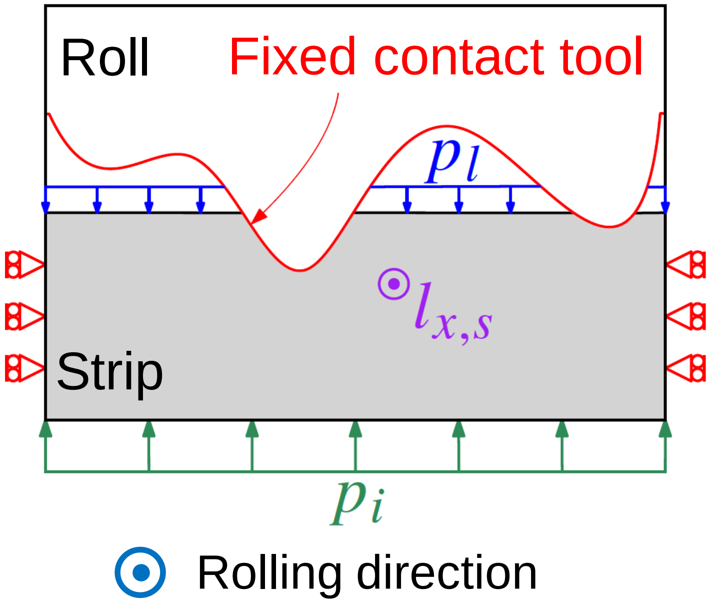

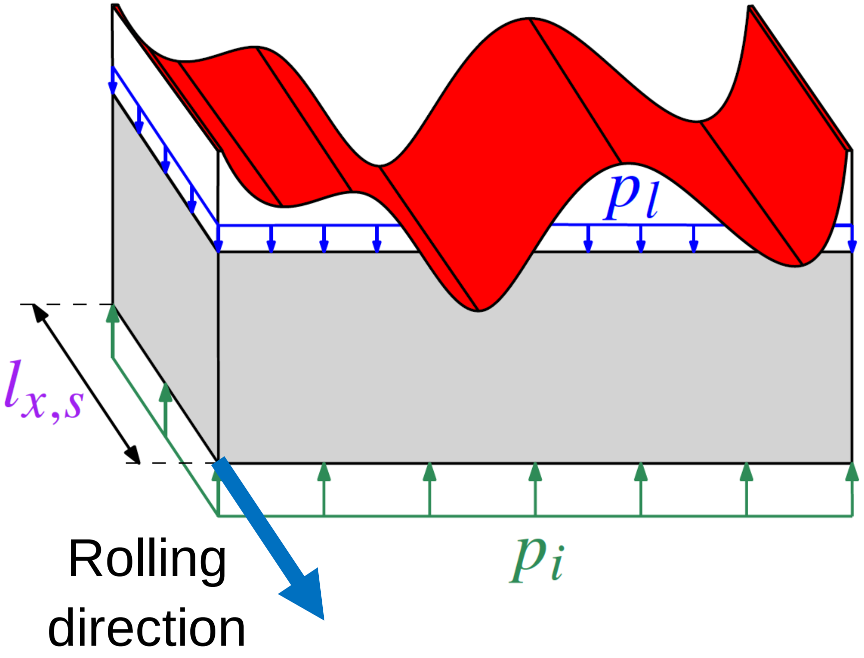

5.3 New coupling procedure

- Full coupling procedure

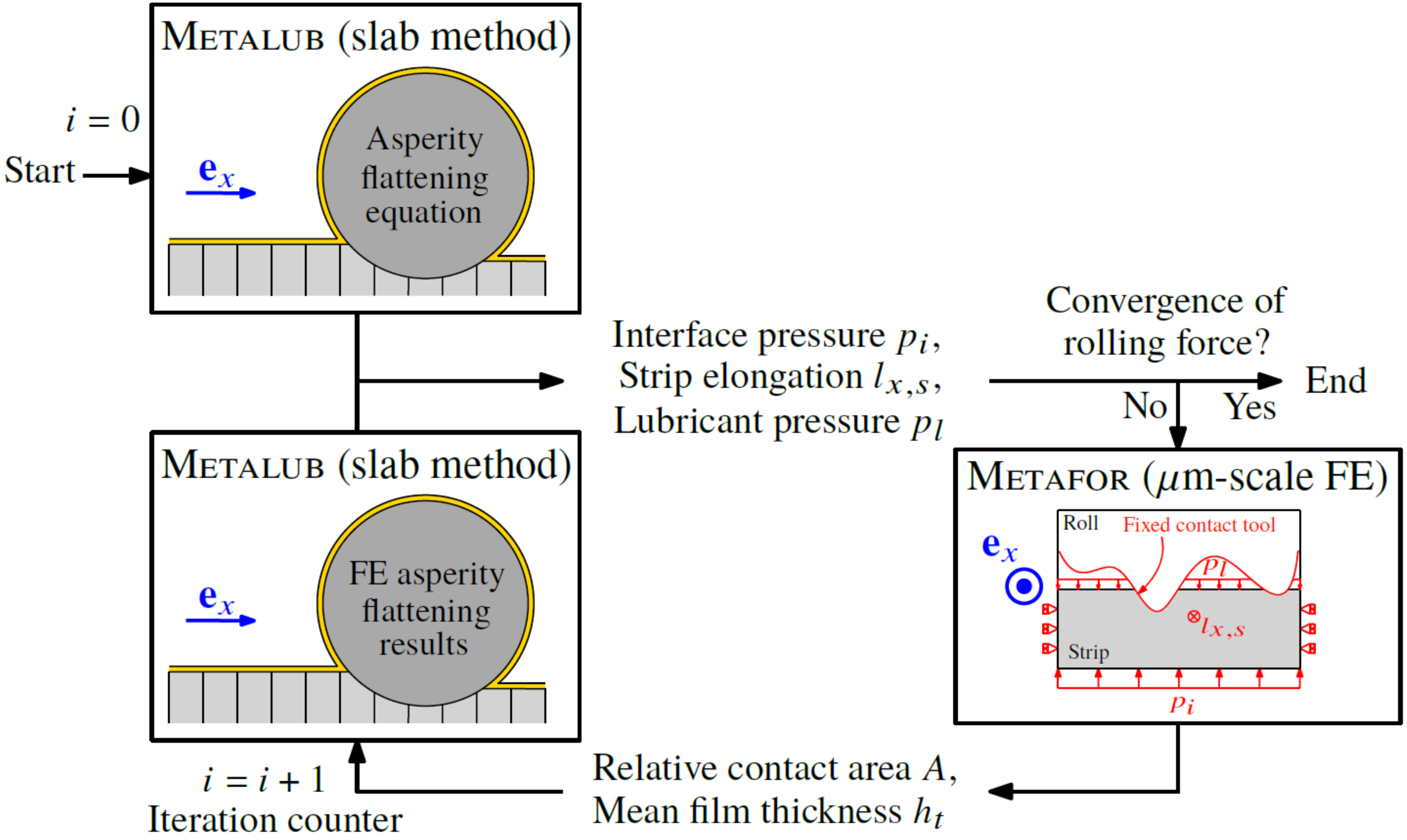

METALUB (slab method)

$i = 0$

Start

Asperity flattening equation

Interface pressure p_i,
Strip elongation $l_{x,s}$,
Lubricant pressure p_l

Convergence of rolling force?

No

Yes

End

METAFOR (μm-scale FE)

Relative contact area A,
Mean film thickness h_t

METALUB (slab method)

FE asperity flattening results

$i = i + 1$
Iteration counter

5.3 New coupling procedure

- Numerical results: first Metafor iteration (Test 5B-4)

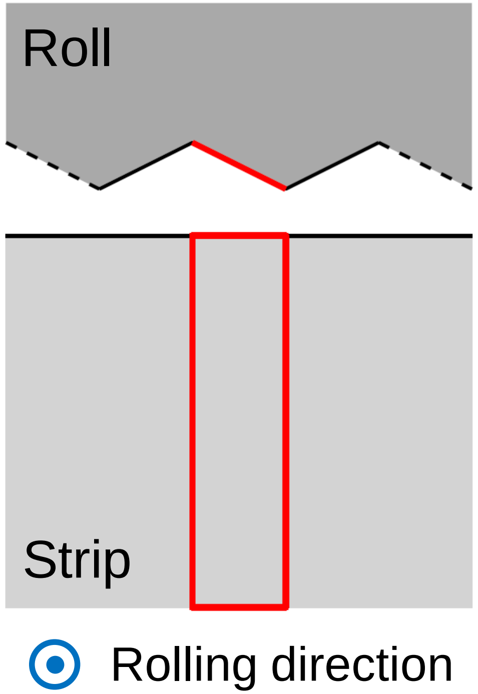

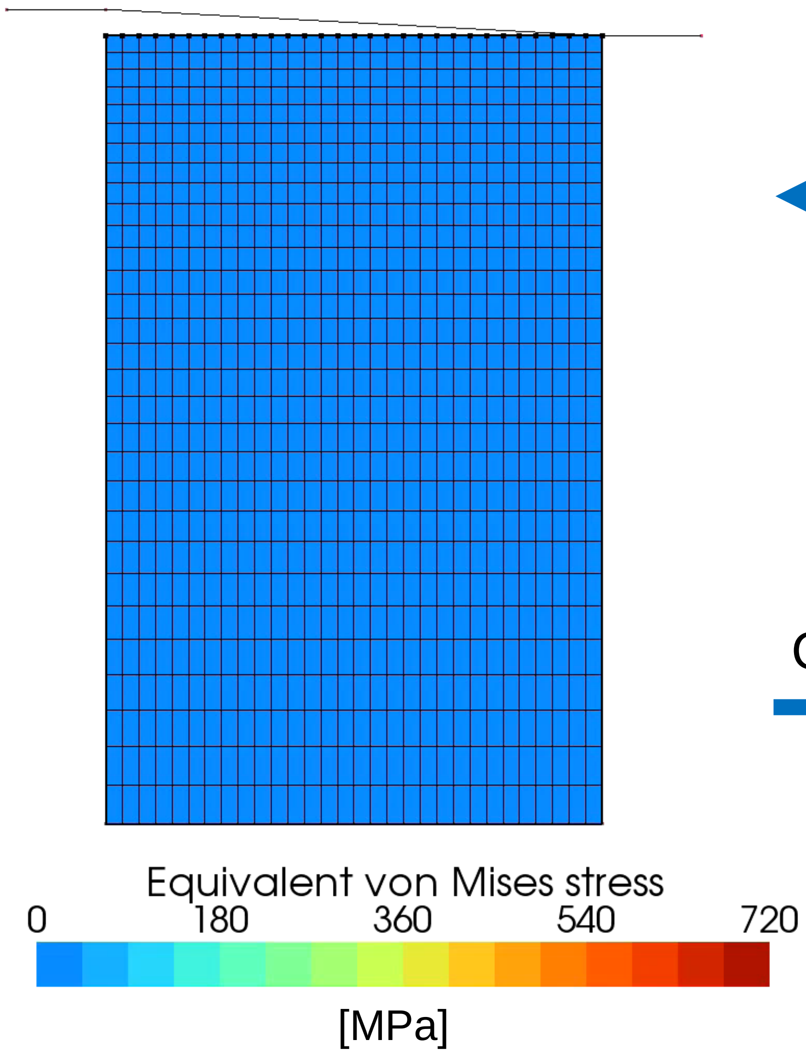

Input

Output

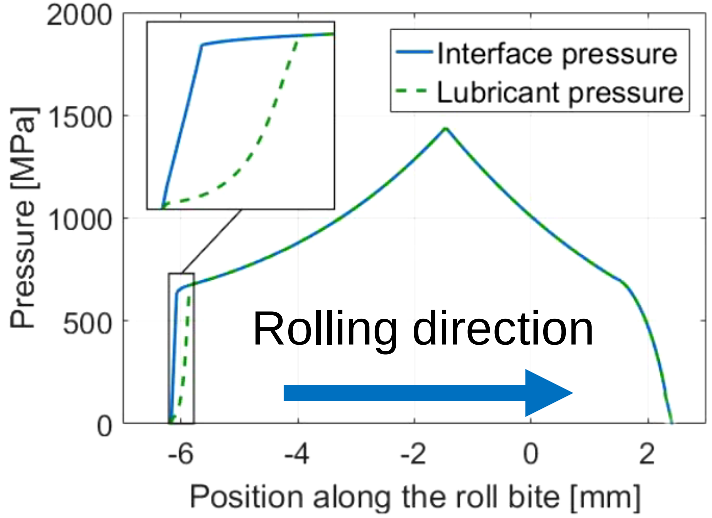

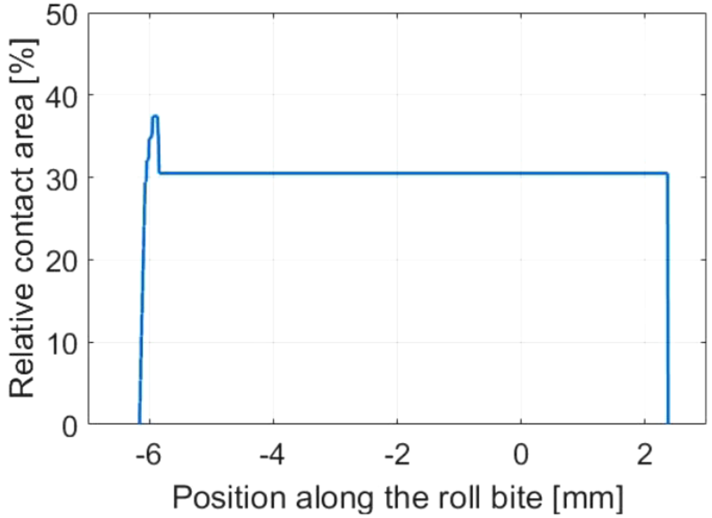

5.3 New coupling procedure

- Shortcomings
    - Mesh dependence in FE model, if lubricant pressure p_l becomes equal to interface pressure p_i
        - Tentative solution: slight reduction of the lubricant pressure

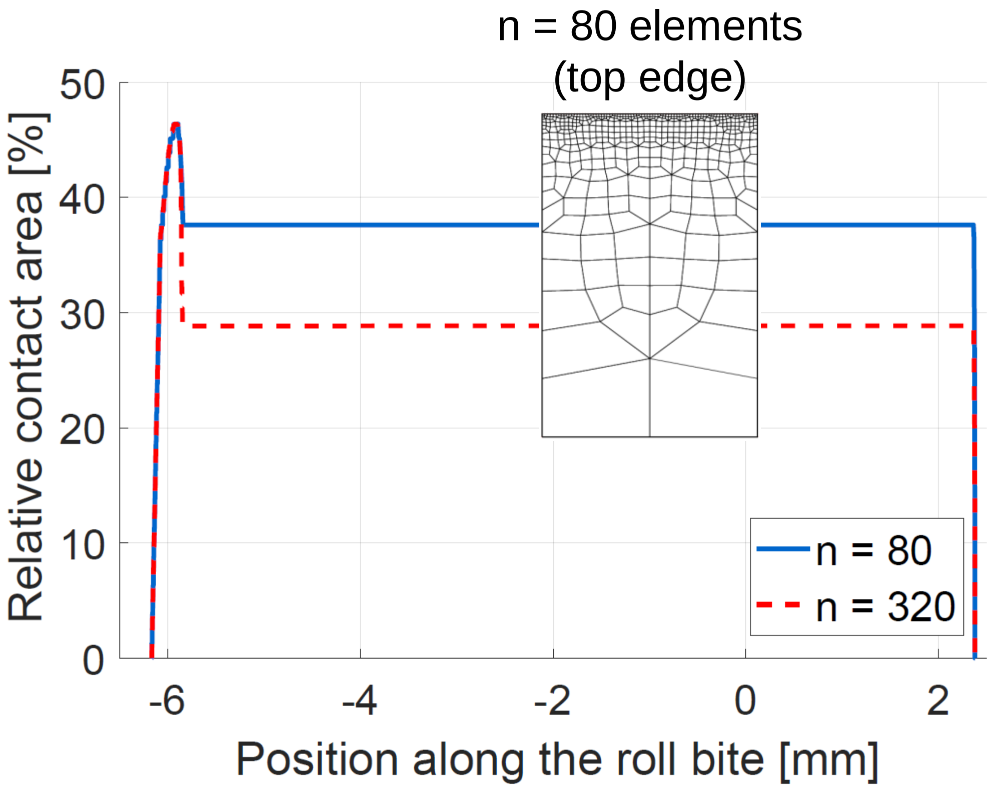

Mesh dependence, if $p_l = p_i$

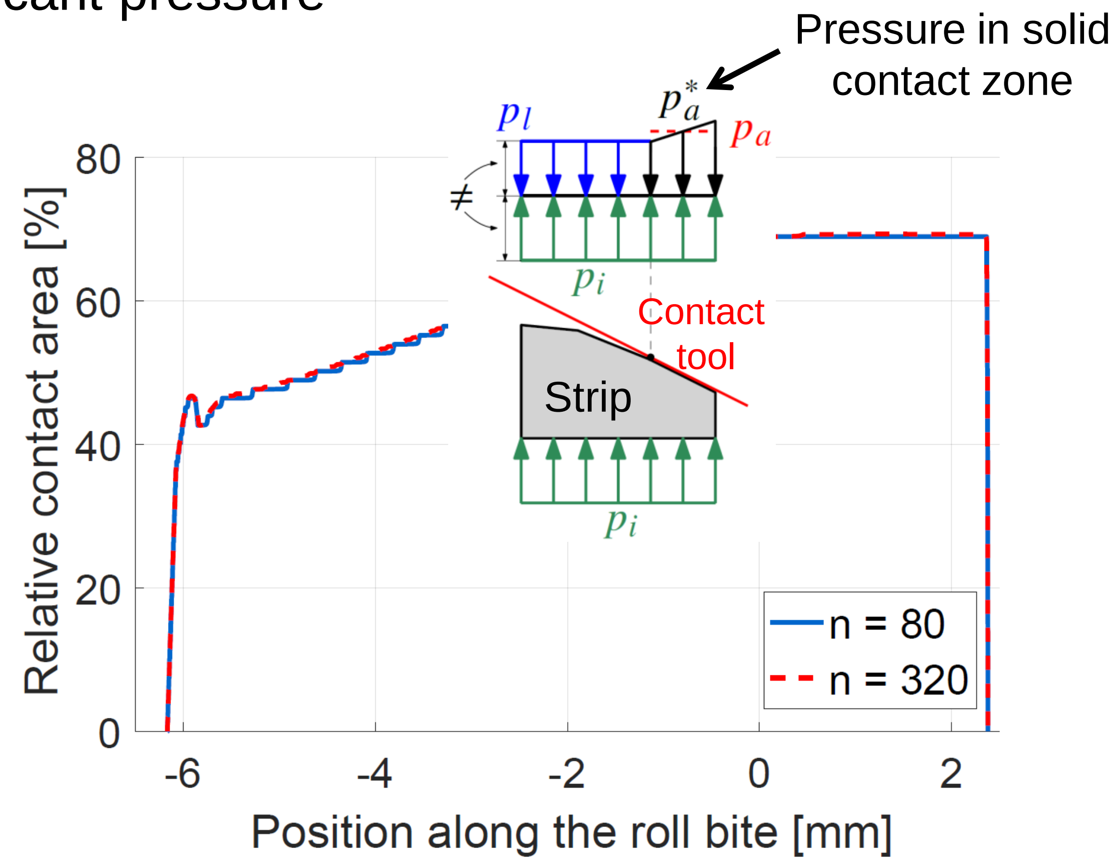

No mesh dependence, if $p_l = 0.95 p_l$

5.3 New coupling procedure

- Shortcomings
  - Insufficient strength/tightness of the coupling procedure
    - Results of coupled Metalub computation based on results of classical Metalub computation (instead FE flattening model) different from results of classical Metalub computation.

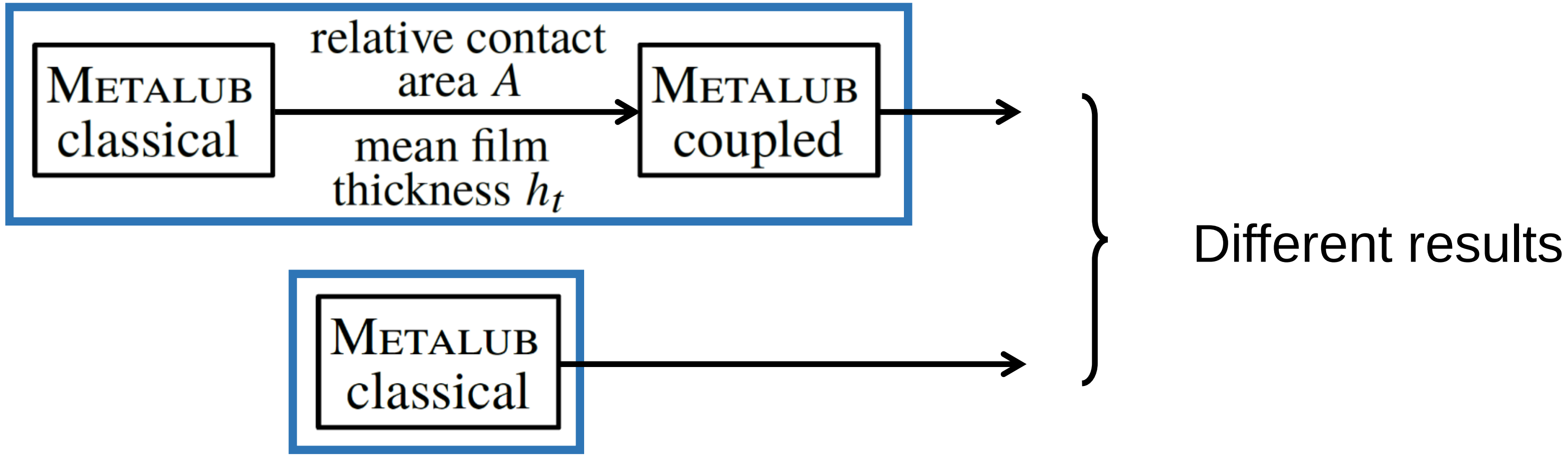

Different results

    - Results should, however, be equal since flattening model unchanged.
    - Tentative solution: different criterion in the adjustment loop of the lubricant flow rate

5.3 New coupling procedure

- Numerical results: full coupling procedure (Test 5B-4)
  - “Convergence” reached
  - Wilson and Sheu’s equation seems to overestimate the relative contact area, which increases friction and thus, the rolling force

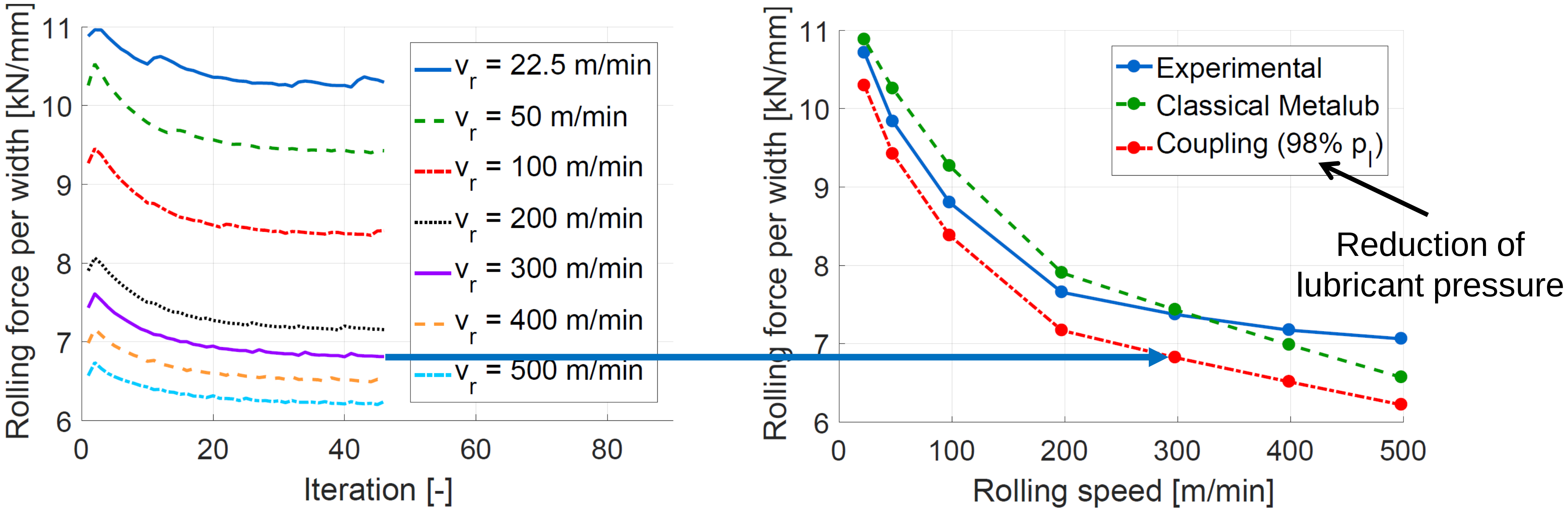

Reduction of lubricant pressure

- Intermediate conclusion
  - Convergence but strong hypotheses required
  - Possible computation-intensive solution but still no MPH lubrication

Outline

1. Introduction
2. Experimental data
3. Metalub model
4. Metalub results
5. FE asperity flattening in Metalub
6. **SPH asperity flattening**
7. Conclusion and outlook

6.1 Motivation

- Most promising model of MPH lubrication: Carretta’s FE model of plane strip drawing

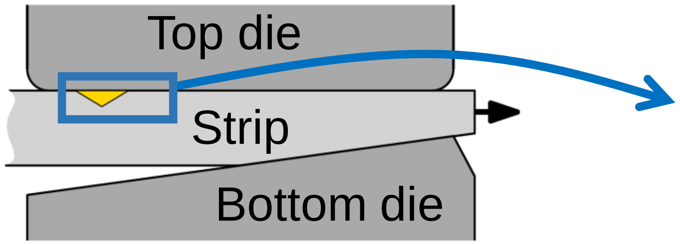

Strip drawing

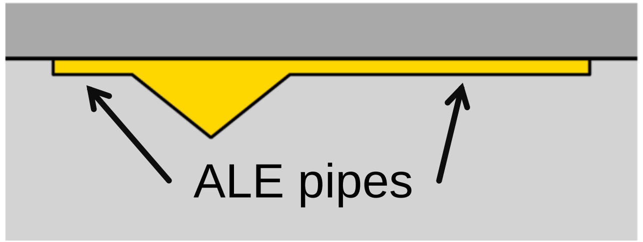

Lubricant pocket with artificial pipes in FE model

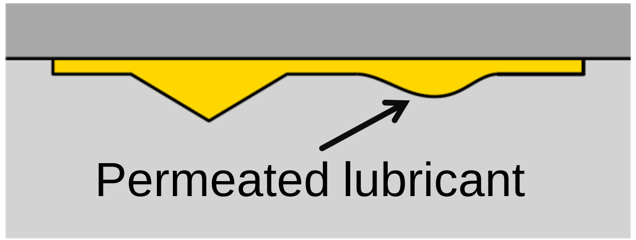

Permeation of lubricant from pocket into solid contact zone

- Limitations:
  - Artificial ALE lubricant pipes to allow permeation
  - Large deformations limited by mesh-distortions
  - Long computation time (10 days)
  - 2D model (3D extension not straightforward)

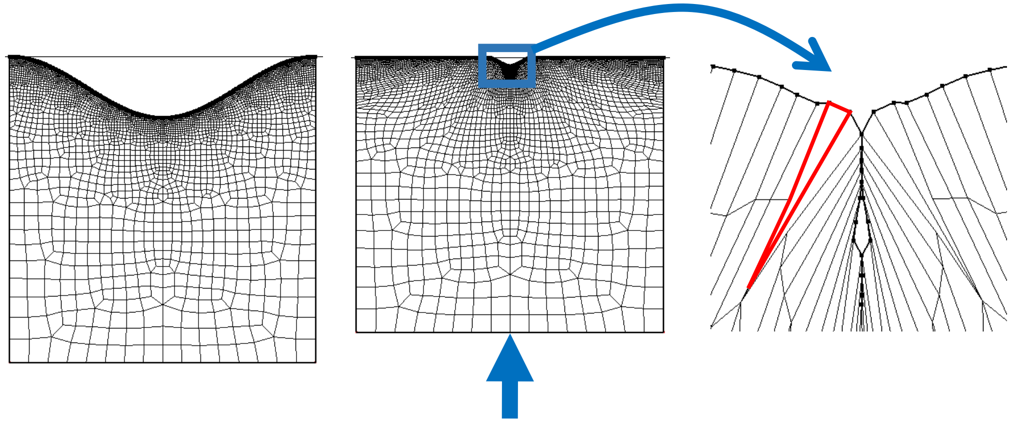

- Objective: explore “Smoothed Particle Hydrodynamics” (SPH) method to model MPH lubrication

6.2 Smoothed particle hydrodynamics

- Eulerian, Lagrangian or Arbitrary Lagrangian Eulerian (ALE) meshes in FE method

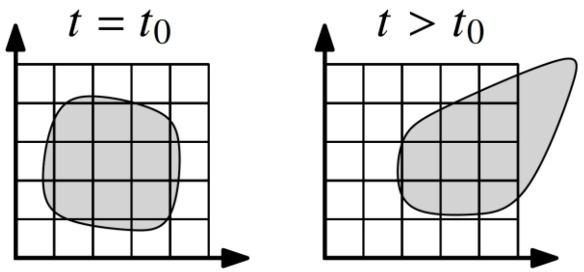

Eulerian:
✓ No mesh distortions
× Difficult boundary tracking

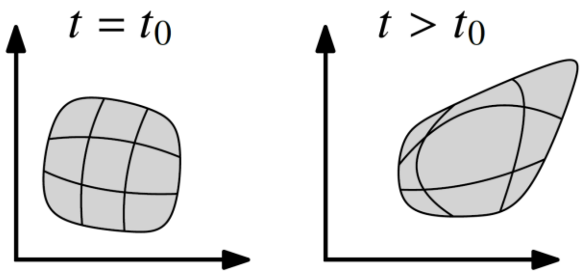

Lagrangian:
× Mesh distortions
✓ Automatic boundary tracking

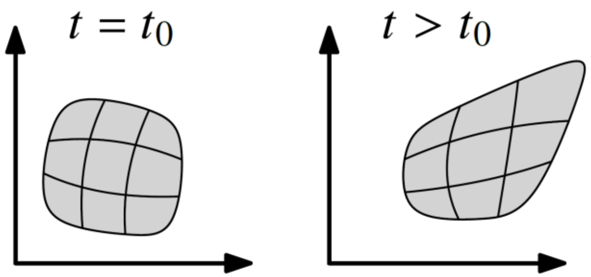

ALE:
✓ No mesh distortions
✓ Automatic boundary tracking
× Mesh motion to be anticipated

- Classical mesh-based versus Lagrangian meshless particle method

Classical mesh-based:
× Difficult boundary tracking or
× Mesh distortions or
× Mesh motion to be anticipated

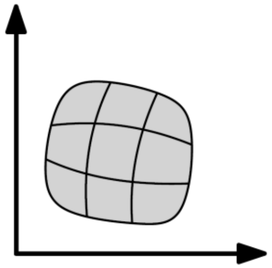

Lagrangian meshless particle:
✓ Automatic boundary tracking
✓ No mesh distortions
✓ No mesh motion to be anticipated

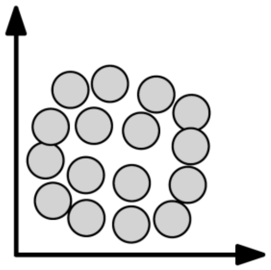

- SPH: Lagrangian meshless particle method

6.2 Smoothed particle hydrodynamics

- Fundamental concepts
  - Kernel approximation

$$f(\mathbf{x}) = \int_{\mathbb{V}} f(\mathbf{x}')\,\delta(\mathbf{x}-\mathbf{x}')\,\mathrm{d}\mathbf{x}' \xrightarrow{\text{Approx.}} f(\mathbf{x}) = \int_{\mathbb{V}} f(\mathbf{x}')\,W(\mathbf{x}-\mathbf{x}',h)\,\mathrm{d}\mathbf{x}'$$

Smoothing length

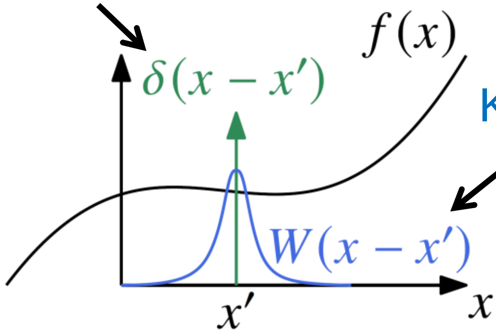
Dirac delta function

Kernel

  - Particle approximation

$$f(\mathbf{x}) = \int_{\mathbb{V}} f(\mathbf{x}')\,W(\mathbf{x}-\mathbf{x}',h)\,\mathrm{d}\mathbf{x}' \xrightarrow{\text{Approx.}} f(\mathbf{x}_a) = \sum_{b\in\mathcal{S}_a} V_b\, f(\mathbf{x}_b)\,W(x_{ab})$$

$$\rightarrow \nabla f(\mathbf{x}_a) = \sum_{b\in\mathcal{S}_a} V_b\, f(\mathbf{x}_b)\,\nabla_a W(x_{ab})$$

Particles in neighborhood of a

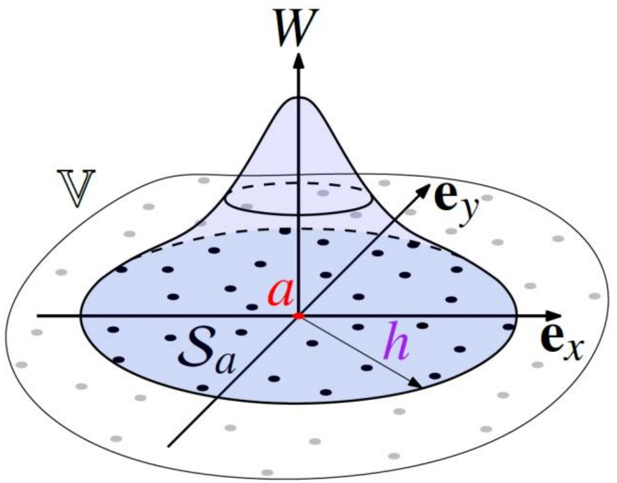

  - Gradient correction (consistency)
    - Zeroth-order completeness: $[\nabla\mathbf{f}(\mathbf{x}_a)]^T = \sum_{b\in\mathcal{S}_a} V_b\,[\mathbf{f}(\mathbf{x}_b)-\mathbf{f}(\mathbf{x}_a)]\otimes\nabla_a W(x_{ab})$
    - First-order completeness: $[\nabla\mathbf{f}(\mathbf{x}_a)]^T = \sum_{b\in\mathcal{S}_a} V_b\,[\mathbf{f}(\mathbf{x}_b)-\mathbf{f}(\mathbf{x}_a)]\otimes\mathbf{K}_a^{-1}\nabla_a W(x_{ab})$

with $\mathbf{K}_a = \sum_{b\in\mathcal{S}_a} V_b\,\nabla_a W(x_{ab})\otimes(\mathbf{x}_b-\mathbf{x}_a)$

6.2 Smoothed particle hydrodynamics

- Eulerian SPH for fluids
  - Variational approach by Bonet and Lok
  - Non-linear compressibility
  - Newtonian viscosity
  - Artificial Monaghan viscosity (stability)

$$m_a \frac{\mathrm{d}\mathbf{v}_a}{\mathrm{d}t} = \sum_{b \in \mathcal{S}_a} \left[V_a V_b \left(\boldsymbol{\sigma}_a \mathbf{K}_a^{-1} + \boldsymbol{\sigma}_b \mathbf{K}_b^{-1} \right) + m_a m_b \Pi_{ab} \right] \nabla_a W(x_{ab}) + m_a \mathbf{b}_a + \sum_{b \in \mathcal{S}_a^c} \mathbf{f}_{ab}^c$$

- Total Lagrangian SPH for solids
  - Tensile instability: total Lagrangian
  - Elasto-J2-plasticity with hardening (P = Piola)
  - Zero-energy mode suppression (HG = HourGlass)

$$m_a \frac{\mathrm{d}\mathbf{v}_a}{\mathrm{d}t} = \sum_{b \in \mathcal{S}_a^0} \left[V_a^0 V_b^0 \left(\mathbf{P}_a \mathbf{K}_{0,a}^{-1} + \mathbf{P}_b \mathbf{K}_{0,b}^{-1} \right) \nabla_a W(X_{ab}) + \mathbf{f}_{ab}^{\mathrm{HG}} \right] + m_a \mathbf{b}_a + \sum_{b \in \mathcal{S}_a^c} \mathbf{f}_{ab}^c$$

- Contact interaction
  - Penalty force

$$\mathbf{f}_{ab}^c = -\frac{4}{3} E^* \sqrt{R^*} \delta^{3/2} \frac{\mathbf{x}_{ab}}{x_{ab}}$$

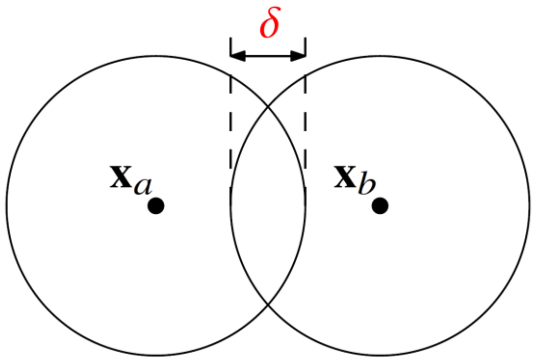

6.2 Smoothed particle hydrodynamics

- Numerical solution method
    - LAMMPS (Plimpton, 1995)
        - Molecular dynamics solver
        - USER-SMD (Ganzenmüller, 2015):
            - Package with this specific SPH formulation
        - Modifications: kernel, post-processing features
    - Computational efficiency
        - Neighbor search: link-cell binning and neighbor lists
        - Domain decomposition with dynamic load balancing
    - Time integration
        - Velocity-Verlet (explicit)
        - Time step stability limit

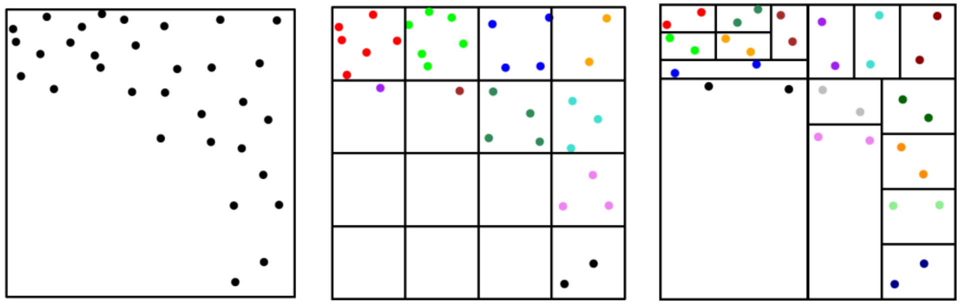

Serial

Parallel

Parallel (balanced)

6.3 Validation tests

- First fluid and fluid-structure interaction (FSI) validation tests of the USER-SMD package
- Tests based on Cerquaglia's thesis (2019) about PFEM-FEM coupling in MN2L research group

- Water sloshing in an oscillating reservoir [Souto-Iglesias et al.]

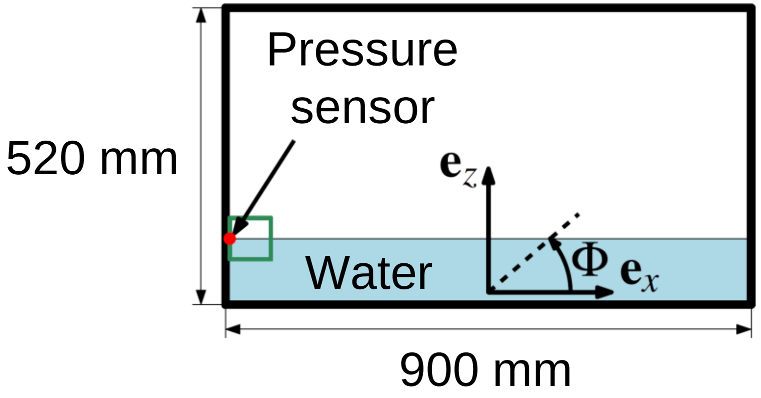

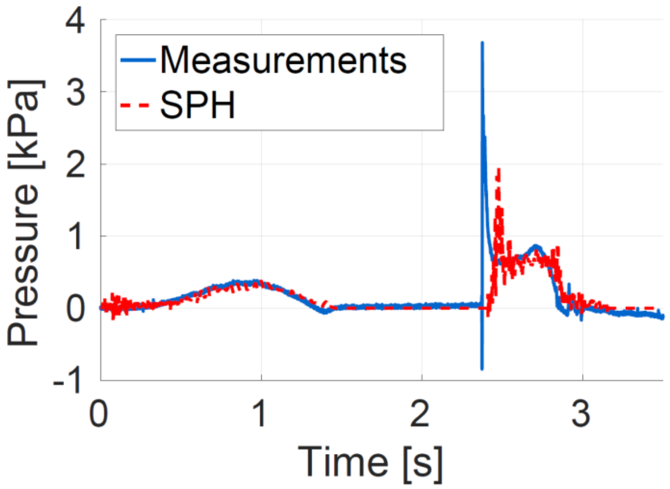

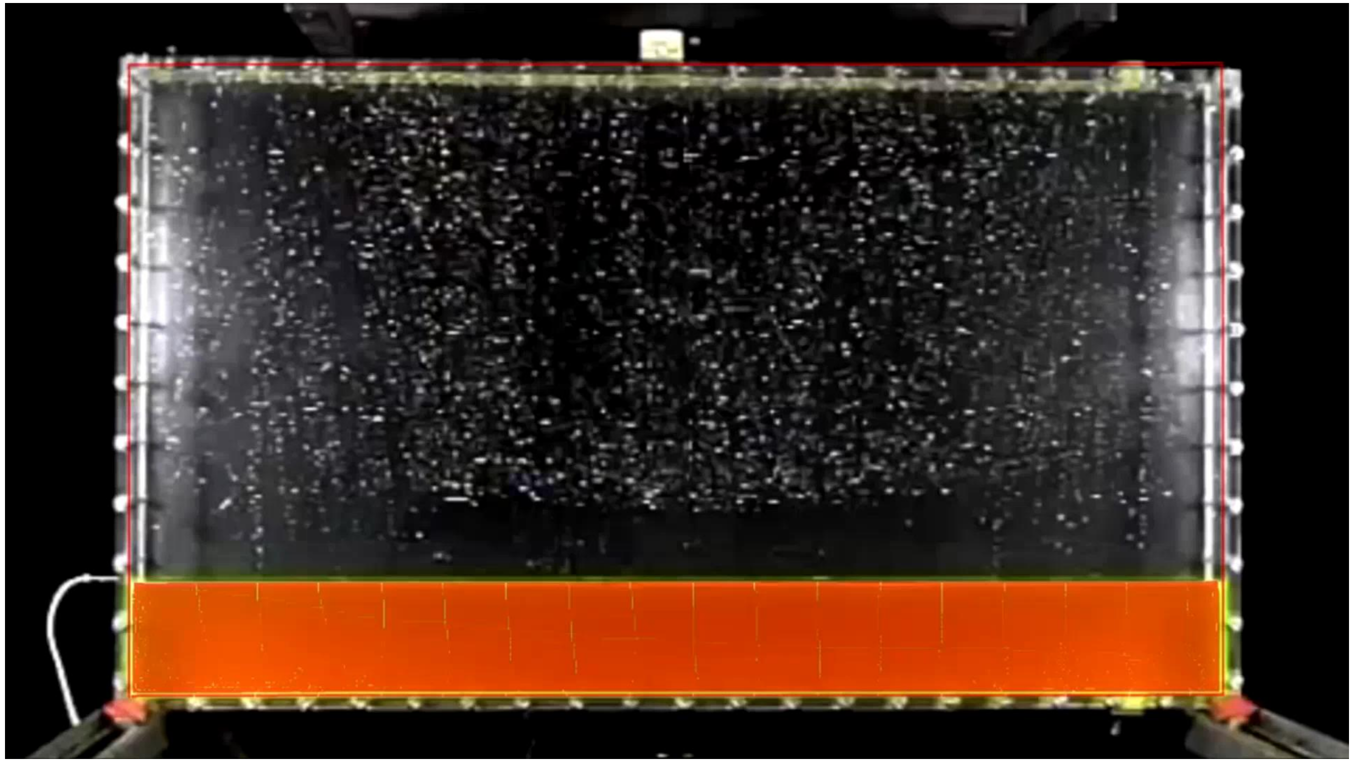

Yellow = real water; red = prediction
(20,000 water particles, 2 h CPU, 3 physical cores)

6.3 Validation tests

- Dam break against an elastic obstacle

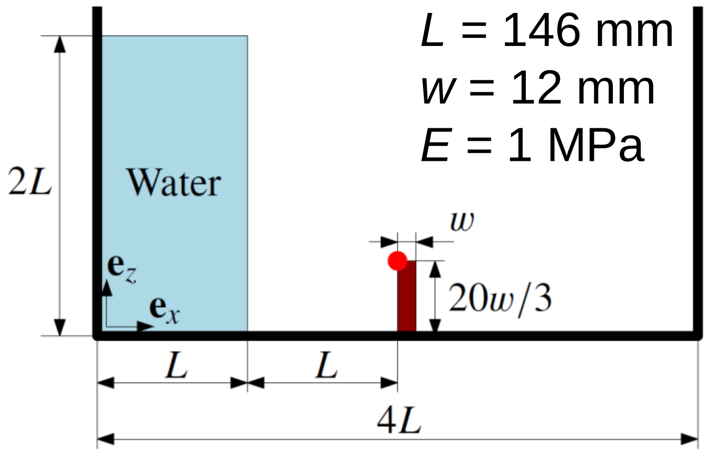

L = 146 mm
w = 12 mm
E = 1 MPa

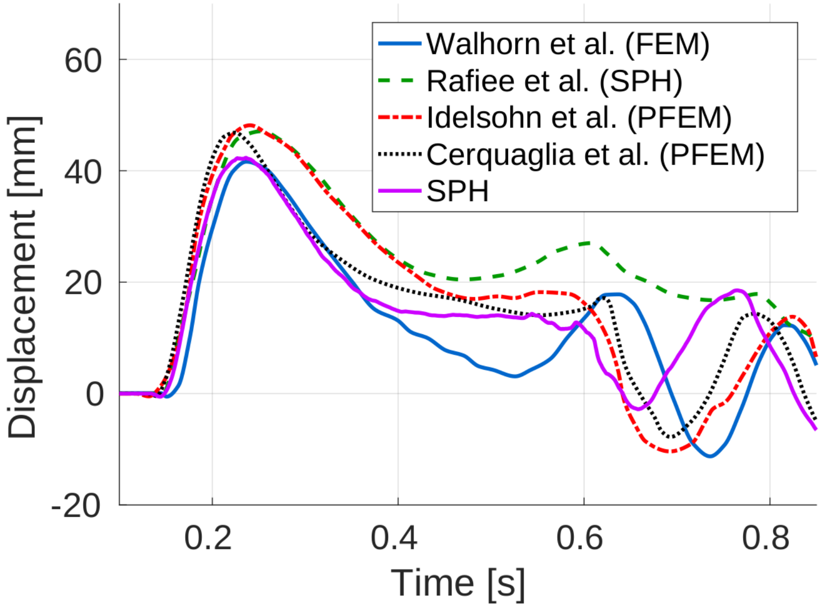

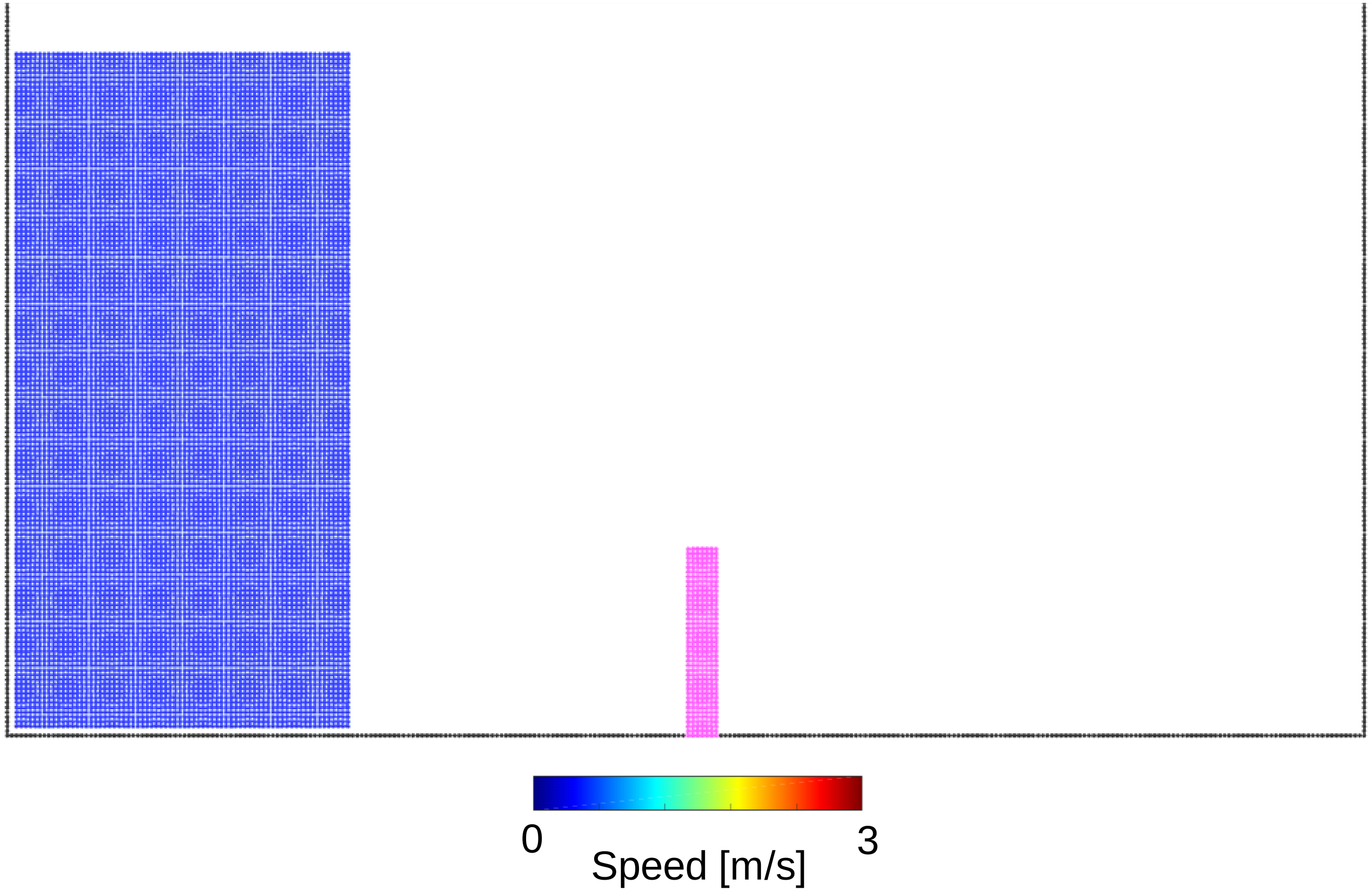

(10,440 water particles, 278 solid particles,
10 min CPU, 3 physical cores)

6.3 Validation tests

- Gravity-driven viscous flow
  - Periodic boundary condition along vertical direction: particles reinjected at the top
  - No-slip boundary condition: fixed boundary particles included in particle sum of fluid particles

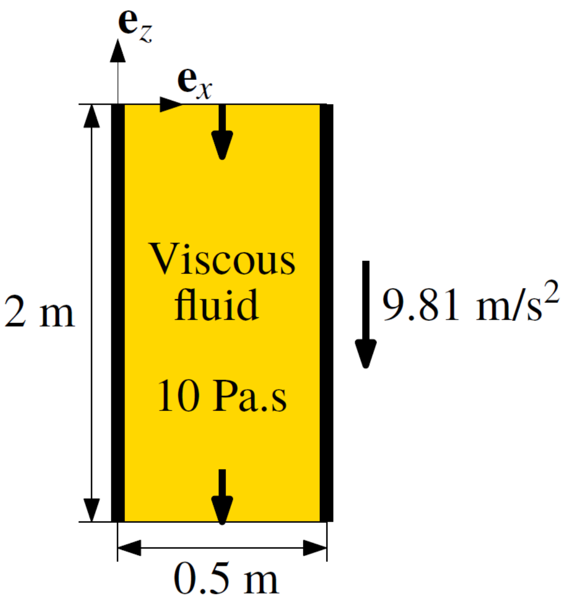

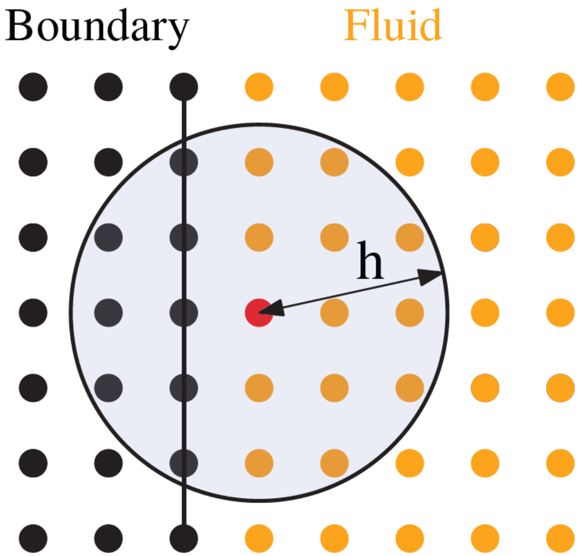

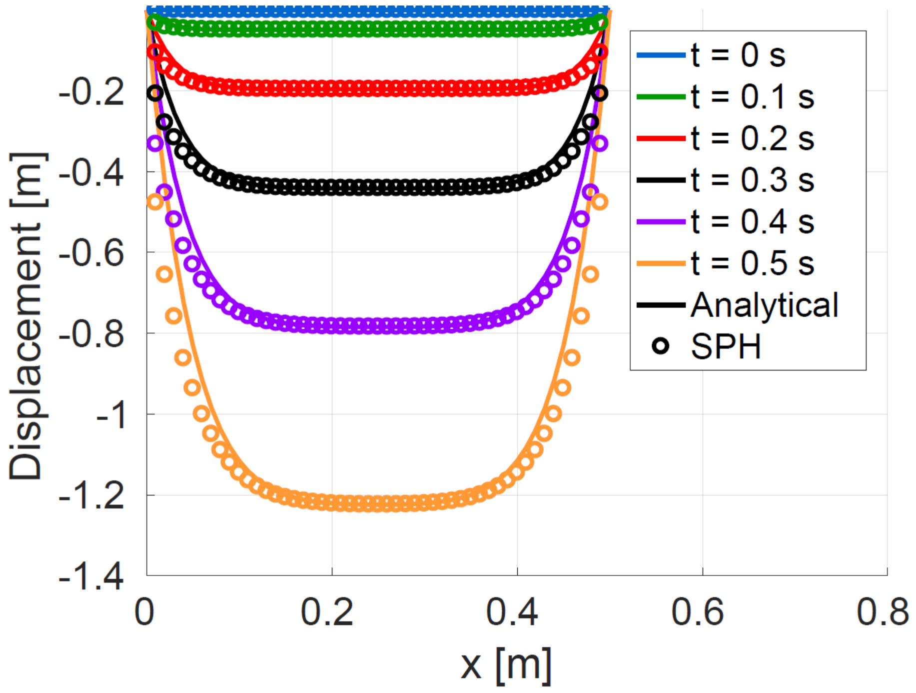

6.4 Asperity flattening

- Problem statement [Shvarts and Yastrebov, 2018]:
  - Lubricated asperity flattening
  - Elastic-perfectly plastic steel
    - Young modulus: 200 GPa
    - Poisson's ratio: 0.28
    - Yield stress: 250 MPa
  - Non-linearly compressible oil
    - Bulk modulus: 2000 + 9.25 p_l [MPa]
  - Relative contact area as a function of pressure

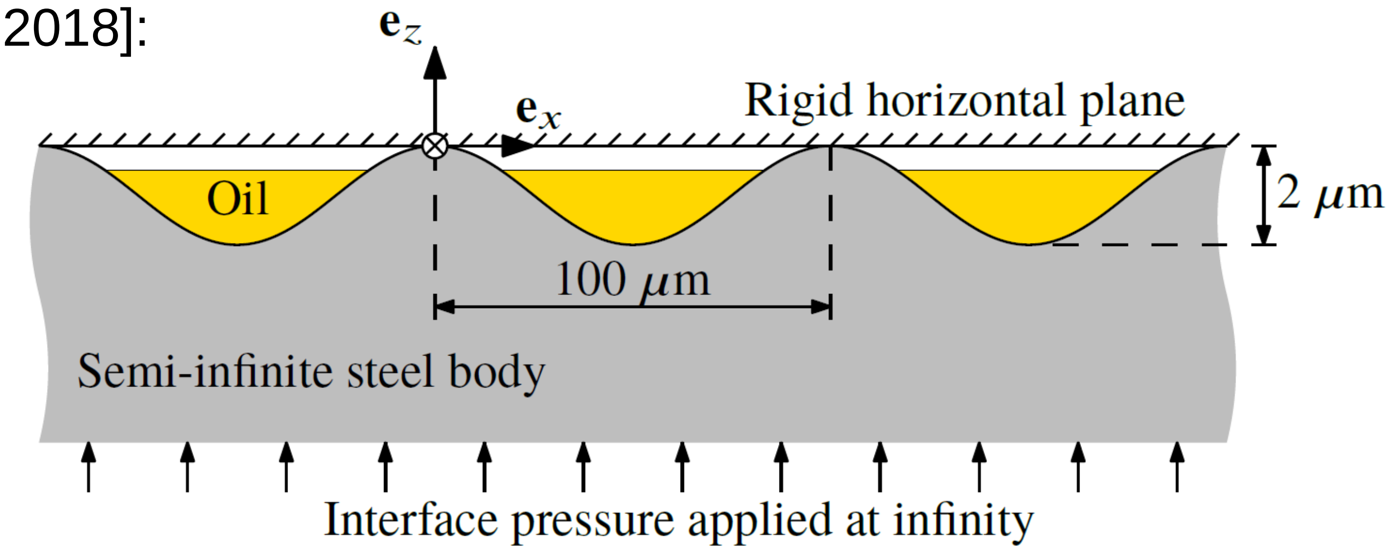

- Progressive resolution
  1. Compression of an elastoplastic solid
  2. Dry asperity flattening
  3. Compression of a fluid
  4. Lubricated asperity flattening

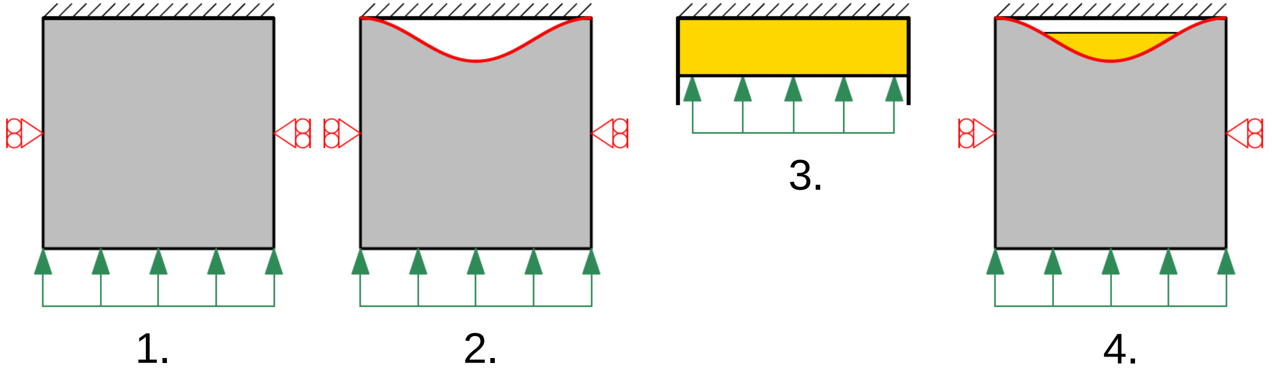

6.4.1 Dry asperity flattening

- Boundary conditions
  - No horizontal displacement of vertical edges
  - Imposed upward speed

- Discretization
  - Coarser boundary than by Lagrangian meshes
  - Asperity amplitude increased
  - ~36,000 particles; 4.5 h CPU time (12 cores)
    - ➔ Local refinement required

- Relative contact area computation

- Successful validation
  - By previous FE model of asperity flattening
  - Without mesh distortions in SPH

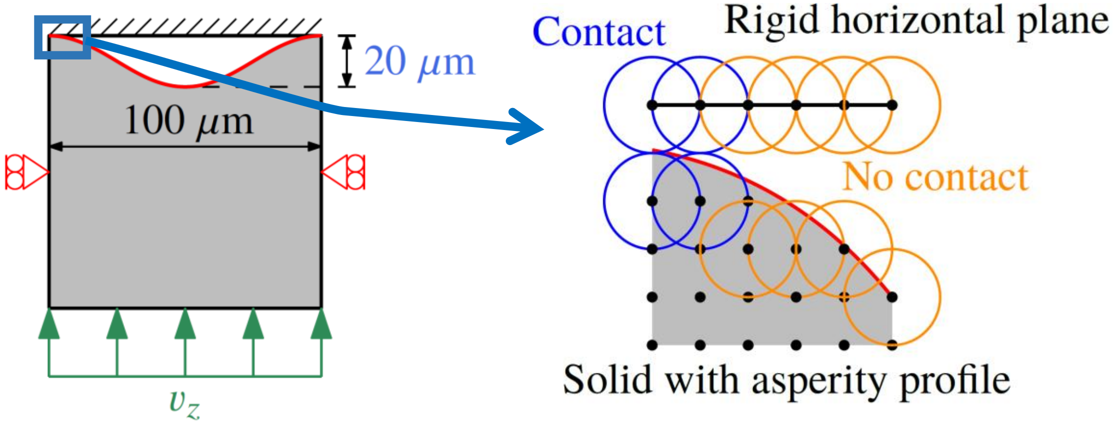

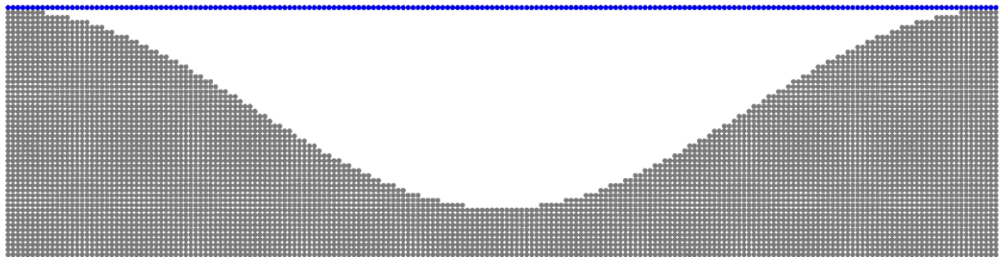

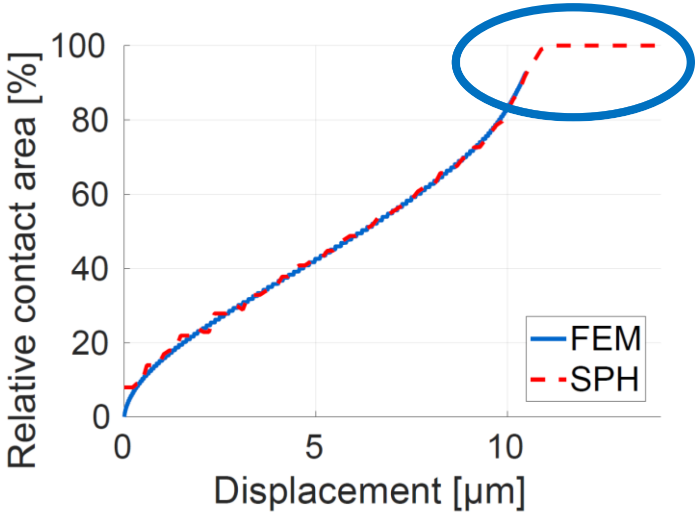

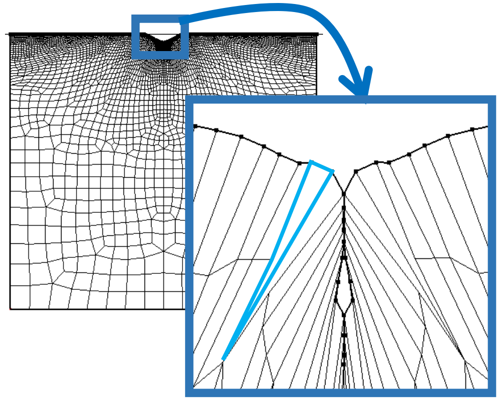

6.4.2 Lubricated asperity flattening

- Previous configuration with oil
- Almost identical solutions when oil is not compressed
- Increase of relative contact area slowed down by oil in SPH
- Infiltration after ~2000 MPa due to penalty contact
  - ➔ Possible solution: boundary condition by Adami et al.
- Artificial permeation at very high pressure (~5000 MPa)
- MPH lubrication? Not yet.
  - Solve shortcomings: boundary conditions, CPU time

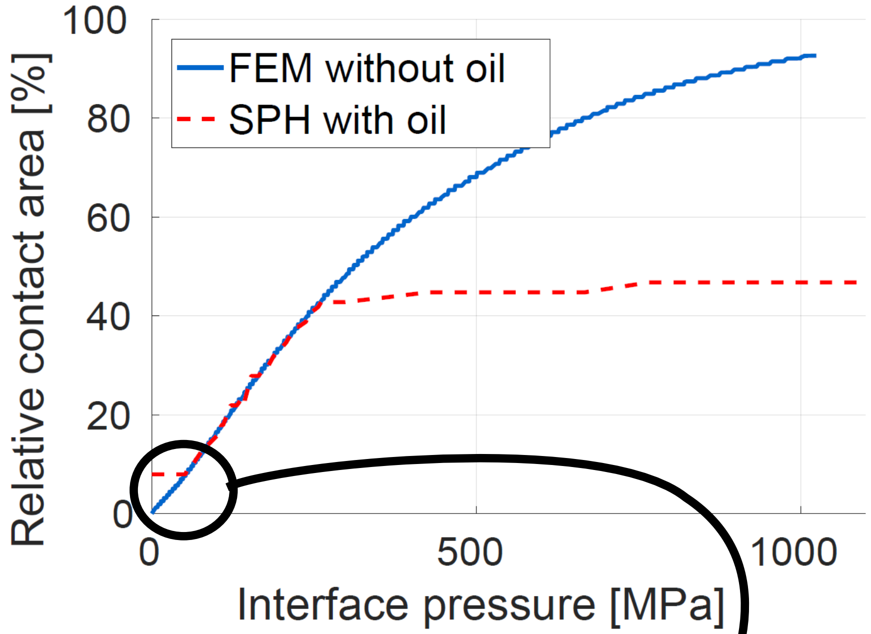

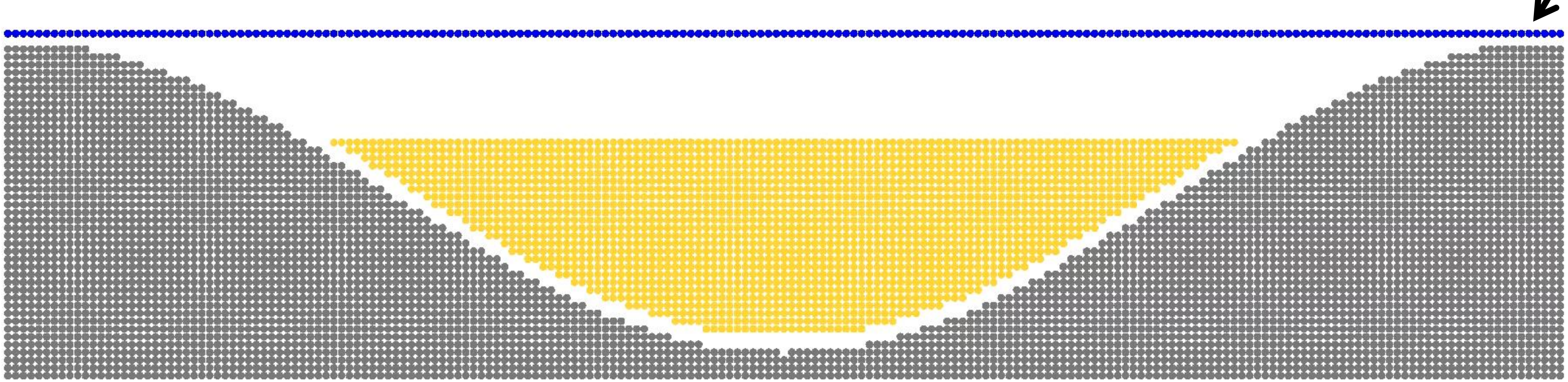

Outline

1. Introduction
2. Experimental data
3. Metalub model
4. Metalub results
5. FE asperity flattening in Metalub
6. SPH asperity flattening
7. **Conclusion and outlook**

Conclusion – Original contributions

- Experimental data

  ➔ Post-processing and analysis of the most comprehensive data of lubricant cold rolling

- Metalub model

  ➔ Re-derivation, documentation, extension and refactoring of the model and its implementation

  ➔ One of the most powerful models of lubricated cold rolling!

- Metalub results

  ➔ Evaluation of Metalub's predictive capabilities and shortcomings based on the previous data

- FE asperity flattening in Metalub

  ➔ First coupling procedures between Metalub and the FE solver Metafor with lubricated asperity flattening including the strip elongation

- SPH asperity flattening

  ➔ First simulation of complex FSI validation tests by LAMMPS USER-SMD

  ➔ First SPH models of dry and lubricated asperity flattening

Outlook

- Incorporation of a full thermal model into Metalub
  - Similar to ThermRoll and within the Metalub software project

- Incorporation of an analytical MPH lubrication model into Metalub
  - Reduction of relative contact area based on variables that favor MPH lubrication according to Ahmed and Sutcliffe (2001)

- Incorporation of a lubricant film formation model into Metalub
  - Computation of lubricant film thickness at the entry based on Cassarini (2007)

- Extension of experimental data
  - Reduction of modeling uncertainties (viscoplasticity, …)

- Improvement of lubricated asperity flattening by SPH
  - Local refinement of discretization by Spreng (2017); boundary condition by Adami et al. (2012)

Thank you for your attention!

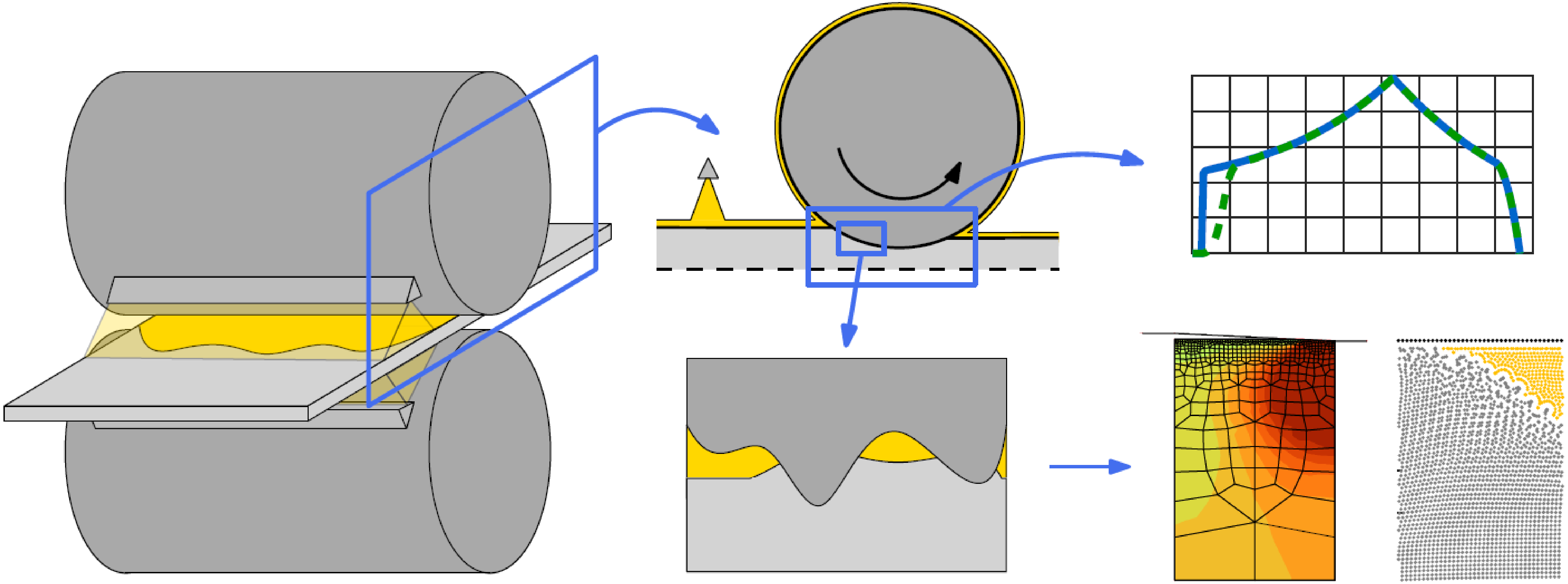

Selected references

- S. Adami, X. Y. Hu, and N. A. Adams. A generalized wall boundary condition for smoothed particle hydrodynamics. Journal of Computational Physics, 231(21):7057–7075, 2012.
- R. Ahmed and M. P. F. Sutcliffe. An experimental investigation of surface pit evolution during cold-rolling or drawing of stainless steel strip. Journal of Tribology, 123(1):1–7, 2001.
- D. R. Bland and H. Ford. Cold rolling with strip tension, Part 3 - An approximate treatment of the elastic compression of the strip in cold rolling. Journal of Iron and Steel Institute, 171:245–249, 1952.
- R. Boman and J.-P. Ponthot. Numerical simulation of lubricated contact in rolling processes. Journal of Material Processing Technology, 125-126:405–411, 2002.
- J. Bonet and T.-S. L. Lok. Variational and momentum preservation aspects of Smooth Particle Hydrodynamic formulations. Computer Methods in Applied Mechanics and Engineering, 180(1–2):97–115, 1999.
- T. Bouache, N. Legrand, and P. Montmitonnet. A numerical heat transfer analysis in mixed film lubrication for cold strip rolling. In M. Steeper, editor, 5th European Rolling Conference, London, 2009.
- Y. Carretta. Modélisation des conditions d’apparition du micro-hydrodynamisme via la méthode des éléments finis dans la perspective d’intégrer ce phénomène dans un modèle numérique de laminage à froid. PhD thesis, Université de Liège, 2014. In French.
- Y. Carretta, J. Bech, N. Legrand, M. Laugier, J.-P. Ponthot and R. Boman. Numerical modelling of micro-plasto-hydrodynamic lubrication in plane strip drawing. Tribology International, 110:378-391, 2017.
- S. Cassarini. Modélisation du film lubrifiant dans la zone d’entrée pour la lubrification par émulsion en laminage à froid. PhD thesis, École Nationale Supérieure des Mines de Paris, 2007. In French.
- M. L. Cerquaglia. Development of a fully-partitioned PFEM-FEM approach for fluid-structure interaction problems characterized by free surfaces, large solid deformations, and strong added-mass effects. PhD thesis, Université de Liège, 2019.
- G. C. Ganzenmüller. Smooth Mach Dynamics package for LAMMPS, Fraunhofer Ernst-Mach Institute for high-speed dynamics. https://lammps.sandia.gov/doc/PDF/SMD_LAMMPS_userguide.pdf, 2015. Version 0.12.
- J. H. Hitchcock. Elastic deformation of rolls during cold-rolling. Roll Neck Bearings. Report of A.S.M.E. Special Research Committee on Heavy-Duty Anti-friction Bearings, pages 33–41, 1935.

Selected references

- G. R. Johnson and W. H. Cook. A constitutive model and data for metals subjected to large strains, high-strain rates and high-temperatures. Proceedings of the 7th International Symposium on Ballistics, pages 541–547, 1983.
- D. A. Korzekwa, P. R. Dawson, and W. R. D. Wilson. Surface asperity deformation during sheet forming. International Journal of Mechanical Sciences, 34(7):521–539, 1992.
- M. Laugier, M. Tornicelli, C. S. Leligois, D. Bouquegneau, D. Launet, and J. A. Alvarez. Flexible lubrication concept. The future of cold rolling lubrication. Proceedings of the Institution of Mechanical Engineers, Part J: Journal of Engineering Tribology, 225(9):949–958, 2011.
- M. Laugier, R. Boman, N. Legrand, J.-P. Ponthot, M. Tornicelli, J. I. Bech and Y. Carretta. Micro-plasto-hydrodynamic lubrication. A fundamental mechanism in cold rolling. Advanced Materials Research, 966-967:228–241, 2014.
- N. Legrand, D. Patrault, N. Labbe, D. Gade, D. Piesak, N. G. Jonsson, A. Nilsson, J. Horsky, T. Luks, P. Montmitonnet, R. Canivenc, R. Dwyer Joyce, A. Hunter, C. Pinna and L. Maurin. Advanced roll gap sensors for enhanced hot and cold rolling processes (rollgap sensors). Research Fund for Coal and Steel, European Commission, 2015.
- N. Marsault. Modélisation du régime de lubrification mixte en laminage à froid. PhD thesis, École Nationale Supérieure des Mines de Paris, 1998. In French.
- W. Meindl. Walzenabplattung unter Berücksichtigung der Kontaktschubspannungen. PhD thesis, Johannes Kepler Universität Linz, 2001. In German.
- S. Plimpton. Fast parallel algorithms for short-range molecular dynamics. Journal of Computational Physics, 117(1):1–19, 1995.
- J.-P. Ponthot. Traitement unifié de la mécanique des milieux continus solides en grandes transformations par la méthode des éléments finis. PhD thesis, Université de Liège, 1995. In French.
- A. G. Shvarts and V. A. Yastrebov. Trapped fluid in contact interface. Journal of the Mechanics and Physics of Solids, 119(1):140–162, 2018.
- A. Souto-Iglesias, E. Botia-Vera, A. Martin, and F. Pérez-Arribas. A set of canonical problems in sloshing. Part 0: Experimental setup and data processing. Ocean Engineering, 38(16):1823–1830, 2011.
- F. Spreng. Smoothed particles hydrodynamics for ductile solids. PhD thesis, Universität Stuttgart. Institut für Technische und Numerische Mechanik, 2017.
- A. Stephany. Contribution à l’étude numérique de la lubrification en régime mixte en laminage à froid. PhD thesis, Université de Liège, 2008. In French.
- M. P. F. Sutcliffe. Surface asperity deformation in metal forming processes. International Journal of Mechanical Sciences, 30(11):847–868, 1988.
- M. P. F. Sutcliffe. Flattening of random rough surfaces in metal-forming processes. Journal of Tribology, 121(3):433–440, 1999.
- W. R. D. Wilson and S. Sheu. Real area of contact and boundary friction in metal forming. International Journal of Mechanical Sciences, 30(7):475–489, 1988.

Acknowledgement

The author, Dominik Boemer, would like to acknowledge the Belgian National Fund for Scientific Research (F.R.S.-FNRS) for its financial support (F.R.S.-FNRS Research Fellowship).

fnrs

FREEDOM TO RESEARCH